



National Library
of Canada

Acquisitions and
Bibliographic Services Branch

395 Wellington Street
Ottawa, Ontario
K1A 0N4

Bibliothèque nationale
du Canada

Direction des acquisitions et
des services bibliographiques

395 rue Wellington
Ottawa (Ontario)
K1A 0N4

NOTICE

The quality of this microform is heavily dependent upon the quality of the original thesis submitted for microfilming. Every effort has been made to ensure the highest quality of reproduction possible.

If pages are missing, contact the university which granted the degree.

Some pages may have indistinct print especially if the original pages were typed with a poor typewriter ribbon or if the university sent us an inferior photocopy.

Reproduction in full or in part of this microform is governed by the Canadian Copyright Act, R.S.C. 1970, c. C-30, and subsequent amendments.

AVIS

La qualité de cette microforme dépend grandement de la qualité de la thèse soumise au microfilmage. Nous avons tout fait pour assurer une qualité supérieure de reproduction.

S'il manque des pages, veuillez communiquer avec l'université qui a conféré le grade.

La qualité d'impression de certaines pages peut laisser à désirer, surtout si les pages originales ont été dactylographiées à l'aide d'un ruban usé ou si l'université nous a fait parvenir une photocopie de qualité inférieure.

La reproduction, même partielle, de cette microforme est soumise à la Loi canadienne sur le droit d'auteur, SRC 1970, c. C-30, et ses amendements subséquents.

**Mechanistic Studies of the Photolysis
of Substituted Benzyl Acetates and Pivalates
and
1-Naphthylmethyl Carbonates and Carbamates**

by

Paula Jane MacLeod

Submitted in partial fulfillment of the requirements for the
Degree of Doctor of Philosophy

at

Dalhousie University
Halifax, Nova Scotia

© Paula Jane MacLeod



National Library
of Canada

Acquisitions and
Bibliographic Services Branch

395 Wellington Street
Ottawa, Ontario
K1A 0N4

Bibliothèque nationale
du Canada

Direction de l'acquisitions et
des services bibliographiques

395 rue Wellington
Ottawa (Ontario)
K1A 0N4

Yves G. Gauthier

Yves G. Gauthier

The author has granted an irrevocable non-exclusive licence allowing the National Library of Canada to reproduce, loan, distribute or sell copies of his/her thesis by any means and in any form or format, making this thesis available to interested persons.

L'auteur a accordé une licence irrévocable et non exclusive permettant à la Bibliothèque nationale du Canada de reproduire, prêter, distribuer ou vendre des copies de sa thèse de quelque manière et sous quelque forme que ce soit pour mettre des exemplaires de cette thèse à la disposition des personnes intéressées.

The author retains ownership of the copyright in his/her thesis. Neither the thesis nor substantial extracts from it may be printed or otherwise reproduced without his/her permission.

L'auteur conserve la propriété du droit d'auteur qui protège sa thèse. Ni la thèse ni des extraits substantiels de celle-ci ne doivent être imprimés ou autrement reproduits sans son autorisation.

ISBN 0-612-08784-0

Canada

Name Paula Jane Macleod

Dissertation Abstracts International is arranged by broad, general subject categories. Please select the one subject which most nearly describes the content of your dissertation. Enter the corresponding four digit code in the space provided.

Organic Chemistry
SUBJECT TERM

0490
SUBJECT CODE

U·M·I

Subject Categories

THE HUMANITIES AND SOCIAL SCIENCES

COMMUNICATIONS AND THE ARTS

Architecture 0729
Art History 0377
Cinema 0900
Dance 0378
Fine Arts 0357
Information Science 0723
Journalism 0391
Library Science 0399
Mass Communications 0708
Music 0413
Speech Communication 0459
Theater 0465

EDUCATION

General 0515
Administration 0514
Adult and Continuing 0516
Agricultural 0517
Art 0273
Bilingual and Multicultural 0282
Business 0688
Community College 0275
Curriculum and Instruction 0727
Early Childhood 0518
Elementary 0524
Finance 0277
Guidance and Counseling 0519
Health 0680
Higher 0745
History of 0520
Home Economics 0278
Industrial 0521
Language and Literature 0279
Mathematics 0280
Music 0522
Philosophy of 0998
Physical 0523

Psychology 0525
Reading 0535
Religious 0527
Sciences 0714
Secondary 0533
Social Sciences 0534
Sociology of 0340
Special 0529
Teacher Training 0530
Technology 0710
Tests and Measurements 0288
Vocational 0747

LANGUAGE, LITERATURE AND LINGUISTICS

Language
General 0679
Ancient 0289
Linguistics 0290
Modern 0291
Literature
General 0401
Classical 0294
Comparative 0295
Medieval 0297
Modern 0298
African 0316
American 0591
Asian 0305
Canadian (English) 0352
Canadian (French) 0355
English 0593
Germanic 0311
Latin American 0312
Middle Eastern 0315
Romance 0313
Slavic and East European 0314

PHILOSOPHY, RELIGION AND THEOLOGY

Philosophy 0422
Religion
General 0318
Biblical Studies 0321
Clergy 0319
History of 0320
Philosophy of 0322
Theology 0469

SOCIAL SCIENCES

American Studies 0323
Anthropology
Archaeology 0324
Cultural 0326
Physical 0327
Business Administration
General 0310
Accounting 0272
Banking 0770
Management 0454
Marketing 0338
Canadian Studies 0385
Economics
General 0501
Agricultural 0503
Commerce Business 0505
Finance 0508
History 0509
Labor 0510
Theory 0511
Folklore 0358
Geography 0366
Gerontology 0351
History
General 0578

Ancient 0579
Medieval 0581
Modern 0582
Black 0328
African 0331
Asia, Australia and Oceania 0332
Canadian 0334
European 0335
Latin American 0336
Middle Eastern 0333
United States 0337
History of Science 0585
Law 0398
Political Science
General 0615
International Law and Relations 0616
Public Administration 0617
Recreation 0814
Social Work 0452
Sociology
General 0626
Criminology and Penology 0627
Demography 0938
Ethnic and Racial Studies 0631
Individual and Family Studies 0628
Industrial and Labor Relations 0629
Public and Social Welfare 0630
Social Structure and Development 0700
Theory and Methods 0344
Transportation 0709
Urban and Regional Planning 0999
Women's Studies 0451

THE SCIENCES AND ENGINEERING

BIOLOGICAL SCIENCES

Agriculture
General 0473
Agronomy 0265
Animal Culture and Nutrition 0475
Animal Pathology 0476
Food Science and Technology 0359
Forestry and Wildlife 0478
Plant Culture 0479
Plant Pathology 0480
Plant Physiology 0817
Range Management 0777
Wood Technology 0746
Biology
General 0306
Anatomy 0287
Biostatistics 0308
Botany 0309
Cell 0379
Ecology 0329
Entomology 0353
Genetics 0369
Limnology 0793
Microbiology 0410
Molecular 0307
Neuroscience 0317
Oceanography 0416
Physiology 0433
Radiation 0821
Veterinary Science 0778
Zoology 0472
Biophysics
General 0786
Medical 0760
EARTH SCIENCES
Biogeochemistry 0425
Geochemistry 0996

Geodesy 0370
Geology 0372
Geophysics 0373
Hydrology 0388
Mineralogy 0411
Paleobotany 0345
Paleoecology 0426
Paleontology 0418
Paleozoology 0985
Palynology 0427
Physical Geography 0368
Physical Oceanography 0415

HEALTH AND ENVIRONMENTAL SCIENCES

Environmental Sciences 0768
Health Sciences
General 0566
Audiology 0300
Chemotherapy 0992
Dentistry 0567
Education 0350
Hospital Management 0769
Human Development 0758
Immunology 0982
Medicine and Surgery 0564
Mental Health 0347
Nursing 0569
Nutrition 0570
Obstetrics and Gynecology 0380
Occupational Health and Therapy 0354
Ophthalmology 0381
Pathology 0571
Pharmacology 0419
Pharmacy 0572
Physical Therapy 0382
Public Health 0573
Radiology 0574
Recreation 0575

Speech Pathology 0460
Toxicology 0383
Home Economics 0386

PHYSICAL SCIENCES

Pure Sciences
Chemistry
General 0485
Agricultural 0749
Analytical 0486
Biochemistry 0487
Inorganic 0488
Nuclear 0738
Organic 0490
Pharmaceutical 0491
Physical 0494
Polymer 0495
Radiation 0754
Mathematics 0405
Physics
General 0605
Acoustics 0986
Astronomy and Astrophysics 0606
Atmospheric Science 0608
Atomic 0748
Electronics and Electricity 0607
Elementary Particles and High Energy 0798
Fluid and Plasma 0759
Molecular 0609
Nuclear 0610
Optics 0752
Radiation 0756
Solid State 0611
Statistics 0463
Applied Sciences
Applied Mechanics 0346
Computer Science 0984

Engineering
General 0337
Aerospace 0538
Agricultural 0539
Automotive 0540
Biomedical 0541
Chemical 0542
Civil 0543
Electronics and Electrical 0544
Heat and Thermodynamics 0545
Hydraulic 0545
Industrial 0546
Marine 0547
Materials Science 0794
Mechanical 0548
Metallurgy 0743
Mining 0551
Nuclear 0552
Packaging 0549
Petroleum 0765
Sanitary and Municipal System Science 0790
System Science 0790
Technology
General 0428
Operations Research 0796
Plastics Technology 0795
Textile Technology 0994

PSYCHOLOGY

General 0621
Behavioral 0384
Clinical 0622
Developmental 0620
Experimental 0623
Industrial 0624
Personality 0625
Physiological 0989
Psychobiology 0349
Psychometrics 0632
Social 0451



Dalhousie University

Date August, 1995

Author Paula Jane MacLeod

Title Mechanistic Studies of the Photolysis of Substituted Benzyl Acetates and Pivalates and 1-Naphthylmethyl Carbonates and Carbamates

Department or School Chemistry

Degree Ph.D. Convocation October Year 1995

Permission is herewith granted to Dalhousie University to circulate and to have copied for non-commercial purposes, at its discretion, the above title upon request of individuals or institutions.

Signature of Author

THE AUTHOR RESERVES OTHER PUBLICATION RIGHTS, AND NEITHER THE THESIS NOR EXTENSIVE EXTRACTS FROM IT MAY BE PRINTED OR OTHERWISE REPRODUCED WITHOUT THE AUTHOR'S WRITTEN PERMISSION.

THE AUTHOR ATTESTS THAT PERMISSION HAS BEEN OBTAINED FOR THE USE OF ANY COPYRIGHTED MATERIAL APPEARING IN THIS THESIS (OTHER THAN BRIEF EXCERPTS REQUIRING ONLY PROPER ACKNOWLEDGEMENT IN SCHOLARLY WRITING) AND THAT ALL SUCH USE IS CLEARLY ACKNOWLEDGED.

To my family
for their love and support

Table of Contents

List of Figures	viii
List of Tables	ix
List of Schemes	x
Abstract	xi
List of Abbreviations and Symbols Used	xii
Acknowledgements	xiv

Chapter 1

The Photochemistry of Benzylic and Indanyl Esters

1.1 Introduction	1
1.2 Results and Discussion on the Photochemistry of the Monosubstituted Benzyl Acetates 1a-f and Pivalates 2a-f	18
1.2.1 Products and Yields on Direct Irradiation of 1a-f and 2a-f	18
1.2.2 Multiplicity of the Reactive Excited State	24
1.2.3 Quantitative Mechanistic Scheme	29
1.2.4 Conclusions	41
1.3 Results and Discussion on the Photochemistry of the Multiple Methoxy Substituted Compounds	42
1.3.1 Introduction	42
1.3.2 Products and Yields on Irradiation of 1g-i and 2g-i	44
1.3.3 Quantitative Mechanistic Scheme for Esters 1g-i and 2g-i	47
1.3.4 Photolysis of Esters 1j-l	54
1.3.5 Conclusions	55
1.4 Results and Discussion of the Photochemistry of Substituted Indanyl Acetates and Pivalates	57
1.4.1 Introduction	57
1.4.2 Preparation and Photolysis of Esters 3-6	62
1.4.3 Quantitative Mechanistic Scheme for Esters 5a-c and 6a-c	68
1.4.4 Photophysical Data for Esters 5a-c and 6a-c	70
1.4.5 Conclusions	77

1.5	Experimental	79
1.5.1	General Procedures	79
1.5.2	Fluorescence Measurements	80
1.5.3	Syntheses of the Benzyl Alcohols 7a-l and the Indanyl Alcohols 19a-c	80
1.5.4	Preparation and Characterization of the Benzyl and Indanyl Esters 1-6	85
1.5.5	Preparative Photolyses	94
1.5.6	Characterization and Preparation of the Photoproducts 8-13 and 21-31	94
	The Methyl Ethers 8a-j , 21 , and 25a-c	94
	The Toluenes, 9a-j , 22 and 26a-c	98
	The Radical Coupling Products 10a-j , 11a-j , 27a-c and 28a-c	100
	The Dimers 12a-j , 28a-c and 29a-c	106
	The Aryl-methanol Products 31a-c	108
1.5.7	Quantitative Photolyses	109
1.5.8	Analytical Determination of the Ether Yields 8a,e,f	110
1.5.9	Oxidation Potential Measurements	110
1.5.10	Quantum Yield Measurements	111

Chapter 2

The Photochemistry of 1-Naphthylmethyl Carbonates and Carbamates

2.1	Introduction	112
2.2	Results and Discussion	116
2.2.1	Synthesis of the 1-Naphthylmethyl Carbonates and Carbamates	116
2.2.2	Excited-State Properties of the Carbonates and Carbamates	116
2.2.3	Photolysis of the Carbonates 31 and 32	118
2.2.4	Photolysis of the Carbamates 33 and 34	125
2.2.5	Conclusions	128
2.3	Experimental	129
2.3.1	General Experimental	129
2.3.2	Synthesis of the Carbonates 31 and 32 and Carbamates 33 and 34	129
2.3.3	Fluorescence Measurements	132
2.3.4	Preparative Photolysis	132
2.3.5	Characterization of the Photoproducts	133
2.3.6	Quantitative Photolysis	136
2.3.7	Photolysis of 1-Naphthylmethyl Phenyl Ether, 38	137
2.3.8	Photolysis of N-(1-Naphthylmethyl)aniline, 43	137

Chapter 3

Conformational Behaviour of Highly Hindered Ethanes: *Meso* and *dl* Dimers of 2,2,2',2'-Tetramethyl-1-1'-biindanyl

3.1	Introduction	138
3.2	Results	143
3.2.1	Crystallography	143
3.2.2	NMR Analysis of the <i>Meso</i> Dimer, 30a	145
3.2.3	Calculations for the <i>Meso</i> Dimer, 30a	149
3.2.4	NMR Analysis of the <i>Racemic</i> Dimer, 29a	153
3.2.5	Calculations for the <i>Racemic</i> Dimer, 29a	157
3.2.6	Conclusions	161
3.4	Experimental	163
3.4.1	General experimental	163
3.4.2	Characterization of the Dimers	163
	References	166

List of Figures

Figure 1.	The π -electron densities for a monosubstituted benzene ring with an electron-withdrawing group ($W = \text{CH}_3$) and an electron-donating group ($D = \text{CH}_3$) for the ground state and the first excited state.	5
Figure 2.	A plot of the rate constant of electron transfer, $\log k_{ET}$, for converting the radical pair to the ion pair as a function of the oxidation potential, E_{OX} , of the 1-naphthylmethyl radical.	11
Figure 3.	A plot of the rate of electron transfer, k_{ET} , for converting the radical pair to the ion pair as a function of the oxidation potential, E_{OX} , of the benzylic radical.	38
Figure 4.	A plot of % conversion vs. time for the photolysis of the indanyl esters 6b,c and 3-methoxy benzyl acetate in aqueous dioxane.	73
Figure 5.	An ORTEP representation of the <i>R,R</i> form of the racemic dimer 29a	144
Figure 6.	400 MHz ^1H NMR spectra of the <i>meso</i> dimer 30a at a) +45 $^\circ\text{C}$; b) +25 $^\circ\text{C}$; and c) -40 $^\circ\text{C}$	146
Figure 7.	The room temperature 400 MHz ^1H NMR (CDCl_3) spectrum of the racemic dimer, 29a	154
Figure 8.	a) A 65 MHz ^{13}C NMR solution spectrum of the racemic dimer, 29a . b) A MAS ^{13}C NMR spectrum from the solid state for the racemic dimer, 29a	156

List of Tables

Table 1.	Quantum Yields for the Formation of 1 Naphthylmethyl Ether from the Photolysis of Substituted 1 Naphthylmethyl Esters in Methanol at 25 °C	9
Table 2.	Product Yields for the Photolysis of Esters 1a-f and 2a-f in Methanol.	20
Table 3.	Photophysical Properties of Esters 1a-f , 2a-f and Alcohols 7a-f in Methanol.	26
Table 4.	Product Yields for the Esters 1 and 2 in Methanol with the Quencher, 2,3-Dimethylbutadiene.	28
Table 5.	Values of k_{11} and F_{ox} for the Radical Pair Generated in the Photolysis of Esters 1a-f	34
Table 6.	Product Yields for the Photolysis of Esters 1g-i and 2g-i	45
Table 7.	Oxidation Potentials and Electron-Transfer Rate Constants for Esters 1g-j	49
Table 8.	Product Yields for the Photolysis of Esters 1j and 2j in Methanol.	54
Table 9.	Product Yields for the Photolysis of Esters 3 and 4 in Methanol	64
Table 10.	Product Yields for the Photolysis of Esters 5a-c and 6a-c in Methanol.	67
Table 11.	Calculated Values of k_{ij} for Esters 6a-c and k_{11} for Esters 5a-c	68
Table 12.	Emission Properties of the Substituted indanyl Alcohols 13a-c and Esters 5a-c and 6a-c in Methanol.	71
Table 13.	Photophysical Data for the Carbonates and Carbamates.	117
Table 14.	Coalescence Temperatures and Kinetic Data for the <i>Meso</i> Dimer.	148
Table 15.	Select Geometrical Data for Conformers of the <i>Meso</i> Dimer.	151
Table 16.	Select Geometrical Data for Conformers of the Racemic Dimer.	158

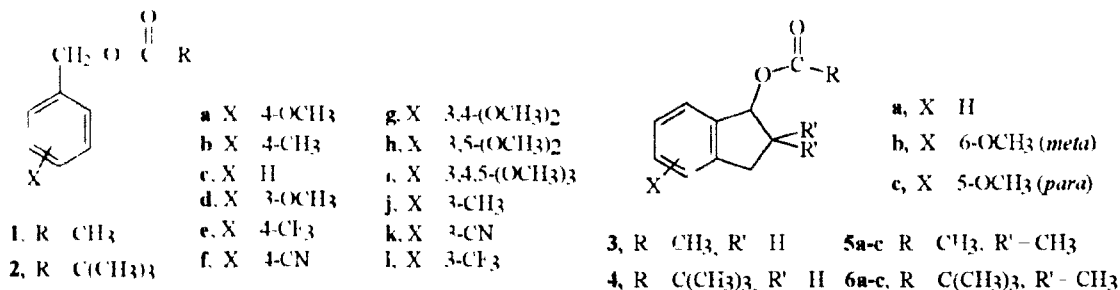
List of Schemes

Scheme 1.	Proposed Mechanism for the Photoreaction of Benzyl Acetates	6
Scheme 2.	Proposed Mechanism for the Photolysis of <i>N</i> -Methylmethyl Esters.	10
Scheme 3.	General Mechanism for Photolysis of a Benzylic Ester	15
Scheme 4	Possible Reaction Pathways to the Singlet and Triplet Excited States of a Benzylic Ester in the Presence of a Quencher.	25
Scheme 5.	Simplified Mechanism for the Photoreaction of Benzylic Esters 1a-f and 2a-f	30
Scheme 6.	Pathways for the Decarboxylation of Carbamic Acids	126

Abstract

Photolysis of a benzylic compound with a leaving group can give products from radical intermediates, ionic intermediates or both. The factors that control the partitioning between these intermediates are not well understood. In fact, different mechanisms have been proposed for the formation of these two intermediates. If the mechanism and factors controlling the reactivity of benzylic substrates were known, then systems could be designed to give specific products. One application is in protecting group chemistry, a functional group could be protected with a benzylic substrate that has been designed to give products exclusively from either ionic or radical intermediates.

Benzylic esters were chosen for study because upon photolysis they give mixtures of products. Esters **1-6** were studied to determine the effect of the following structural variations on product distribution: substituents on the aromatic ring, the R group, and conformational mobility.



The proposed mechanism is homolytic cleavage from the singlet excited state to give a radical pair, a benzylic radical and an acyloxy radical. The radical pair then partitions between two pathways: decarboxylation of the acyloxy radical followed by coupling or electron transfer between the radical pair to give the ion pair. Heterolytic cleavage to give ion pairs directly is, at most, a minor pathway. Substituents changed product ratios by changing the oxidation potential of the benzylic radical and thus the rate of electron transfer. The R group changed the rate of decarboxylation.

The major effect of substituents on the photochemistry of the conformationally restricted esters, **3-6**, was also changing the oxidation potential of the benzylic radical. However, quantum yield studies showed that the substituents also have an electronic effect and can increase or decrease the efficiency of homolytic cleavage. Comparison of the results of esters **1** and **2** with those for **3-6** revealed a third effect of substituents. In a benzylic ester, where the bond that is cleaving is conformationally mobile, substituents can also alter the population of ground-state conformers and change quantum yields of reaction.

The photochemistry of 1-naphthylmethyl phenyl and benzyl carbonates and carbamates was also studied. Again, the mechanism was homolytic cleavage to give a radical pair. The important competing pathways were decarboxylation and electron transfer.

List of Abbreviations and Symbols Used

aq	aqueous
anal.	analysis
Ar	aromatic
calcd	calculated
δ	chemical shift
DMSO	dimethylsulfoxide
E_{ox}	oxidation potential
ϵ	molar extinction coefficient
eV	electron volt
GC	gas chromatography
GC/FID	gas chromatograph with a flame ionization detector
HPLC	high performance liquid chromatography
IR	infrared
J	coupling constant
k_{α}	rate constant of α -cleavage
k_{CO_2}	rate constant of decarboxylation
k_{D}	rate constant of diffusion
k_{ET}	rate constant of electron transfer
k_{F}	rate constant of fluorescence
k_{γ}	rate constant of hydrogen atom abstraction
k_{I}	rate constant of heterolytic cleavage

k_{IR}^{IP}	rate constant of internal return from the ion pair
k_{IR}^{RP}	rate constant of internal return from the radical pair
k_{ISC}	rate constant of intersystem crossing
k_R	rate constant of homolytic cleavage
λ	reorganization energy
λ_{MAX}	wavelength of maximum absorption
LCAO	linear combination of atomic orbitals
MO	molecular orbital
MS	mass spectrometry
NMR	nuclear magnetic resonance
Ph	phenyl
Φ	quantum yield of reaction
ϕ	state efficiency
S_0	ground state
S_1	singlet excited state
SCE	saturated calomel electrode
τ_S	singlet lifetime
τ_T	triplet lifetime
T_1	triplet excited state
THF	tetrahydrofuran
TLC	thin layer chromatography
UV	ultraviolet

Acknowledgements

I sincerely thank Dr. James A. Pincock for his guidance during my studies at Dalhousie. I appreciate the numerous opportunities he has provided to enrich my education.

I thank my coworkers, especially Susan Swansburg and Sandra Nevill, for their input and constructive criticism of papers, posters and talks over the past few years. I also thank them for making life in the lab interesting.

Finally, I thank my husband Ian for his support and especially for his patience and understanding during preparation of this thesis.

Financial support was provided by the Faculty of Graduate Studies Dalhousie University, Department of Chemistry Dalhousie University, The Natural Sciences and Engineering Research Council of Canada and the Killam Foundation.

Chapter 1

The Photochemistry of Benzylic and Indanyl Esters

1.1 Introduction

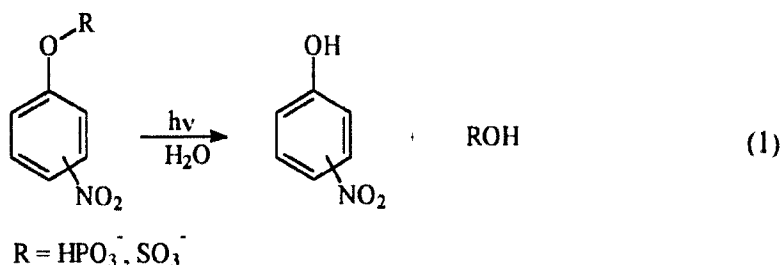
A solvolysis reaction is a type of substitution reaction in which a leaving group is replaced by the solvent. When the leaving group is attached to a benzylic carbon atom the solvolysis can proceed by either an S_N1 or S_N2 mechanism. The S_N1 mechanism is favored for benzylic compounds that lead to the formation of stabilized cations, for instance when the ring is substituted with electron-donating groups. The relationship between substituents on the aromatic ring and the rate of solvolysis can be correlated using the well-known Hammett equation.¹ For example, the rate of solvolysis of cumyl chlorides in ethanol correlates with σ^+ values and gives a Hammett ρ value of -4.54.¹ The large value of ρ indicates the reaction is very sensitive to substituents and the negative sign indicates that the reaction is facilitated by electron-donating groups. For these reactions a *para* methoxy compound would undergo solvolysis four orders of magnitude faster than a *meta* methoxy substituted compound. The kinetics, structural effects, and mechanisms of solvolysis reactions have been discussed elsewhere in greater detail.^{2,3}

As will be discussed, the reactions of benzylic substrates with leaving groups have also been studied photochemically. To be photoreactive, the bond connecting the leaving group to the benzylic carbon must be lower in energy than the difference in energy between the ground and excited states of the benzylic substrate. This condition is satisfied for many groups, such as esters, that do not readily undergo ground-state

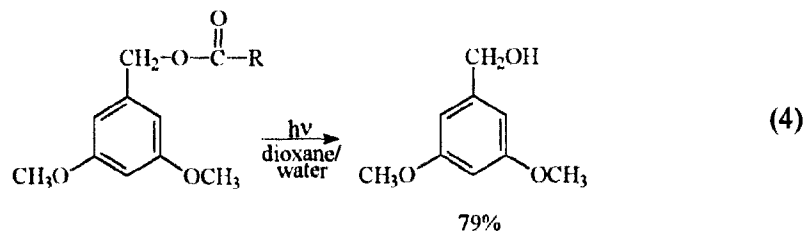
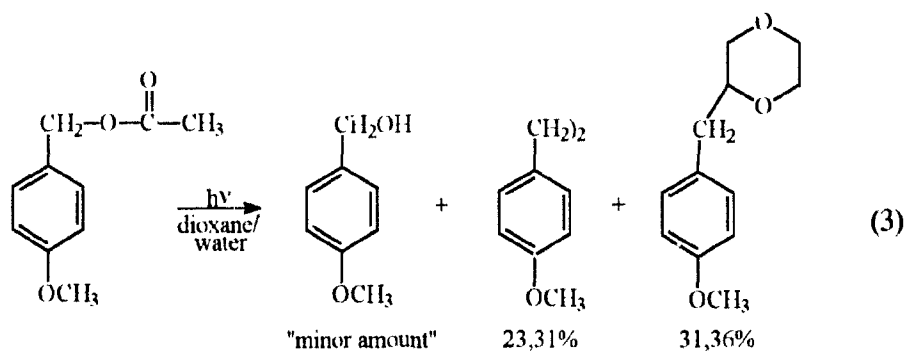
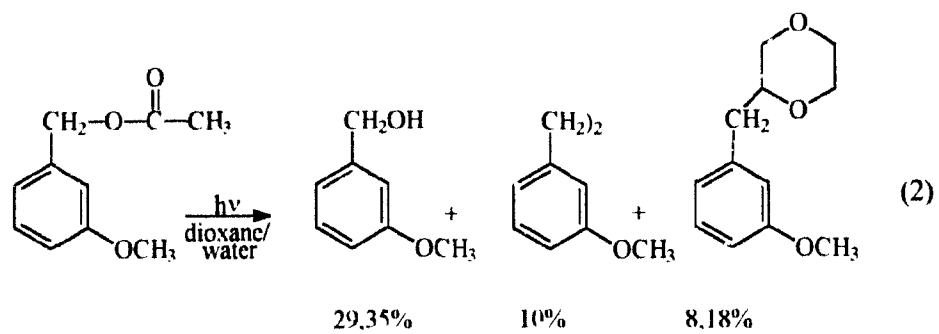
solvolyses. Photochemical cleavage of the bond between the benzylic carbon and the leaving group can give an ion pair (photosolvolysis), radical pair, or both.

Substituents on the aromatic ring have been shown to influence the efficiency of photosolvolysis reactions and affect the partitioning between ion pair and radical pair intermediates in cases where both are formed. These substituent effects are not well understood.

One of the earliest studies that illustrated the effects of aromatic substituents on a photosolvolysis reaction was by Havinga *et al.*⁴ in 1956 on the photohydrolysis of isomeric nitrophenyl phosphate and sulphate esters, eq 1. Upon irradiation, the esters hydrolysed to nitrophenol and the corresponding inorganic acid. In the excited state hydrolysis was enhanced by an electron-withdrawing group in the *meta* position. However, ground-state hydrolysis is enhanced by an electron-withdrawing group in the *para* position because the intermediate phenoxy anion is stabilized by resonance delocalization of the negative charge.



Zimmerman and Sandel's⁵ studies on the photolysis of methoxy substituted benzyl acetates in aqueous dioxane, eqs 2-4, provide another example of photoreaction

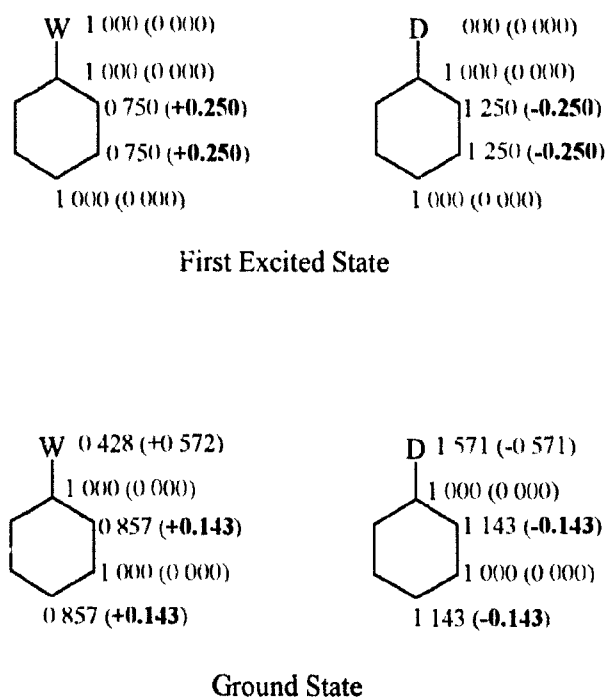


substituent effects. Benzyl alcohol, a photosolvolysis product, was formed from trapping the intermediate benzylic cation by the nucleophilic solvent, water. In addition, products from radical intermediates, benzylic dimers and solvent coupling products, were also formed. The yields of the products are given in eqs 2-4.⁶ The yield of photosolvolysis product, benzyl alcohol, was greater for the *meta* methoxy substituted isomer than for the *para* methoxy substituted ester. The only product reported from photolysis of 3,5-dimethoxybenzyl acetate was 3,5-dimethoxybenzyl alcohol, eq 4. As well, the *meta* methoxy isomer reacted more efficiently ($\Phi_R = 0.13$) than the *para* methoxy isomer ($\Phi_R = 0.016$). Based on ground-state reactions one would expect the *para* methoxy isomer to give a higher yield of ion-derived product and react more efficiently than the *meta* isomer because the *para* methoxy substituent stabilizes the intermediate benzylic cation.

Again, excited-state substituent effects are contrary to ground-state expectations. To rationalize the difference between ground-state and excited-state substituent effects, Zimmerman used simple Hückel LCAO MO π -electron densities. The calculated π -electron densities for a benzene ring with an electron-withdrawing group (W) and an electron-donating group (D) for both the ground state and the first excited state are shown in Figure 1.⁵ As expected, an electron-withdrawing group in the ground state results in decreased electron densities at the *ortho* and *para* positions while an electron-donating group gives increased electron density at these positions. In the excited state an electron-withdrawing group decreases electron density at the *ortho* and *meta* positions while an electron-donating group increases electron density at

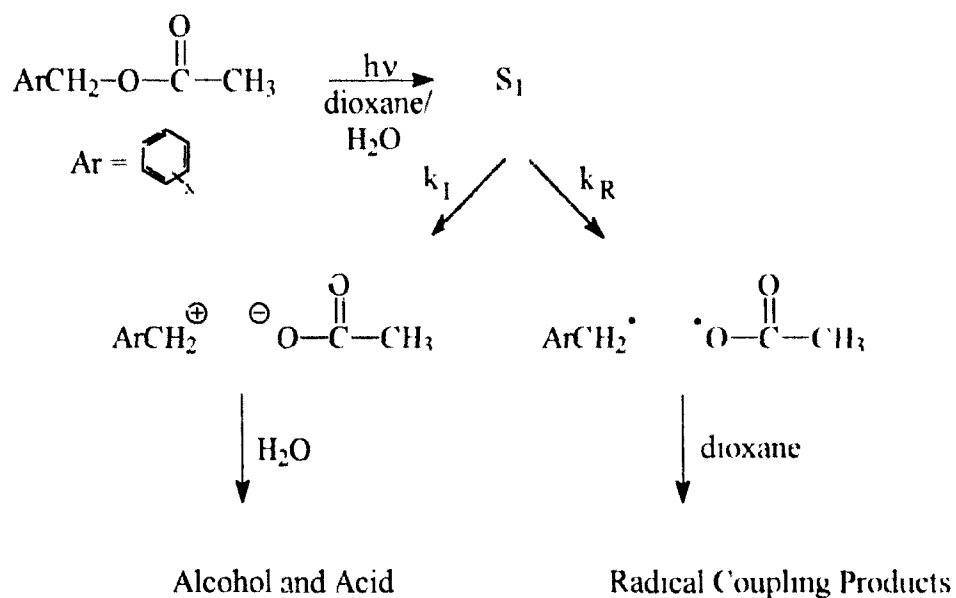
these positions. The ability of a substituent in the excited state to alter electron density at the *meta* positions was termed the "*meta* transmission effect" or more simply the *meta* effect.⁵

Figure 1. The π -electron densities for a monosubstituted benzene ring with an electron-withdrawing group ($W = \text{CH}_2^+$) and an electron-donating group ($D = \text{CH}_2^-$) for the ground state and the first excited state. The numbers in brackets are the charges.



Based on the above observations, Zimmerman proposed a mechanism for the photo-reaction of benzyl acetates (Scheme 1).⁵ Irradiation gives the singlet excited state of the ester, S_1 , which cleaves heterolytically, with a rate constant k_1 , to give

Scheme 1. Proposed Mechanism for the Photoreaction of Benzyl Acetates.

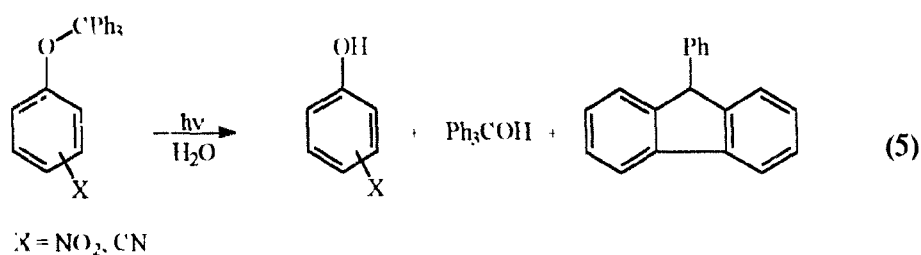


ionic intermediates and homolytically, with a rate constant k_R , to give radical intermediates. The ionic intermediates are trapped by water to give solvolysis products, an alcohol and a carboxylic acid, while the radical intermediates couple to give dimers and coupling products between the benzylic radical and dioxane.

The product ratios (% yield benzyl alcohol / % yield radical products) are controlled by the ratio of the rate constants (k_I/k_R) for forming the intermediate ion pair and radical pair. Photolysis of the *meta* methoxy substituted ester gives more benzyl alcohol than the *para* methoxy substituted one because heterolytic cleavage is facilitated by the presence of the *meta* methoxy group due to the *meta* effect. When

two *meta* methoxy groups are present the rate constant for heterolytic cleavage is increased such that homolytic cleavage can no longer compete and only the photosolvolysis product is observed, eq 4.

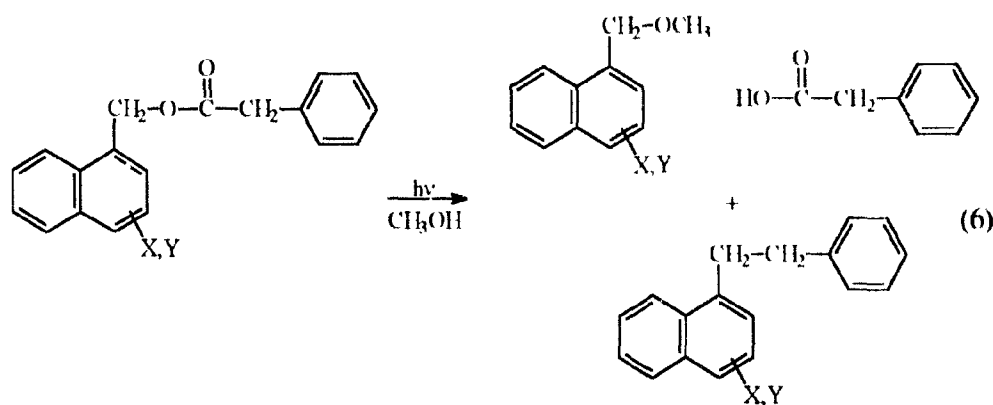
To test the generality of the *meta* effect, Zimmerman *et al.*⁷ studied the effect of electron-withdrawing groups, NO₂ and CN, on the photohydrolysis of phenyl trityl ethers, eq 5. The intermediate in the reaction is a phenoxide anion. Consistent with the prediction of the *meta* effect the ethers were more reactive when the electron-withdrawing group was *meta*.



Since Havinga⁴ and Zimmerman's^{5,7} work, there have been many observations of both increased photoreactivity of *meta* substituted benzylic compounds and increased yields of ion-derived products. For example, Wan *et al.*⁸ found that *meta* methoxy substituted benzyl alcohols photodehydroxylated more efficiently than the *para* methoxy isomer. *Meta* substituents were also found to be more electron donating than the corresponding *para* substituents for the photohydration of styrenes.⁹ However, there are also studies that do not support the *meta* effect. Givens *et al.*¹⁰ studied substituent effects on the photosolvolysis of benzyl phosphates and found a normal ground-state order for reactivity. The *para* substituted compound was the most

reactive. McKenna *et al.*¹¹ observed decreased yields of ionic cleavage for the photolysis of 3,5-dimethoxybenzyl ammonium salts.

Studies by Pincock and DeCosta¹² on the photoreaction of substituted 1-naphthylmethyl esters of phenylacetic acid, eq 6, also do not support the argument of the *meta* effect. Products were formed from both an intermediate ion pair and radical pair. Trapping of the ion pair by methanol gave the photosolvolysis products



1-naphthylmethyl ether and phenylacetic acid. The initial radical pair is a 1-naphthylmethyl radical and a phenylacetyloxy radical. The phenylacetyloxy radical decarboxylates to give a benzylic radical that couples with the 1-naphthylmethyl radical.

Quantum yields, ϕ , for formation of the 1-naphthylmethyl ether were measured. The assumption was made that the cation was formed exclusively by heterolytic cleavage and the quantum yields were used to calculate rate constants for cation formation, k_1 (Table 1). The results did not support the argument of the *meta*

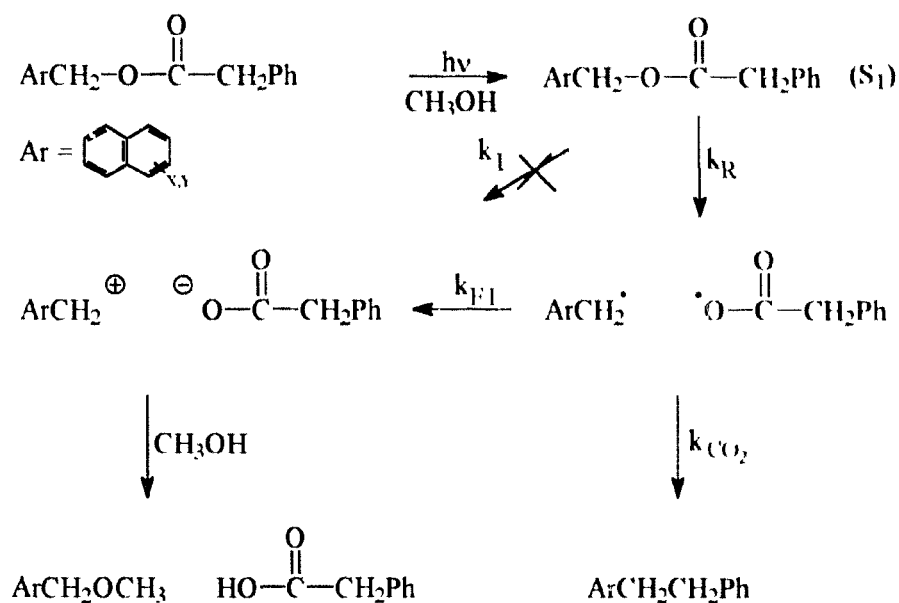
Table 1. Quantum Yields for the Formation of 1-Naphthylmethyl Ether from the Photolysis of Substituted 1-Naphthylmethyl Esters in Methanol at 25 °C.¹³

Ester	ϕ ether	τ_1 (ns)	$k_1 \times 10^5 \text{ s}^{-1}$	%ether	$\log k_{ET}$	E_{OX} (V)
H	<0.005	49	<1.0	84	10.4	0.47
3-OCH ₃	0.008	11	7.3	31	9.44	0.52
4-OCH ₃	0.017	7.3	23	74	10.15	0.04

effect with $k_1^S(4\text{-CH}_3\text{O}) > k_1^S(3\text{-CH}_3\text{O})$. Neither were their results consistent with a normal ground-state order because $k_1^S(3\text{-CH}_3\text{O}) \gg k_1^S(\text{H})$. Also, these rate constants did not agree with the product distributions observed because the highest yield of ether was observed for the unsubstituted ester (smallest rate constant) and the lowest yield for the 3-OCH₃ substituted ester.

To rationalize their observations Pincock and DeCosta proposed the mechanism shown in Scheme 2. The singlet excited state of the 1-naphthylmethyl ester cleaves homolytically to give a radical pair, the 1-naphthylmethyl radical and the phenylacetyloxy radical. The radical pair then partitions between two pathways. The phenylacetyloxy radical can decarboxylate and then couple with the 1-naphthylmethyl radical to give product or the radical pair can form the ion pair by electron transfer. The important pathway for forming the ion pair is the electron-transfer pathway and not heterolytic cleavage. The substituents on the aromatic ring change the rate constant of electron transfer, k_{ET} , for converting the radical pair to the ion pair, by changing the oxidation potential, E_{OX} , of the 1-naphthylmethyl radical. The rate of decarboxylation is constant and the yield of ion-derived product varies as a function

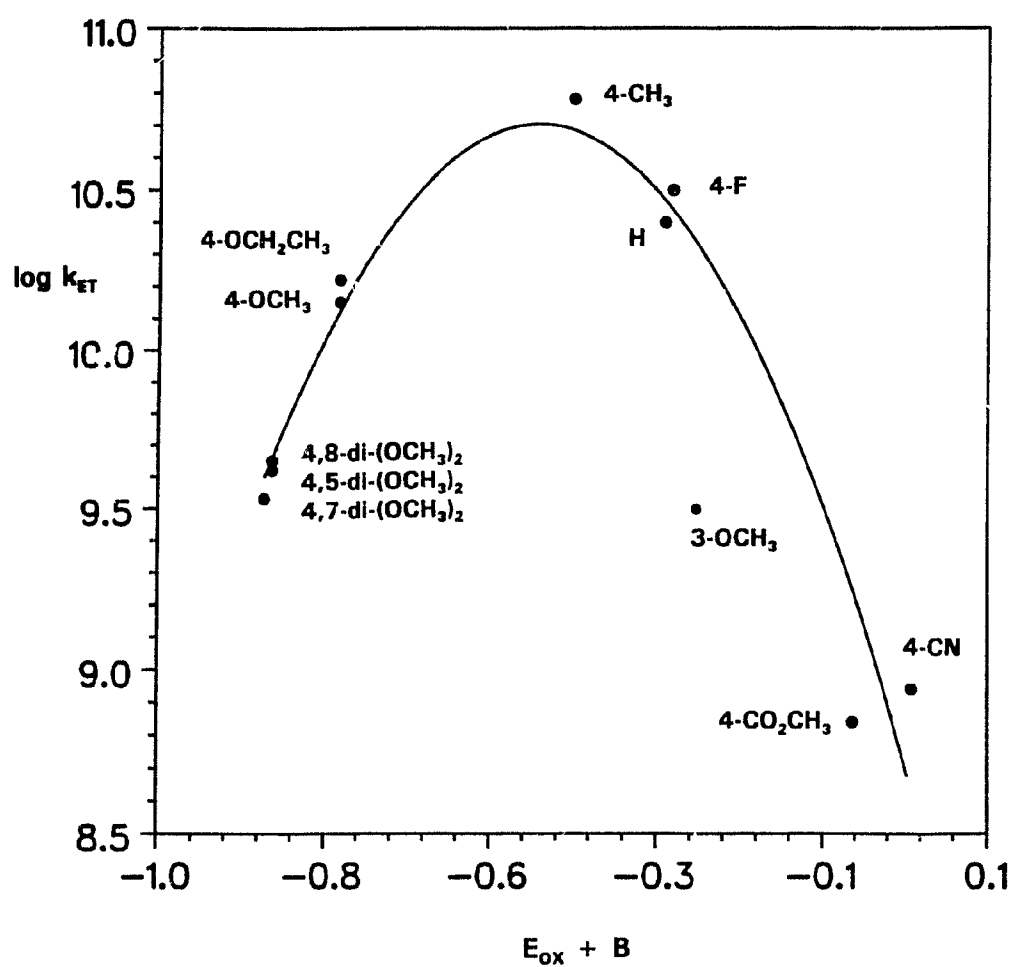
Scheme 2. Proposed Mechanism for the Photolysis of 1-Naphthylmethyl Esters.



of E_{OX} . The plot of $\log k_{\text{ET}}$ vs. E_{OX} , shown in Figure 2, is parabolic. The electron-transfer rate constant increases as the oxidation potential of the 1-naphthylmethyl radical decreases, however, a point is reached where the rate constant for electron transfer decreases although the electron-transfer process is becoming thermodynamically more favourable.

Marcus's¹⁴ theory predicts a parabolic relationship between the free energy of activation (ΔG^\ddagger) for electron-transfer reactions and the free energy for electron transfer, ΔG° , eq 7.

Figure 2. A plot of the rate constant of electron transfer, $\log k_{ET}$, for converting the radical pair to the ion pair as a function of the oxidation potential, E_{OX} , of the 1-naphthylmethyl radical.¹³



$$\Delta G^\ddagger = \frac{Z_1 Z_2 e^2 F}{D r_{12}} + \frac{\lambda}{4} \left(1 + \frac{\Delta G^{o'}}{\lambda} \right) \quad (7)$$

The first term in eq 7 is the gain or loss in electrostatic free energy as the precursor complex is formed. The Z_1 and Z_2 values are the charges on the precursors, e is the electronic charge, F is the ionic strength, D is the dielectric constant of the pure solvent and r_{12} is the distance between the two precursors. If one of the precursors has zero charge the first term will be zero. This will be the case for all of the photoreactions discussed because the electron transfer is occurring between in-cage radical pairs.

The second term is the parabolic one where λ is the reorganizational energy, which accounts for the energy changes necessary for the reaction to reach the transition state. It includes bond shortening/lengthening, torsional motions and solvent reorganization. This term allows radical pairs to have a lifetime in polar solvents. When radical pairs are formed in a polar solvent, exergonic electron transfer to form the ion pairs is not instantaneous because the reorganization energy is a barrier. $\Delta G^{o'}$ is the standard free energy of electron transfer corrected for the separation of the ions, r_{12} , in a solvent of dielectric constant D , eq 8.

$$\Delta G^{o'} = \Delta G^o - \frac{e^2}{D r_{12}} \quad (8)$$

Marcus theory provides an understanding of the factors that control the rate of electron transfer between a donor and an acceptor molecule. The rate of electron

transfer is related to the free energy of activation by eq 9. Combining eqs 7 and 9 gives a relationship between the rate of electron transfer and free energy which is frequently used because of its simplicity. The region where $\log k_{ET}$ decreases with increasing ΔG^\ddagger is called the Marcus inverted region.

$$k_{ET} = A \exp\left(\frac{-\Delta G^\ddagger}{RT}\right) \quad (9)$$

The trend of the ether yields in Table 1, $H > 4-OCH_3 > 3-OCH_3$, is observed because the esters span both the normal and the Marcus inverted region. As the substituent is changed from 3-OCH₃ to H to 4-OCH₃ the oxidation potentials of the 1-naphthylmethyl radicals decrease, thus, k_{ET} should increase. However, k_{ET} is smaller for the 4-OCH₃ substituted ester than for the unsubstituted ester because it is in the Marcus inverted region. Thus, the ether yield is maximized for the unsubstituted ester.

Zimmerman's results⁵ can also be explained by Marcus theory. All three of the benzylic esters studied could be in the inverted region and the rate constants for electron transfer would decrease in the following manner: $k_{ET}(4-OCH_3) < k_{ET}(H) < k_{ET}(3-OCH_3)$. This is consistent with the observation that the 3-OCH₃ gave the highest yield of ether product. Inclusion of the heterolytic cleavage may not be necessary to explain Zimmerman's results.

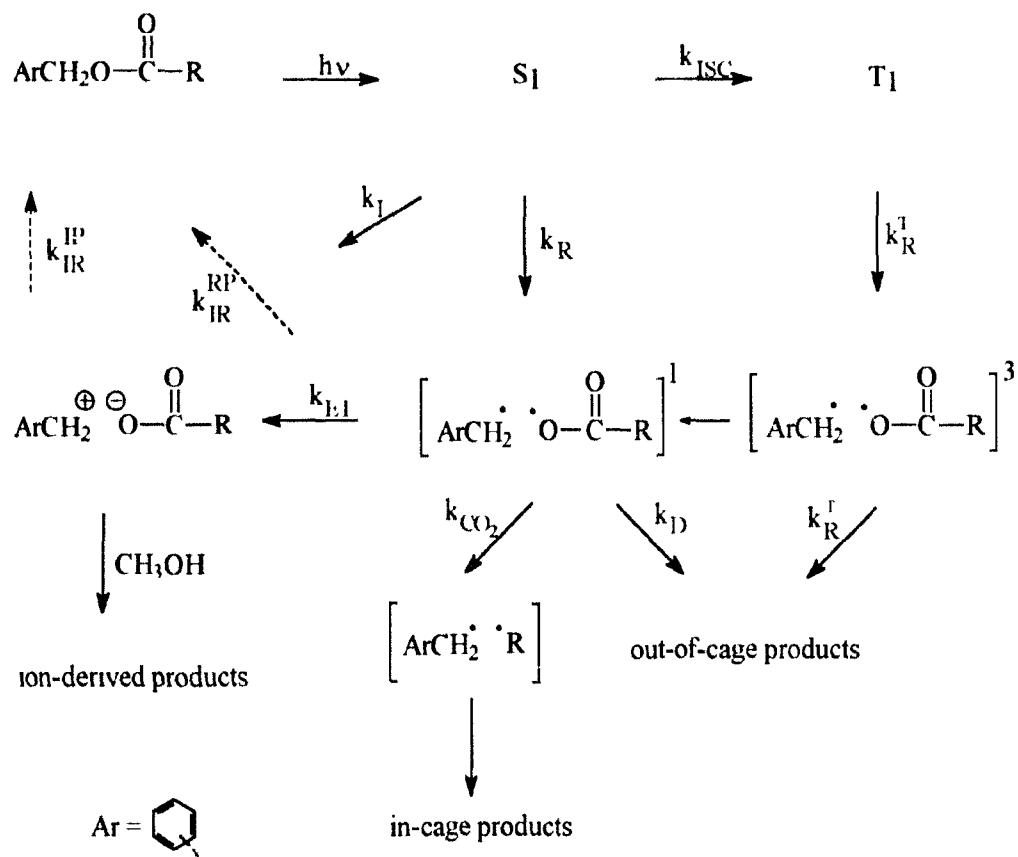
Two different mechanisms have been proposed for the photoreaction of two very similar substrates. The two competing reaction pathways in the mechanism proposed by Zimmerman and Sandel⁵ for the photolysis of benzylic esters are

homolytic cleavage and heterolytic cleavage from the excited singlet state. However, the important competition in the mechanism proposed by Pincock and DeCosta¹² is between ground-state reactions that occur after the excited-state cleavage. The above two proposals are mechanistic extremes and it is possible that for some substrates the mechanism could be a combination of these. A more detailed discussion of the possible reaction pathways in a benzylic photoreaction follows.

The initial event of a benzylic ester photoreaction is the absorption of light by the aromatic chromophore inducing a $\pi\text{-}\pi^*$ transition forming the excited singlet state, S_1 . Besides fluorescence and internal conversion, the excited singlet state can decay by the pathways shown in Scheme 3. For benzyl acetate, the energy of the excited singlet state is on the order of 444 kJ/mol (106 kcal/mol) above the ground state. Thus, the energy provided by excitation is sufficient to induce cleavage of the benzylic C-O bond that has a bond strength of about 272 kJ/mol (65 kcal/mol) for esters.¹⁵ The singlet excited state can cleave homolytically, k_R , to generate an in-cage radical pair, the benzylic radical and the acyloxy radical. The acyloxy radical can decarboxylate, in-cage or out-of-cage, to form an alkyl radical that couples with a benzylic radical. The in-cage radical pair can also diffuse apart and dimerize or form other out-of-cage radical coupling products. The in-cage radicals can also recombine in a process called internal return, k_{IR}^{RP} .

The excited singlet state can also cleave heterolytically, k_I , to give an ion pair that is trapped by the nucleophilic solvent. As with the radical pairs, the ion pairs can recombine, k_{IR}^{IP} . The ion pairs can also be formed by electron transfer between the

Scheme 3. General Mechanism for Photolysis of a Benzylic Ester.



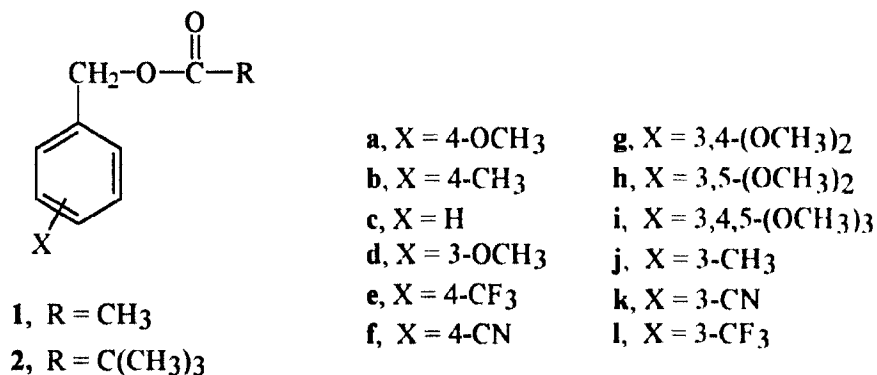
radical pair, k_{IT} .

In addition to cleaving, the excited singlet state can intersystem cross, k_{ISC} , to form the triplet state, T_1 . The triplet excited state is still energetic enough (335 kJ/mol, 80 kcal/mol for unsubstituted benzene) to cleave the C-O bond. This process would generate triplet radical pairs that can combine to give the same radical coupling products as the out-of-cage singlet radical pairs. The triplet radical pairs

cannot undergo electron transfer to form the ion pair, which must be a singlet.

The final product ratios will be a reflection of the various rate constants involved in these processes. If all the rate constants were known predictions could be made about product ratios. This chapter describes the studies of many aspects of the benzylic ester photoreaction. This research assessed the importance of many of the reaction pathways and clarified the role substituents have on determining product ratios and reaction efficiencies.

The results presented in Chapter 1 are divided into three sections, 1.2-1.4. The first section, 1.2, discusses the photochemistry of the benzyl acetates, **1a-f**, and benzyl pivalates, **2a-f**.^{16,17} This work is an extension of the initial work done by Zimmerman and Sandel⁵ on benzylic ester photochemistry. The substituents **a-f** were



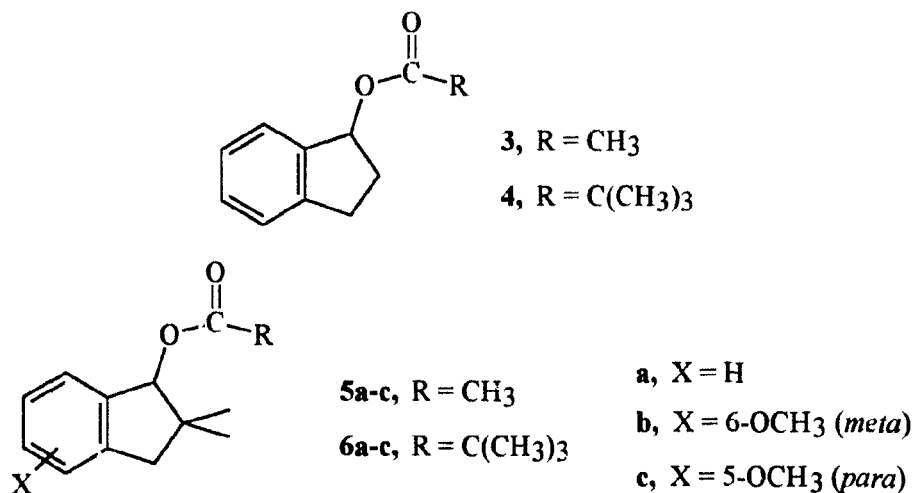
chosen such that the incipient benzylic radicals spanned a wide range of oxidation potentials allowing the importance of the electron-transfer pathway to be explored.

Both the acetate and pivalate esters were studied because changing the rate of decarboxylation of the resulting acyloxy radicals is a good probe for ground-state

reactions that occur after the initial excited-state homolytic cleavage. Also, the importance of triplet reactivity was determined by doing triplet quenching studies.

The results of the photochemistry of the multiple methoxy substituted benzyl acetates **1g-i** and benzyl pivalates **2g-i** are discussed in section 1.3. These compounds were studied to determine the importance of the heterolytic cleavage pathway. According to the argument of the *meta* effect, heterolytic cleavage should be enhanced for these esters. Also the photochemistry of several *meta* substituted benzyl acetates, **1j-l**, was studied and will be discussed.

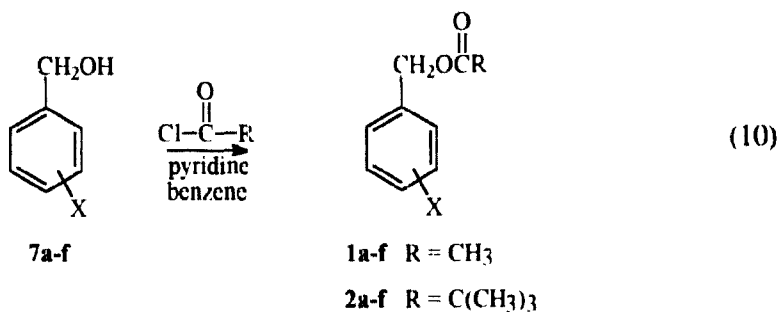
The results of the photochemistry of the indanyl esters, **3**, **4**, **5a-c** and **6a-c** are discussed in section 1.4. The C-O bond in these esters is rigid and any effects the substituents have on the conformation of the C-O bond are eliminated. This allows the electronic effects of the substituents to be analysed independently of conformational effects. Experimental details and compound characterizations are given in the experimental section, 1.5.



1.2 Results and Discussion on the Photochemistry of the Monosubstituted Benzyl Acetates 1a-f and Pivalates 2a-f

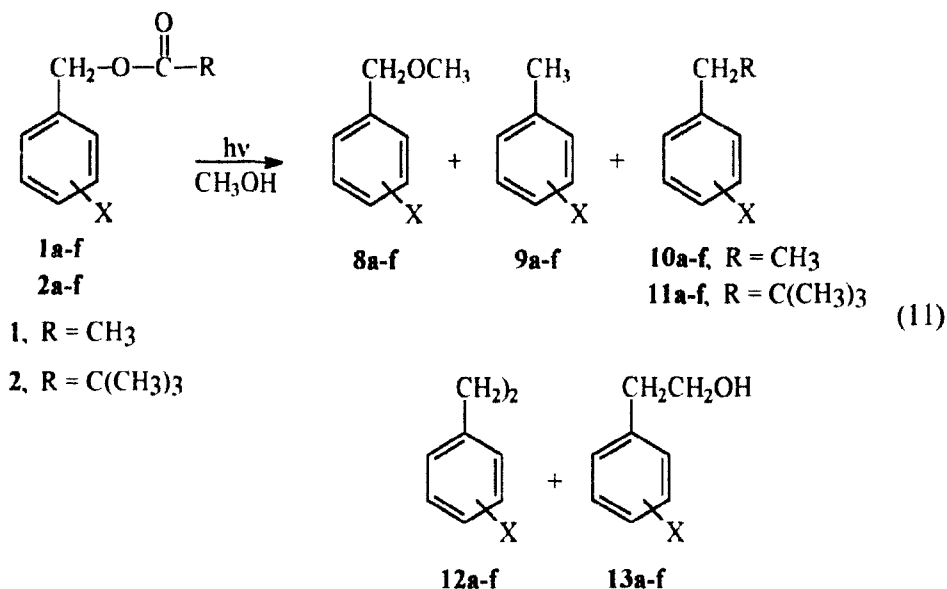
1.2.1 Products and Yields on Direct Irradiation of 1a-f and 2a-f

Esters **1a-f** and **2a-f** were prepared by reacting the corresponding alcohols, **7a-f**, which were either commercially available or prepared by standard methods, with acid chloride, eq 10. The esters were photolysed in methanol and the progress of the



reaction was monitored by GC or HPLC. The photolysis was stopped after most of the ester had reacted (>90%) and the products were isolated by chromatography. Further details concerning synthesis and photolysis of the esters can be found in the experimental section, 1.5.

The products isolated from the reaction mixture are the five benzylic products shown in eq 11. The products were identified by spectroscopic methods (NMR, MS). No attempt was made to isolate or quantify the low molecular weight carboxylic acids, acetic (from **1**) and pivalic (from **2**), which were formed along with the ethers, **8**. A quantitative photolysis was done to determine the yields of these photoproducts, which are given in Table 2. Complete details are given in the experimental section.



The products shown in eq 11 can be rationalized in terms of an intermediate ion pair and radical pair. The methyl ether, **8**, is the only benzylic product formed from the ion pair. The ether yields in Table 2 agree with Zimmerman's observations,⁵ eqs 2-4. The yield of ether is higher for 3-methoxybenzyl acetate (32%) than for the 4-methoxy substituted isomer (1.7%). However, the yield of ether drops substantially for the pivalate esters, **2**, relative to the corresponding acetate esters, **1**. The yield of ether is only 10% for the 3-methoxy substituted pivalate ester. The excited singlet state behaviour of the acetate and the pivalate esters is essentially the same, as will be shown in section 1.2.2. Therefore, the differences in ether yields between the acetate and pivalate esters cannot be due to differences in excited-state cleavage but must be a consequence of processes that occur after excited-state bond cleavage. The obvious

Table 2. Product Yields^a for the Photolysis of Esters **1a-f** and **2a-f** in Methanol.

Esters, 1 , 2	% 8 ether	% 9 toluene	% 10/11 ^b coupled	% 12 dimer	% 13 alcohol	% Total
1a , X = 4-OCH ₃	1.7 ^c	nd	14	48	25	89
2a	nd	13	48	24	4	89
1b , X = 4-CH ₃	8 ^c	2	14	52	21	97
2b	nd	14	53	31	nd	98
1c , X = H	26	nd	19	23	26	94
2c	5	14	45	18	6	88
1d , X = 3-OCH ₃	32	nd	14	38	12	96
2d	10	17	46	20	nd	93
1e , X = 4-CF ₃	1.0 ^c	14	24	17	nd	56
2e	nd	38	34	13	nd	85
1f , X = CN	0.3 ^c	5	16	67	5	95
2f	nd	16	43	32	nd	91

^aThe numbers represent the yield of the benzylic fragment based on the amount of reacted starting material. Therefore, the molar yield of the dimer, **12**, is multiplied by 2. Estimated error based on reproducibility of injections and multiple runs is about $\pm 2\%$. However, note footnote c.

^bThis is the product that results from coupling after decarboxylation. For the acetate esters, **1**, the product is **10** and for the pivalate esters, **2**, the product is **11**.

^cThe yields of the methyl ether from the acetate esters are important for analyzing the results. For cases where this yield is low, analyses were done more carefully and the estimated error is $\pm 0.2\%$.

nd, Not determined but $< 0.5\%$.

difference (Scheme 3, p 15) is the rate of decarboxylation (k_{CO_2}) of the pivaloyloxy radical, $(\text{CH}_3)_3\text{CCO}_2\cdot$, compared to the acetyloxy radical, $\text{CH}_3\text{CO}_2\cdot$. Decarboxylation of the pivaloyloxy radical is faster because it gives a *tert*-butyl radical whereas decarboxylation of the acetyloxy radical gives the less stable methyl radical. Rate constants for decarboxylation of these radicals have been determined previously;¹⁸ $k_{\text{CO}_2} = 1 \times 10^9 \text{ s}^{-1}$ for the acetyloxy radical and $11 \times 10^9 \text{ s}^{-1}$ for the pivaloyloxy radical.

Products **9-13** are formed from the radical pair. The dimer, **12**, is formed from coupling of two benzylic radicals and 2-arylethanol, **13**, is formed from coupling of a benzylic radical with a hydroxymethyl radical. Clearly, these products can only arise after the initially formed radical pair has diffused apart, *i.e.*, out-of-cage products. For most acetates (except **1c**, X = H, and **1d**, X = 3-OCH₃, where the ion pair is a more important intermediate), the sum of the yields for these two out-of-cage products, **12** and **13**, is over 70%. Clearly, diffusional escape from the solvent cage is important. This is expected based on the rate constants for diffusion and decarboxylation. A rate constant for diffusional escape of the radical pair of $6 \times 10^9 \text{ s}^{-1}$ can be calculated using the simple diffusional escape¹⁹ equation assuming 6 Å spheres in a solvent like methanol of viscosity 5.5 mpoise. Diffusional escape is six times faster than decarboxylation of acetyloxy radical, $k_{\text{CO}_2} = 1 \times 10^9 \text{ s}^{-1}$, thus out-of-cage processes dominate. The yields of dimer for the pivalate esters show that out-of-cage radical reactions are less important. Decarboxylation of the pivaloyloxy radical ($(\text{CH}_3)_3\text{CCO}_2\cdot$), $k_{\text{CO}_2} = 11 \times 10^9 \text{ s}^{-1}$ is faster than diffusional escape and in-cage processes dominate.

The pathway for formation of the hydroxymethyl radicals, that couple with benzylic radicals to give product **13**, is not certain but for the acetate esters probably occurs by a methyl radical, formed after decarboxylation of the acetyloxy radical, abstracting a hydrogen atom from methanol. This process would be exothermic by ~ 50 kJ/mol (12 kcal/mol). The acetyloxy radical would decarboxylate before it could abstract a hydrogen atom based on a rate constant obtained by laser flash photolysis,²⁰ for hydrogen atom abstraction from ethyl ether by the ((4-methoxyphenyl)acyl)oxy radical ($\text{ArCO}_2\cdot$) of $< 10^6 \text{ M}^{-1}\text{s}^{-1}$. Decarboxylation will be preferred to hydrogen atom abstraction from the solvent because the decarboxylation is two orders of magnitude faster than the hydrogen atom abstraction. Also, benzylic radicals do not efficiently abstract hydrogen atoms from methanol because the process is endothermic by ~ 29 kJ/mol (6 kcal/mol), as calculated from bond dissociation energies,¹⁵ and dimerization dominates.²¹

For the pivalate esters, once the radical pair diffuses, the ratio of dimerization of the benzylic radicals to form **12**, relative to solvent coupling to form **13**, favours **12**. The *tert*-butyl radicals probably abstract hydrogen atoms from the solvent at a slower rate than does the methyl radical. The hydrogen abstraction by the *tert*-butyl radical is exothermic by only ~ 6 kJ/mol (1.4 kcal/mol).¹⁵ For this reason and for steric reasons, the hydrogen abstraction should be slow.

Toluene, **9**, and the coupling product, **10** ($\text{R} = \text{CH}_3$) or **11** ($\text{R} = \text{C}(\text{CH}_3)_3$), can be formed either in-cage after decarboxylation or out-of-cage. For the pivalate esters, products **9** and **11** are probably formed predominantly in-cage because

decarboxylation is faster than diffusion. The ratio of coupling to disproportionation (11/9), is 3.2 ± 0.4 and is essentially substituent independent (ignoring the 4-CF₃ case, 2e, which has a very different and unexplained value of 0.9). For the acetate esters, disproportionation is impossible and coupling to ethylbenzene, 10 (R = CH₃), is the only in-cage product derived from the radical pair. Because decarboxylation is slower than diffusion for the acetyloxy radicals some ethylbenzene is probably also formed out-of-cage.

Using the known decarboxylation rate constants and the product yields given in Table 2 rate constants for diffusion, k_D , and electron transfer, k_{ET} , can be calculated. However, before this can be done it is necessary to determine if triplet-state reactivity is important. If the triplet excited state cleaves, the products formed will be identical to the out-of-cage products from the singlet radical pair, 12-13. Without knowing the rate constants k_{ISC} and k_R^T a quantitative analysis would be extremely difficult, if possible.

Also, in terms of analyzing substituent effects on the relative yield of products derived from the ion pair versus the radical pair, the importance of triplet reactivity is critical. If for one substituent triplet state reactivity is a major pathway ionic intermediates will be less important overall. If for another substituent triplet reactivity is only a minor pathway then the ionic intermediates would be relatively more important and greater yields of ion-derived product would be formed. In this case the enhanced yields of ion-derived product would not be a result of the substituent enhancing the process that forms the ionic intermediates.

1.2.2 Multiplicity of the Reactive Excited State

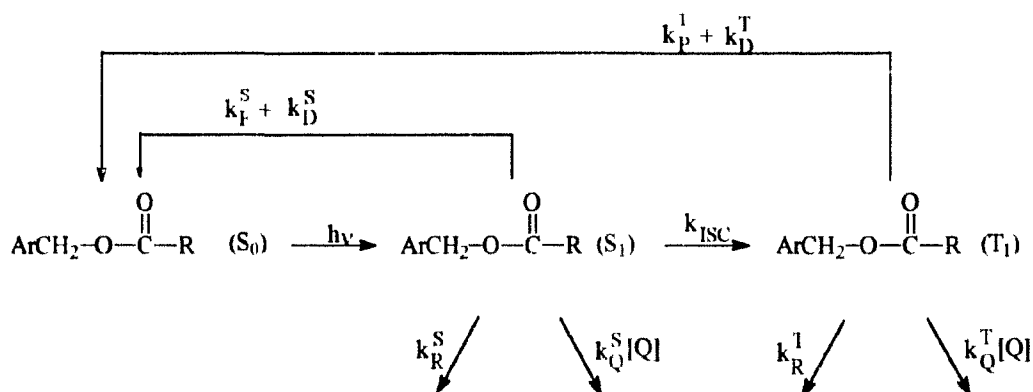
Product yields in benzylic photocleavage reactions are well known²² to depend on the multiplicity (singlet versus triplet) of the reactive excited state. For reactive singlet states both radical pairs and ion pairs can be formed and the radical pairs can form products both in-cage and out-of-cage. Triplet states give triplet radical pairs so only products derived from radical intermediates are possible. Usually out-of-cage processes dominate since in-cage coupling reactions are spin forbidden. Only low yields of out-of-cage radical products were detected for the 1-naphthylmethyl esters¹⁷ (eq 6, p 8). However, for the benzylic esters **1** and **2** the yields of out-of-cage products were substantial suggesting that triplet states might be involved. To test this possibility either triplet sensitization or quenching experiments were necessary.

In a sensitization study the triplet of the compound is formed directly by triplet energy transfer from another chromophore. For benzylic compounds this is very difficult to do as exemplified by Cristol's^{23,24} detailed studies on substituted benzyl chlorides. The triplet energies of benzylic substrates are high and triplet sensitizers of high enough triplet energy to allow unambiguous exothermic triplet energy transfer are not available. Another potential problem is electron transfer sensitization, as has been demonstrated for 1-naphthylmethyl iodide.²⁵ Moreover, sensitizers such as ketones are good hydrogen atom abstractors in their n, π^* triplet excited state and are incompatible with methanol as the solvent.

Because of the problems with sensitization experiments, triplet reactivity was investigated by selective quenching of the triplet state with 2,3-dimethylbutadiene.

The basic idea is shown in Scheme 4 where the rate constants are defined as follows: k_R^S , reaction of the singlet; k_Q^S , quenching of the singlet by quencher Q; k_D^S , radiationless decay of the singlet; k_f^S , fluorescence of the singlet; k_{ISC} , intersystem crossing of the singlet to the triplet; k_R^T , reaction of the triplet; k_Q^T , quenching of the triplet by quencher Q; k_P^T , phosphorescence of the triplet; and k_D^T , radiationless decay of the triplet.

Scheme 4. Possible Reaction Pathways for the Singlet and Triplet Excited States of a Benzylic Ester in the Presence of a Quencher.



Singlet lifetimes, τ_s , and fluorescence quantum yields, ϕ_F , for **1** and **2** were measured²⁶ and are reported in Table 3. For comparison, values for the singlet excited-state properties of the corresponding benzylic alcohols, **7a-f**, were also measured. The k_Q^S values for the pivalate esters, **2**, were determined from Stern-Volmer plots of I_F^0/I_F versus diene concentrations.¹⁷ Combining the singlet lifetimes, τ_s , with the Stern-Volmer slopes, $k_Q^S \tau_s$, gave the k_Q^S values shown in Table 3.

Table 3. Photophysical Properties of Esters **1a-f**, **2a-f** and Alcohols **7a-f** in Methanol.

Ester or Alcohol	$\tau_s \times 10^{9a}$ (s ⁻¹)	ϕ_f^b	$k_Q^s \times 10^{9c}$ (M ⁻¹ s ⁻¹)	$\tau_T \times 10^{6d}$ (s ⁻¹)	$k_Q^T \times 10^{9e}$ (M ⁻¹ s ⁻¹)
1a , X = 4-OCH ₃	6	0.17		3	8
2a	6	0.16	2.3		
7a	7	0.17			
1b , X = 4-CH ₃	22	0.12		0.4	4
2b	23	0.11	2.9		
7b	25	0.15			
1c , X = H	12	0.04		nd ^f	nd
2c	14	0.03	nd ^f		
7c	21	0.07			
1d , X = 3-OCH ₃	<1	<0.01		0.8	3
2d	<1	<0.01	>3		
7d	7	0.16			
1e , X = 4-CF ₃	8	0.11		nd	nd
2e	7	0.11	nd		
9e	13	0.09			
1f , X = CN	11	0.10		>3	>3
2f	10	0.10	11		
7f	11	0.10			

^aBy single photon counting of fluorescence.

^bBy comparison with a value of 0.13 for toluene in methanol.²⁷

^cBy Stern-Volmer quenching studies of fluorescence spectra.

^dBy triplet-triplet absorption using laser flash photolysis.

^eBy Stern-Volmer quenching studies of triplet-triplet absorption.

^fNot determined, see text.

^gNo triplet-triplet absorption observable.

nd, Not determined.

Quenching of the excited singlet states of substituted naphthalene rings by dienes has been reported previously^{28, 29} and is very efficient. The same is true for these substituted benzenes. In agreement with the naphthalene work, there is an electron transfer component to this quenching with the diene as the donor and the aromatic as the acceptor. The rate constant for quenching ($11 \times 10^9 \text{ M}^{-1}\text{s}^{-1}$) approaches the diffusional limit³⁰ in methanol ($18 \times 10^9 \text{ M}^{-1}\text{s}^{-1}$) for the more easily reduced substrate, 4-cyano, **2f**.

The singlet lifetimes and quantum yields of fluorescence are essentially identical for the acetate, **1**, and pivalate, **2**, esters. Changes in the carboxylic acid part of the ester do not affect the excited-state properties of the aromatic chromophore, as was also observed for the 1-naphthylmethyl esters.¹² Therefore, only the triplet values, τ_T and k_Q^T , for the acetate esters have been determined by laser flash photolysis³¹ (LFP) and are given in Table 3. As expected, the τ_T values are in the microsecond range, three orders of magnitude longer than the τ_S values. Therefore, the triplet state can be selectively quenched. The concentration of quencher used to selectively quench the triplet state and not the singlet state was determined using eqs 12 and 13, where %S and %T are the percentages of the excited

$$\%S = \frac{100k_Q^S[Q]}{k_Q^S[Q] + 1/\tau_S} \quad (12)$$

$$\%T = \frac{100k_Q^T[Q]}{k_Q^T[Q] + 1/\tau_T} \quad (13)$$

Table 4. Product Yields for the Esters **1** and **2** in Methanol with the Quencher, 2,3-Dimethylbutadiene.

Ester	[Q] × 10 ¹ mol/L	%T	%S	%8	%9	%10/11	%12	%13
1a , X = 4-OCH ₃	0			2	1	14	48	25
	1.0	96	0.5	2	1	13	20	30
2a , X = 4-OCH ₃	0			nd	13	48	23	4
	1.0	96	0.5	nd	10	35	20	6
1b , X = 4-CH ₃	0			8	2	14	52	21
	2.0	76	11	7	2	11	54	14
1d , X = 3-OCH ₃	0			32	1	14	38	nd
	6.6	94	<2	3 ¹	1	13	18	nd
2d , X = 3-OCH ₃	0			10	17	46	20	nd
	6.6	94	<2	15	13	46	19	nd
1f , X = 4-CN	0			2	5	16	67	5
	1.2	92	13	5	5	19	49	7

nd, Not determined, <0.5%.

state quenched in each case. As shown in Table 4, the concentration of diene used, in most cases, quenched >90% of the triplet states and <2% of the singlet states.

The product yields for the photolysis of a selected set of the esters **1** and **2** in the presence of 2,3-dimethylbutadiene are reported in Table 4 along with the yields for unquenched direct irradiations. The direct and quenched irradiations gave essentially the same product yields in almost all cases. The exception is the decreased yield of dimers, **12**; presumably some out-of-cage benzylic radicals are reacting with the diene quencher. This comparison of product mixtures in direct and triplet quenched reactions is the classic "fingerprint" method.³² The results in Table 4 suggest that triplet excited states and triplet radical pairs can be ignored.

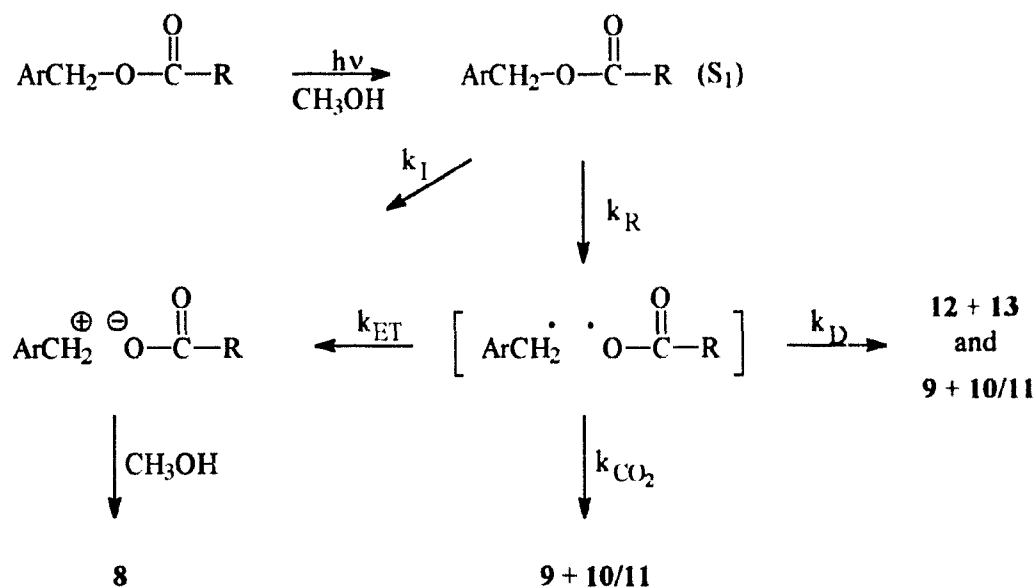
1.2.3 Quantitative Mechanistic Scheme

On the basis of the multiplicity experiments, Scheme 3 (p 15) can be simplified by removing any reaction pathways involving the triplet excited state and triplet radical pairs. Another concern was the importance of the internal return pathways. Internal return could have a major influence on product yields if, for instance, internal return occurs from the ion pair and if the efficiency of this process is substituent dependent. The result would be a decrease in the yield of products derived from the ion pair independent of the pathway and efficiency of its formation.

The efficiency of internal return for both radical pairs and ion pairs as a function of substituents for 1-naphthylethyl esters has been studied.³³ It was shown that internal return of the radical pair was substituent dependent, increasing for

electron-withdrawing substituents, whereas internal return of the ion pair was substituent independent. The predominant pathway for internal return was via the radical pair. However, inclusion of the internal return pathways did not significantly change the calculated rate constants k_{ET} and k_D . For the worst case, ignoring internal return changed the calculated electron-transfer rate constants, k_{ET} , by a factor of 2. An error of this magnitude will have no influence on the conclusions (*vide infra*). Therefore, the assumption can be made that internal return does not interfere with the distribution of products derived from either the radical or the ion pair. Removing the internal return pathways and those involving the triplets leaves only the reaction pathways shown in Scheme 5 to be considered. Scheme 5 can be used to obtain the

Scheme 5. Simplified Mechanism for the Photoreaction of Benzylic Esters **1a-f** and **2a-f**.



rate constants k_{ET} and k_D using the product yields in Table 2 (p 20) and the known rate constants of decarboxylation,¹⁸ k_{CO_2} .

The pivalate ester data will be analyzed first because the yields of the ion-derived products are low, therefore, these substrates serve as good probes for the reactivity of the radical pair. The two competing pathways of the radical pair, decarboxylation and diffusional escape from the solvent cage (k_{CO_2} and k_D in Scheme 5), form products **9-13**. For the pivalate esters, the yields of the methanol incorporated alcohol, **13**, are negligibly low for most cases (*vide supra*). The known rate constant for decarboxylation of the pivaloyloxy radical, $(CH_3)_3CCO_2^{\cdot}$, can be used as a "radical clock"³⁴ for diffusional escape. This is not straightforward, however, because the radical disproportionation product, **9**, and the radical coupling product, **11**, will be formed either from in-cage radical pairs or from a reencounter of out-of-cage radical pairs. A reasonable assumption can be made that once the radical pair has separated by diffusion, reencounters leading to disproportionation, **9**, and coupling, **11**, should occur at the same rate as reencounters leading to the dimer, **12**.

$$\frac{Yield\ (9+11)}{Yield\ 12} = \frac{(k_{CO_2} + k_D/2)}{(k_D/2)} \quad (14)$$

This is true because the concentration of the two radicals, $ArCH_2^{\cdot}$ and $(CH_3)_3C^{\cdot}$, will be the same; eq 14 then applies. This equation simply says that **9** and **11** are formed by two routes and that half the out-of-cage radicals form **9** and **11** and the other half **12**. Rearranging eq 14 gives eq 15. Because k_{CO_2} ($11 \times 10^9\ s^{-1}$) is known, k_D can be evaluated from product yield data for each substrate. For the six compounds, **2a-f**,

$$k_D = \frac{2k_{CO_2}}{\frac{Yield\ 9+11}{Yield\ 12} - 1} \quad (15)$$

studied an average value of $(2 \pm 1) \times 10^{10} \text{ s}^{-1}$ was obtained which is similar to the value of $6 \times 10^9 \text{ s}^{-1}$ calculated from the simple diffusional separation equation¹⁹ (*vide supra*). The conclusion to be reached from the pivalate chemistry is that greater than 90% of the reactivity can be rationalized in terms of homolytic cleavage of S_1 to give a radical pair followed by competition between two pathways, in-cage decarboxylation and diffusional escape.

For the acetate esters, the higher yields of the ether indicate that the ion pair is now a more important intermediate. The intermediate ion pair can be formed by direct heterolytic cleavage from the singlet excited state, by electron transfer between the radical pairs or from both pathways. The data for the acetate esters will be analyzed in two ways. First, the data will be analyzed assuming that the ion pair is formed exclusively from the electron-transfer pathway. The data will then be analyzed a second time including a contribution for heterolytic cleavage.

If there is no contribution from heterolytic cleavage in forming the ion pair, *i.e.*, $k_R \gg k_I$, the rate constants for electron transfer, k_{ET} , can be determined using eq 16, where the yield of ether, **8**, is simply expressed as a ratio of the possible

$$Yield\ \mathbf{8} = \frac{k_{ET}}{(k_{ET} + k_{CO_2} + k_D)} \quad (16)$$

reaction pathways of the radical pair. Rearranging eq 16 gives eq 17. The only

$$k_{ET} = \frac{(k_{CO_2} + k_D)}{\left(\frac{1}{\text{Yield } \mathbf{8}}\right)^{-1}} \quad (17)$$

unknown in eq 17 is k_{ET} because k_{CO_2} ($1 \times 10^9 \text{ s}^{-1}$) is known and k_D should be very similar to that obtained from the pivalate results ($2 \times 10^{10} \text{ s}^{-1}$). Thus k_{CO_2} and k_D are serving as "radical clocks"³⁴ for k_{ET} . Any error in these values will be transferred to k_{ET} , but only as a scaling factor and not by changing their relative magnitudes. The values of k_{ET} obtained this way are given in Table 5 along with the oxidation potentials of the substituted benzylic radicals in acetonitrile.³⁵ Because the yield of ether, **8**, is very low for most cases, considerable care has been taken to ensure that these values are as reliable as possible. Multiple samples, GC injections, and standards were used. For the values below 10%, the estimated error is about $\pm 0.2\%$. For the 4-cyano case, the value is just above detection limits but still measurably greater than zero.

A second possibility is that the ion pair is formed by both heterolytic cleavage and electron transfer between the radical pair. For the pivalate esters the assumption will be made that the electron-transfer pathway is not competitive with decarboxylation. Thus all of the ion pairs for the pivalate esters result from direct heterolytic cleavage of the C-O bond in the excited singlet state (k_I^S). The only product formed from the ion pair is the methyl ether, **8**. Therefore, the ether yields represent the maximum possible contribution of the heterolytic cleavage pathway.

Table 5. Values of k_{ET} and E_{OX} for the Radical Pair Generated in the Photolysis of Esters **1a-f**.

Ester	% 8	$k_{\text{ET}} \times 10^9 \text{ s}^{-1}$	E_{OX}^{a} (V)
1a , X = 4-OCH ₃	1.7 ^b	0.12 ± 0.01	0.26
1b , X = 4-CH ₃	8.0 ^b	0.61 ± 0.02	0.51
1c , X = H	26 ^c (21)	$2.5 \pm 0.3^{\text{d}}$ $(1.8 \pm 0.4)^{\text{e}}$	0.73
1d , X = 3-OCH ₃	32 (22)	$3.3 \pm 0.3^{\text{d}}$ $(2.0 \pm 0.5)^{\text{e}}$	0.79
1e , X = 4-CF ₃	1.0 ^b	0.071 ± 0.014	1.00 ^f
1f , X = 4-CN	0.3 ^b	0.021 ± 0.014	1.08

^aValues taken from ref 35. However, note footnote f.

^bError estimated at $\pm 0.2\%$.

^cError estimated at $\pm 2\%$.

^dCalculated assuming that the total yield of ion pairs (that give ether **8**) are formed by electron transfer in the radical pair. See text.

^eCalculated assuming that a percentage of the ion pairs, estimated from the pivalate data, is formed by direct heterolytic cleavage. See text.

^fNot determined but obtained from the $\rho\sigma^+$ plot using $\sigma^+ = 0.54$ and the literature value³⁵ of $\rho = 0.475 \text{ V}/\sigma^+$

Heterolytic cleavage is greatest for the 3-methoxy compound, **2d**, at 10%, drops to 5% for the unsubstituted compound, **2c**, and is undetected (<0.5%) for the other substituted compounds. This agrees with the prediction⁵ of the *meta* effect for enhanced excited-state heterolytic cleavage with the electron-donating substituent at the *meta* position. However, it is important to emphasize that this process is only a minor component in the overall mechanism, accounting for less than 10% of the reactivity.

The singlet excited-state behaviour for the acetates and pivalates, as determined by fluorescence quantum yields and singlet lifetimes, is essentially identical (Table 3). This is expected since the alkyl group is remote from the benzylic chromophore. Therefore the efficiency of direct heterolytic cleavage for the acetates should parallel that for the pivalates and should also be maximized for the 3-methoxy case. Because decarboxylation is slower for the acetate esters, the yield of ether represents the sum of the yield of ion pair intermediate derived from both the heterolytic cleavage pathway and the electron-transfer pathway. The ether yields from the pivalate esters can be used as an estimate of the yield of ether resulting from heterolytic cleavage for the acetate esters. Examination of the pivalate ether yields in Table 2 shows that this correction is only necessary for the 3-methoxy and unsubstituted acetate esters with 10% of the ether for the 3-methoxy one and 5% of the ether for the unsubstituted one being attributed to direct heterolytic cleavage. There was no detectable yield of ether for the other pivalate esters. Subtracting the pivalate ether yields from the acetate ether yields attributes the remaining 22% and 21% for the 3-methoxy and unsubstituted compounds, respectively to the electron-transfer pathway. The ether

yields with a correction made for heterolytic cleavage have also been used to calculate rate constants of electron transfer using eq 17 and are given in brackets in Table 5.

Examination of the data in Table 5 reveals that the relationship between E_{ox} and k_{ET} is not linear. Previously, electron-transfer rate data for conversion of the radical pair to the ion pair, for 1-naphthylmethyl esters,¹² has been analyzed by Marcus' theory³⁶ of electron transfer. Marcus theory was also used to analyze the data in Table 5 for the benzylic system. This required fitting the k_{ET} values to eq 18, 19, and 20. The fitting parameters are: ν_v , the vibrational modes that are important

$$k_{ET} = \sum_{j=0}^{\infty} F_j V^2 \frac{(4\pi^3)^{1/2}}{(h^2 \lambda_s k_B T)^{1/2}} \exp\left(-\frac{(j h \nu_v + \Delta G_{ET} + \lambda_s)^2}{4 \lambda_s k_B T}\right) \quad (18)$$

$$F_j = \frac{e^{-S} S^j}{j!} \quad (19)$$

$$S = \frac{\lambda_v}{h \nu_v} \quad (20)$$

in the vibrational electronic coupling; λ_s , the solvent reorganization energy; λ_v , the nuclear reorganization energy; and V , the matrix coupling term. The fit also required values of ΔG_{ET} (as a function of substituents) as given by eq 21 where F is the

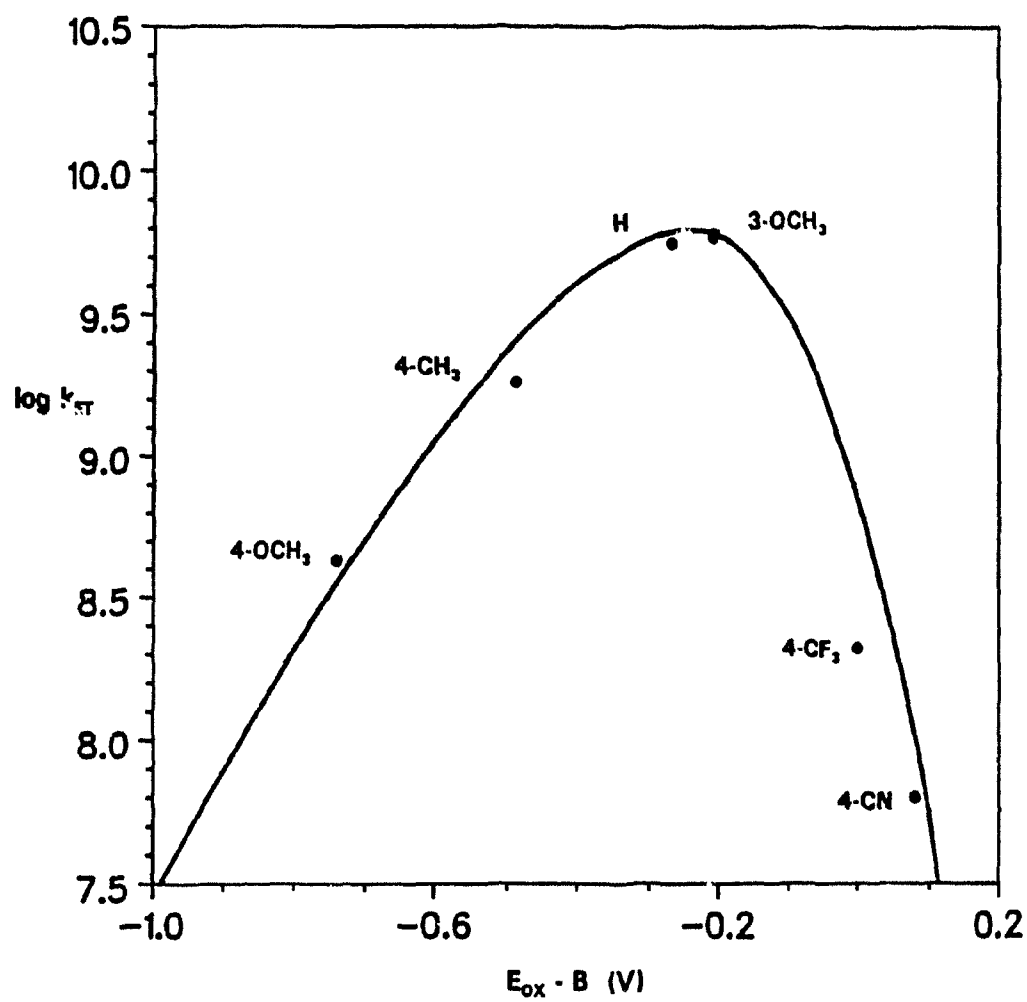
$$\Delta G_{ET} = F(E_{ox} + E_{RED}) + \Delta i - e^2/Dr_{12} \quad (21)$$

Faraday constant, E_{OX} is the oxidation potential of the substituted benzylic radical in acetonitrile (Table 5), E_{RPD} is the reduction potential of the acyloxy radical, and A is an unknown factor that corrects for the fact that the measured values of E_{OX} are in acetonitrile but the photochemistry was done in methanol. The value of A is assumed to be independent of substituents on the aryl ring so that eq 21 simplifies to eq 22 where B replaces all the constant terms in eq 21. The data in Table 5 was fitted to

$$\Delta G_{FT} = FE_{OX} - B \quad (22)$$

eqs 18-22.¹⁷ A value of 1500 cm^{-1} was assigned to ν_v that is typical of both carbon-carbon skeletal vibrations in the arylmethyl species and the carbonyl stretch in the carboxylate anion.³⁸ A better fit was obtained when the k_{ET} values corrected for heterolytic cleavage were used. This fit is shown in Figure 3. The fitting parameters obtained were $V = 4.0 \text{ cm}^{-1}$, $\lambda_v = 0.1 \text{ eV}$, $\lambda_s = 0.2 \text{ eV}$, and $B = -1.0 \text{ V}$. The fit was not significantly worse when the values of k_{ET} uncorrected for heterolytic cleavage were used. Based on this analysis the decision about which of these mechanisms is preferred is therefore not possible, but the major conclusion is clear. Homolytic cleavage of the carbon-oxygen bond in the excited singlet state of the ester is the major photochemical pathway and rationalizes greater than 90% of the product yield data even for the 3-methoxy case. For the other substituted esters greater than 95% of the reaction proceeds by this mechanism. The substituents possibly influence the efficiency of direct heterolytic cleavage but, if so, this is only a minor pathway in the reaction of benzylic esters. The major influence of substituents on product ratios is

Figure 3. A plot of the rate of electron transfer, k_{IT} , for converting the radical pair to the ion pair as a function of the oxidation potential, E_{ox} , of the benzylic radical. The fit is to eqs 18-22.



changing the oxidation potential of the benzylic radical and thus the yield of ion pair product formed from the electron-transfer pathway.

The plot in Figure 3 is qualitatively similar to that obtained previously for the radical pair to ion pair process for 1-naphthylmethyl esters¹² (Figure 2, p 11). The quantitative differences will be discussed below. The plot in Figure 3 clearly shows that the electron-transfer process is slow for electron-withdrawing groups (X = 4-CN, X = 4-CF₃) resulting in very low yields of the methyl ether that is formed from the ion pair. The electron-transfer rate is a maximum for the 3-methoxy and the unsubstituted cases and then decreases in the inverted region as the process becomes thermodynamically more favourable for electron-donating groups (X = 4-CH₃, X = 4-OCH₃). The reason for the high yield of the ion-derived product for the 3-methoxy esters is mainly a result of the increased rate of electron transfer relative to those of the other substituents, not enhanced heterolytic cleavage.

Returning to the quantitative aspects of the fit of the electron-transfer data (eq 18-22) the major difference between the results for the 1-naphthylmethyl-phenylacetyloxy radical pair (NaphthylCH₂ · O-(CO)CH₂Ph)¹² and the present results for the benzylic-acetyloxy radical pair (PhCH₂ · O-(CO)-CH₃) is the very large decrease in the rate of electron transfer for the latter. The largest rate constant in Figure 3 is $2.0 \times 10^9 \text{ s}^{-1}$ for the 3-methoxy substituted benzylic ester as compared to a maximum of $5.5 \times 10^{10} \text{ s}^{-1}$ for the 4-methyl substituent in the 1-naphthylmethyl case. The total reorganization energy, λ , of 0.3 eV for the benzylic substrates is similar to, but smaller than, the 0.5 eV determined for the 1-naphthylmethyl compounds. This

lower value of reorganization energy would increase the rate of electron transfer for the benzylic radical pairs. Therefore, the large decrease in the rate of electron transfer is due entirely to the large drop in the value of the matrix coupling term V from 12.4 to 4.0 cm^{-1} . Because this term is well known to be distance dependent,^{19,40} this observation suggests that the radical pair is further separated for the benzylic radical pairs before electron transfer takes place, perhaps because diffusion is more rapid for the smaller radical pair species. Whatever the reasons for this decreased value, the consequences are obvious. Electron transfer in the radical pair is slow enough so that it no longer dominates diffusional escape (k_D), particularly for the acetates, or decarboxylation (k_{CO_2}), particularly for the pivalates. Overall, ion pairs are much less important reaction intermediates.

The reorganization energy values are also different for the benzylic radical pair ($\lambda_v = 0.1$ eV and $\lambda_s = 0.2$ eV) compared to the 1-naphthylmethyl case ($\lambda_v = 0$ eV and $\lambda_s = 0.5$ eV). The asymmetry in the Marcus "parabola" in the inverted region requires inclusion of nuclear reorganization, λ_v . The value obtained for λ_v of 0.1 eV is small but reasonable on the basis that the electron is being transferred from a nonbonding MO of the benzylic radical to, at least superficially, a nonbonding MO on the acetyloxy radical. Pincock and Decosta¹² tried to estimate λ_v by MO calculations of the bond length and angle changes required for converting the radical pair ($\text{PhCH}_2 \cdot \cdot \text{O}_2\text{CCH}_3$) to the ion pair ($\text{PhCH}_2^+ \cdot \text{O}_2\text{CCH}_3$) and obtained a value of ~ 0.2 eV. This value can be attributed entirely to the change from an asymmetric structure (unequal C-O bond lengths) in the acyloxy radical to a symmetric one for the acetate anion

(equal C-O bond lengths). The solvent reorganization energy, λ_s , of 0.2 eV seems small since typical values of 0.5 eV are obtained for electron transfer over short distances.^{12,39,40} However, the only precedent in the literature for charge separation electron transfer in radical pairs is from our laboratory¹² so comparative discussions are difficult.

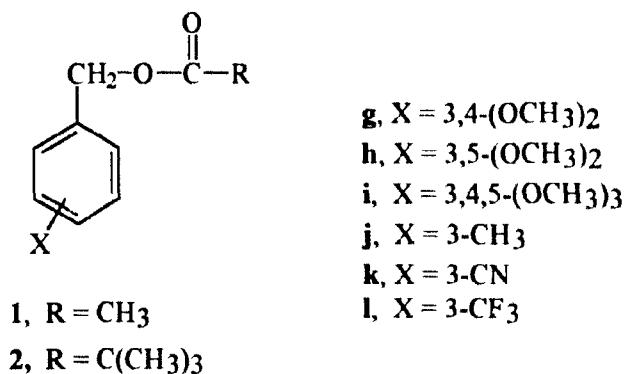
1.2.4 Conclusions

Most of the reactivity of benzylic esters can be attributed to homolytic cleavage of the excited singlet state with the ion pair being formed mainly from electron transfer between the initially formed radical pair. Rate constants for electron transfer have been determined and fitted to Marcus theory. For the 3-methoxy substituted esters it appeared that heterolytic cleavage from the singlet excited state was beginning to be competitive with homolytic cleavage. The next section of this chapter discusses the effect of multiple methoxy substitution on this competition. As well, an attempt was made to determine the effect of electron-withdrawing groups in the *meta* position on the heterolytic cleavage and these results will also be discussed.

1.3 Results and Discussion on the Photochemistry of the Multiple Methoxy Substituted Compounds

1.3.1 Introduction

The product yield studies of esters **1a-f** and **2a-f** in section 1.2 indicated that for the 3-methoxy substituted esters the heterolytic pathway was beginning to be competitive with homolytic cleavage. Therefore, the photochemistry of other methoxy substituted esters, **1g-i** and **2g-i**, was studied. Clearly, the 3,5-dimethoxy derivatives



(**1h**, **2h**) where the *meta* effect would be enhanced are obvious choices. Both the acetate, **1**, and pivalate, **2**, esters were studied because the change in the decarboxylation rate constant¹⁸ allowed the electron-transfer rate to be monitored.

The 3,4-dimethoxy derivatives (**1g**, **2g**) were chosen as another useful probe of the mechanism. If the *meta* effect is important and the critical competition occurs between heterolytic and homolytic cleavage then photolysis of the 3,4-dimethoxy substituted esters, **1g** and **2g**, should give product ratios (radical vs. ionic) similar to the 3-methoxy substituted esters, **1e** and **2e**, *i.e.*, the additional 4-methoxy group

would do little to change the dominant effect of the 3-methoxy group. However, if it is the competition between decarboxylation and electron transfer that is important then photolysis of the 3,4-dimethoxy substituted esters, **1g** and **2g**, should give product ratios similar to the 4-methoxy substituted esters, **1f** and **2f**, because the benzylic radicals for these esters would have very similar oxidation potentials, *i.e.*, the additional 3-methoxy group would do little to change the dominant effect of the 4-methoxy group.

In addition, because the *meta* effect prediction is not exclusive to the methoxy group and because previous work had only included *meta* methoxy, a study of other *meta* substituents seemed of interest. Therefore, a series of *meta* substituted benzyl acetates, **1j-l**, was also studied.

The effect of *meta* substituents and multiple substituents in benzylic ester photochemistry has not been extensively explored. Wan *et al.*⁴¹ have compared the reactivity of positional isomers of substituted benzyl acetates. A few substituents (CH₃, F, Cl) in the three possible positions of benzyl acetate were examined. The esters were photosolvolysed in 50% aqueous acetonitrile. The *ortho* isomer was the most reactive, followed by the *meta* isomer. The *para* isomer was the least reactive. This effect was observed independent of the substituent. Their conclusion was that in S₁ substituent effects appear to follow an *o* > *m* > *p* rule.

Wan *et al.*⁴² have also studied the effect of multiple methoxy substitution on the photohydroxylation of benzyl alcohols. They found that the effects of the methoxy groups were additive. The reactivity pattern of the disubstituted compounds follows

the rule $o,o > o,m > m,m$.

The photochemistry of dimethoxybenzenes has been studied in aqueous sulfuric acid.^{43,44} The singlet excited state of 1,3-dimethoxybenzene was found to protonate regioselectively at the 2- position to give an intermediate cyclohexyldienyl cation. Laser flash photolysis studies of the photoprotonation of 1,3-dimethoxybenzenes in 1,1,1,3,3,3-hexafluoroisopropyl alcohol (HFIP) were done by McClelland and coworkers.⁴⁵ Again, protonation was found to be selective at the 2- position. A transient was observed and assigned as the intermediate cyclohexyldienyl cation. In contrast, in the ground state, there is a strong preference for protonation at the 4- position.^{46,47,48} These observations are consistent with the predictions of the *meta* effect.⁵

1.3.2 Products and Yields on Irradiation of 1g-i and 2g-i

The esters **1g-i** and **2g-i** were prepared by reacting the benzyl alcohols **7g-i** with acid chloride (eq 10, p 18) and photolysed in methanol with a low-pressure mercury lamp. The major benzylic products were formed, eq 23, analogous to the products formed from esters **1a-f** and **2a-f**. Again, no attempt was made to isolate or quantify the low molecular weight carboxylic acids, acetic and pivalic, which were formed along with the ethers, **8g-i**. The yields of these products are given in Table 6. The formation of the five benzylic products shown in eq 23 can be rationalized by the mechanism shown in Scheme 5 (p 30). The ion pair is trapped by methanol to give the ether, **8**. The remaining products are radical derived. The benzylic radical forms

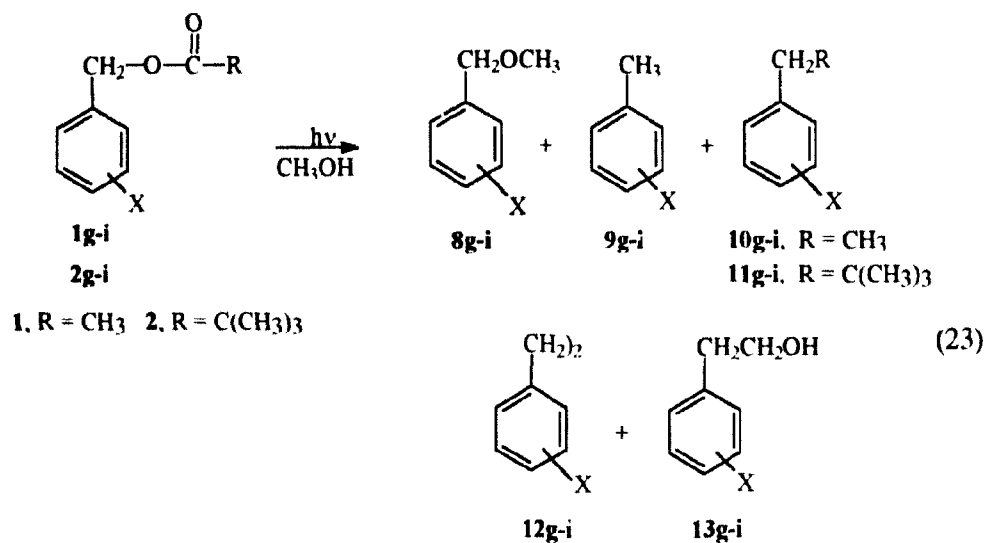


Table 6. Product Yields^a for the Photolysis of Esters **1g-i** and **2g-i** in Methanol.

Esters, 1g-i 2g-i	% 8g-i ether	% 9g-i toluene	% 10/11g-i ^b coupled	% 12g-i ^c dimer	% 13g-i alcohol
1g , 3,4-(OCH ₃) ₂	43	<1	7	28	nd
2g	7	11	25	36	nd
1h , 3,5-(OCH ₃) ₂	56	5	23	2	nd
2h	14	23	44	10	nd
1i , 3,4,5-(OCH ₃) ₃	66	nd	15	11	nd
2i	20	22	45	5	nd

^aThe yields are absolute yields based on consumed ester. Estimated error, $\pm 2\%$.

^bFor esters **1** the product is **10**, R = CH₃. For esters **2** the product is **11**, R = C(CH₃)₃.

^cTwice the molar yield.

nd, Not determined, <0.5%.

9 in a significant yield by in-cage disproportionation for $R = C(CH_3)_3$. These toluene products are only formed in minor amounts for the acetates where there is no readily available source of a hydrogen atom. The benzylic radicals can also either couple with the alkyl radical (R') to form **10/11**, the other in-cage product, or couple out-of-cage with itself to form **12**, the dimer.

Examination of the product yields in Table 6 allows some qualitative conclusions to be made. A simple first approach is an examination of the ether yields because the ethers are the only benzylic products formed from the ionic intermediates. For the acetates, there is a correlation between the ether yields and the methoxy substitution pattern. As predicted by the *meta* effect, the 3-methoxy substituted ester as well as the 3,4-dimethoxy substituted one, gave a higher yield of ether product, **8**, 32% and 43%, respectively than the 4-methoxy substituted ester (2%). The ether yield from the 3,5-dimethoxy substituted ester (56%) was almost double that for a single *meta* methoxy group and was even greater for the 3,4,5-trimethoxy substituted ester (66%). As predicted by the *meta* effect, the yield of product from the ionic intermediate is enhanced as methoxy groups are added to the aromatic ring.

An interesting result is the effect of a 4-methoxy group in the presence of a 3-methoxy group for the acetate esters. When the acetate ester is substituted with a 4-methoxy group only, very little ether product (2%) is formed. However, when there is a 3-methoxy group in combination with a 4-methoxy group, the latter seems to have a larger effect. The yield of the ether from the 3,4-dimethoxy substituted ester is 43% whereas it is only 32% from the 3-methoxy substituted ester. This is an increase of

9%, while a 4-methoxy group alone increases the ether yield by only 2% relative to the unsubstituted ester. These substituent effects are not additive in a simple way.

The same trends are observed for the pivalate esters. As the number of methoxy groups is increased, the yield of ether is enhanced. If the available data were only those for the acetates or the pivalates, the conclusion would likely be made that *meta* methoxy groups enhance the efficiency of heterolytic cleavage. However, when the results of the two esters are compared the yield of ether from the acetate esters ($R = CH_3$) is much higher than for the corresponding pivalate esters ($R = C(CH_3)_3$). Therefore, the *meta* effect, which is based only on excited-state electron densities and thus enhanced heterolytic cleavage efficiencies, cannot completely explain the differences.

The alkyl group (R) of the esters has virtually no effect on the photophysical properties of esters (*vide supra*) and therefore, any differences in ether yields as a function of R must be a consequence of ground-state processes that occur after excited-state bond cleavage. Rate constants for the ground-state processes can be estimated allowing the data in Table 6 to be analyzed quantitatively.

1.3.3 Quantitative Mechanistic Scheme for Esters 1g-i and 2g-i

Examination of the data in Table 6 for the pivalate product yields shows that, as for the esters 2a-f, the reactivity of the radical pair is quite important. Again, the product yield data will be analyzed assuming that, for the pivalate esters, the ion pair is formed entirely by direct heterolytic cleavage. This pathway is now more important

than it was for the pivalates **2a-f**. The maximum yield of ether occurs for the 3,4,5-trimethoxy substituted compound, **2i**, and it accounts for 20% of the total product yield. However, 80% of the reactivity is still attributed to the radical pair. The yields of the radical products and eq 15 (p 32) were used to determine values for k_D , that are given in Table 7. For ester **2g** calculation of k_D is not mathematically possible because the yield (**9** + **11**) = yield (**12**). However, examination of eq 14 reveals that in order for this to be true $k_D/2$ must be much greater than $k_{\alpha O_2}$, therefore, k_D would have to be greater than $2.2 \times 10^{11} \text{ s}^{-1}$. This is not possible. The calculated value of k_D for **2h** (3,5-(OCH₃)₂) is $3.9 \times 10^9 \text{ s}^{-1}$ and $1.6 \times 10^9 \text{ s}^{-1}$ for **2i** (3,4,5-(OCH₃)₃). These rate constants are very different from the average value of k_D , $2 \times 10^{10} \text{ s}^{-1}$, calculated for the monosubstituted pivalate esters **2a-f**. There are no obvious reasons why the rate constants of diffusion are so different for ester **2g** compared to esters **2h** and **2i** or why the calculated diffusional rate constants for esters **2g-i** are so different from the monosubstituted esters **2a-f**.

For the acetate esters the ether is a major product. The ether yields reflect both heterolytic cleavage and electron transfer because decarboxylation of $\text{CH}_3\text{CO}_2^\cdot$ is slower. Again, the ether yields from the pivalate esters will be used to estimate what fraction of the ether yield for the acetate esters is formed by heterolytic cleavage. After this subtraction, the remaining yield of ether is the fraction formed by the electron-transfer process (Table 7). This yield can then be used to determine k_{ET} from eq 17, p 33. The only unknown in eq 17 is k_{ET} because $k_{\alpha O_2}$ ($1 \times 10^9 \text{ s}^{-1}$) is known and the value of k_D was determined above. The values of k_{ET} obtained in this way are

Table 7. Oxidation Potentials and Electron-Transfer Rate Constants for Esters **1g-j**.

Ester	% 8 ^a	$k_D \times 10^9 \text{ s}^{-1}$	$k_{ET}^b \times 10^9 \text{ s}^{-1}$	$E_{ox} \text{ (V)}$
1g , 3,4-(OCH ₃) ₂	36	nd	nd	0.26 ^c
1h , 3,5-(OCH ₃) ₂	42	3.9	3.5	0.77 ^d
1i , 3,4,5-(OCH ₃) ₃	46	1.6	2.2	0.26 ^d
1j , 3-CH ₃	19	17	4.2	0.70 ^e

^aObtained by subtracting the yield of **8** for the pivalate ester from the corresponding acetate ester in Table 6.

^bCalculated from eq 17 with $k_{CO_2} = 1 \times 10^9 \text{ s}^{-1}$

^cFrom ref 35.

^dThis work, see experimental section.

^eNot measured but assumed equal to that of **1a** and **1i**.

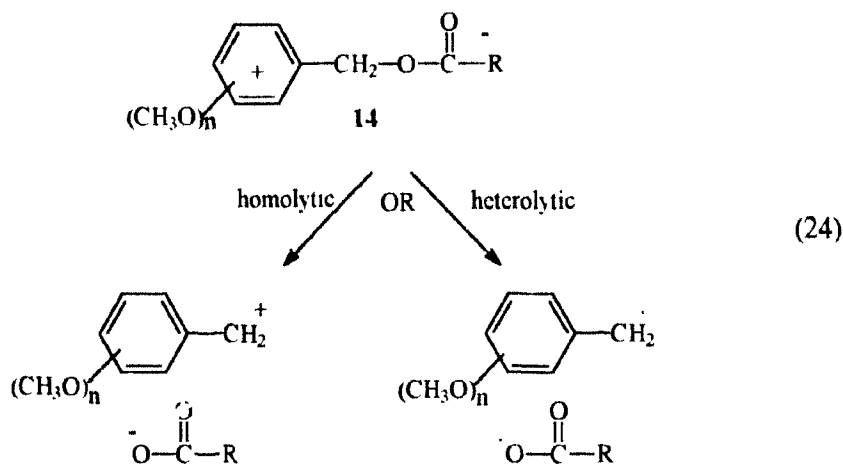
nd, Not determined, see text.

given in Table 7, along with the known values¹⁵ for the oxidation potentials of the substituted benzylic radicals in acetonitrile. The rate constant of electron transfer for the 3,4,5-trimethoxy substituted ester is very different than that for the 4-methoxy substituted ester which has a similar oxidation potential, Table 5. The lack of agreement between the rate constants of diffusion and electron transfer for the multiple methoxy substituted esters and those values calculated for the monosubstituted esters (*vide infra*) suggests that the simple equations used to calculate k_D and k_{ET} are incorrect for the multiple methoxy substituted esters.

One assumption used to analyse the data was that the photophysical behaviour of the acetates and the pivalates are identical. If this is not true the analysis would no longer be correct. This is an unlikely possibility because, as was mentioned earlier, the singlet excited-state behaviour of the acetate esters **1a-f** and the pivalate esters **2a-f** was shown to be identical. Unfortunately, the multiple methoxy substituted compounds do not detectably fluoresce so the fluorescence quantum yields or lifetimes for compounds **1g-i** and **2g-i** cannot be compared.

A second explanation is that there is another reaction pathway that has not yet been considered that perturbs product ratios and thus the equations used for data analysis would be incorrect. One possibility that has been studied is intramolecular electron transfer between the more easily oxidized methoxy substituted rings and the ester carbonyl to form a charge transfer species, **14**, eq 24. There is literature precedence^{49,50} for this process in arylmethyl esters of aromatic carboxylic acids

(ArCH₂O(CO)Ar) where the ester functional group is more easily reduced than the aliphatic esters studied here. However, the presence of multiple methoxy groups



would lower the oxidation potential of the ring and enhance this possibility. If **14** was formed preferentially for one alkyl group over another (*i.e.*, ester **1** compared to ester **2**) and if **14** fragmented preferentially either homolytically or heterolytically as in eq 24, this would provide an additional pathway to form ion pairs or radical pairs respectively. This new pathway would then alter the product ratios from the normal excited-state bond cleavage.

Normally intramolecular electron transfer is detected by a decrease in the fluorescence quantum yield for the esters compared to related compounds that lack the ester functionality, for example, toluenes. The lack of fluorescence for esters **1g-i** and **2g-i** makes these experiments impossible. Because of this difficulty methoxynaphthalenes were tested as model compounds. The oxidation potential of 1-

methoxynaphthalene ($E_{1/2} = 1.38$ V in acetonitrile vs. SCE)^{51a} is similar to that for a dimethoxy substituted benzene ($E_{1/2} = 1.45$ V for 1,2-dimethoxybenzene in acetonitrile vs. SCE)^{51b} and the oxidation potential of 1,4-dimethoxynaphthalene ($E_{1/2} = 1.10$ V in acetonitrile vs. SCE)^{51c} is similar to that of a trimethoxy substituted benzene ($E_{1/2} = 1.12$ V for 1,2,4-trimethoxybenzene in acetonitrile vs. SCE).^{51d} However, no quenching of the fluorescence was observed for either methoxynaphthalene compound in methanol solution containing up to 4 M ethyl acetate. Given that the lifetime of 1-methoxynaphthalene⁵² is 10 ns, the rate constant for quenching must be less than 10^9 $M^{-1}s^{-1}$. This is orders of magnitude smaller than the rate constants for the other reaction pathways.

When comparing the acetate and pivalate esters, differences in their excited-state properties have been ruled out as a reason for the large differences in the yield of the ether. This means that differences in the rates of ground-state processes following the bond cleavage must be responsible. One possibility is the intervention of internal return of either the radical pair (k_{IR}^R) or the ion pair (k_{IR}^I) to the starting ester, as shown in Scheme 3. If ion pair return is important, the yield of the ether will drop relative to the yield expected from the bond cleavage processes. This could explain the lower than expected ether yield for **1h**. Another possibility is that internal return in the radical pair is more efficient for the acetate esters. This is a real possibility because the lifetime of the radical pair will be longer for the $CH_3CO_2^{\cdot}$ than for the $(CH_3)_3CCO_2^{\cdot}$ radical. The lifetime is decreased for the latter because it decarboxylates an order of magnitude more rapidly. Internal return of the ion pair could therefore

amplify the importance of the direct heterolytic cleavage (k_1^b) for the acetates **1g,i** and increase the yield of the ether in the photoreaction of these esters.

Internal return in the photolysis of 1-naphthylethyl esters³³ has been studied. Excluding internal return and using the simple reaction mechanism shown in Scheme 5 resulted in only a minor perturbation on the calculated rate constants. However, to be sure that this was also true for benzylic esters the internal return process has been studied for esters **1i** and **2i**.³³ Internal return was monitored by preparing ¹⁸O labelled esters and measuring ¹⁸O scrambling during the photolysis by mass spectrometry. The importance of internal return in the ion pair was determined by doing a ground-state solvolysis where the only possible intermediate is the ion pair. The results showed no significant differences in internal return efficiencies between the acetate and pivalate esters. As well, the percentage of internal return was small and reaffirms that it can be excluded from the reaction mechanism.

The above experiments rule out many possible explanations for the differences in the rates of electron transfer for esters **1g-i** compared to the monosubstituted esters. The most likely explanation is that di- and trisubstituted compounds have different fitting parameters for the Marcus equation, *i.e.*, reorganization energies and matrix coupling terms, and should not be expected to have rates of electron transfer comparable to the monosubstituted benzylic esters. This could also be true for *meta* substituted compounds, because they might not necessarily have the same fitting parameters as the *para* isomers.

1.3.4 Photolysis of Esters 1j-l

The *meta* substituted esters **1j-l** were prepared and their photochemistry was studied to construct a Marcus plot for the *meta* substituted esters. The photochemistry of esters **1j** and **2j** was studied first. Upon photolysis in methanol the typical benzylic products were formed, eq 23, and the yields are given in Table 8. When the esters **1k** and **1l** were photolysed in methanol the usual benzylic products were formed (eq 23, p 45) however, the products as well as the ester isomerized. For instance, on irradiation

Table 8. Product Yields^a for the Photolysis of Esters **1j** and **2j** in Methanol.

Ester	% 8j ether	% 9j toluene	% 10/11j ^b coupled	% 12j dimer	% 13j alcohol
1j	26	2	18	17	nd
2j	7	10	45	24	nd

^aEstimated error, $\pm 2\%$.

^bFor ester **1** the product is **10**, R = CH₃. For ester **2** the product is **11**, R = C(CH₃)₃.

^cTwice the molar yield

nd, Not detected, <0.5%.

of the 3-cyano substituted ester (**1k**), products with the cyano group in both the 3- and 4- positions were formed along with the 4-cyano substituted ester.

Reliable results on the primary product distribution for the 3-cyano and 3-trifluoromethyl substituted esters could not be obtained because of this complication.

The mechanism for these positional isomerizations on the aromatic ring is presumed to be the known benzvalene rearrangement.⁵⁴ This reaction, which is quite inefficient ($\Phi = 0.05$ for benzene-1,3,5-d₃),⁵⁵ was competitive with the reaction pathways that formed the benzylic cleavage products. This had not been a problem with other substituents, but the electron-withdrawing groups make the esters **1k** and **1l** quite unreactive to benzylic cleavage. A study of a series of *meta* substituted esters where the resulting benzylic radical has a range of oxidation potentials will not be possible because data for the two most convenient substituents that raise the oxidation potential of the benzylic radical, trifluoromethyl and cyano, cannot be obtained. However, the substituent dependence of the benzvalene rearrangement reactions is of interest and is being investigated further.

Besides the methoxy substituents, the only other *meta* substituent to be studied was the methyl group, esters **1j** and **2j**. A value of k_{ET} ($4.2 \times 10^9 \text{ s}^{-1}$) was calculated using eq 17 (p 33) and is shown in Table 7. This value of k_{ET} is similar to the value for the unsubstituted benzylic radical that has a very similar oxidation potential.

1.3.5 Conclusions

Although numerical analysis of the results for the multiple methoxy compounds was inconclusive, qualitative conclusions can be made. The goal of this section was to determine if the heterolytic cleavage pathway could be enhanced by addition of methoxy groups to the aromatic ring. Examination of the ether yields revealed that for the 3,4,5-(OCH₃)₃ substituted pivalate ester the ether yield was 20%. At most 20%

of the reactivity for this compound can be explained by terms of heterolytic cleavage of the singlet excited state. Homolytic cleavage is still the dominant reaction pathway. Also, the data indicate that the rates of electron transfer for these compounds cannot be predicted based on the results for a series of monosubstituted esters. For the one *meta* substituted compound that was studied, 3-CH₃, the calculated rate of electron transfer was comparable to the rate of electron transfer for a *para* substituted compound with a similar oxidation potential.

1.4 Results and Discussion of the Photochemistry of Substituted Indanyl Acetates and Pivalates

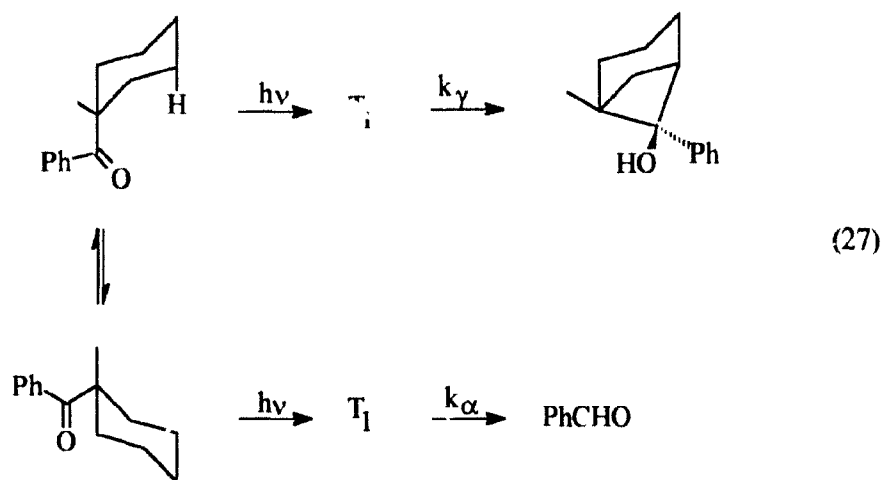
1.4.1 Introduction

The first two sections of results in this chapter have established the mechanism for benzylic ester photoreactions. The results suggest that the reactivity of these esters can be attributed predominantly to homolytic cleavage of the excited singlet state. However, there is still one question that needs to be investigated further. The efficiency of photochemical reactions generating benzylic cations is often enhanced by the presence of a *meta* methoxy group. Zimmerman⁵ explained this observation in terms of the *meta* effect. The electronic distribution around the benzene ring in the excited state when the ring is *meta* methoxy substituted enhances heterolytic cleavage. This pathway is enhanced and thus the overall efficiency of the reaction increases. However, the results in the previous two sections strongly suggest that heterolytic cleavage is only a minor pathway. Therefore, how does the *meta* methoxy group increase the reaction efficiency? One possibility is that the *meta* methoxy group enhances homolytic cleavage. However, for completeness, there is another possibility that will be explored, the substituents could be altering the ground-state populations of the two benzylic conformers and ultimately influencing reaction rates.

For benzylic compounds ($\text{Ar-CH}_2\text{-X}$), there are two stable conformers of the C-X bond, one with the X group in the plane of the ring, **15**, and the other with the X group perpendicular to the plane of the ring, **16**. For photochemical benzylic cleavage reactions, the reactive conformer will be the one with the C-X bond homo-conjugated

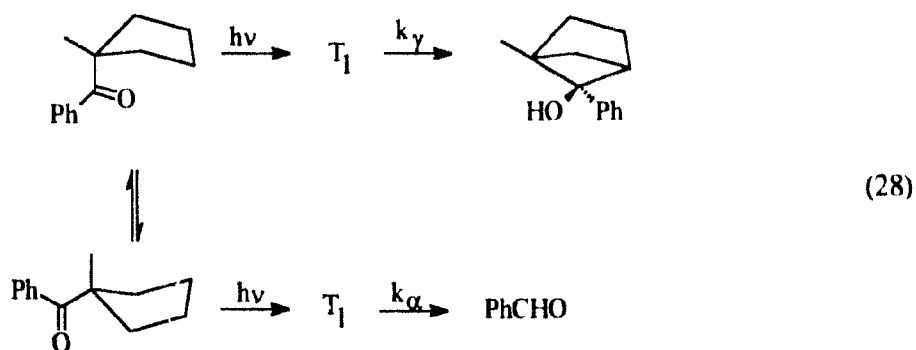
Examples of this are rare in ground-state chemistry but not for photochemical reactions⁵⁷ because the rates of reaction can be fast enough to be competitive with conformational motion.

A good example of the importance of conformational motion in photochemical reactions was reported by Lewis *et al.*⁵⁸ on the photochemical α -cleavage and γ -hydrogen abstraction reactions of cycloalkyl phenyl ketones. There are two stable conformers of these compounds. By ring inversion, the phenylketone moiety can be either axial or equatorial. For 1-methylcyclohexyl phenyl ketone, eq 27, the cleavage (k_α) and abstraction (k_γ) reactions are more rapid than ring



inversion. This is an example of a system that does not follow the Curtin-Hammett or the Winstein-Holness equation. Product quantum yields were found to be dependent upon both conformational populations in the ground state and the efficiency of product formation from the conformers, not only on the relative rate constants, k_α and k_γ .

On the other hand, for 1-methylcyclopentyl phenyl ketone, eq 28, where the ring inversion is much faster, product ratios were only dependent upon the relative rate constants of reaction, k_x and k_y .

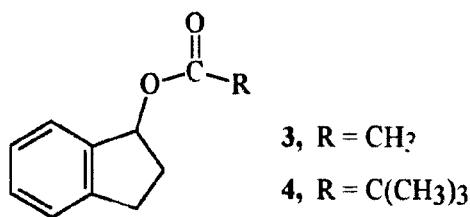


For benzylic compounds the barrier to rotation and the preferred conformation can be determined by the J-method,⁵⁹ a high resolution NMR technique. This method is applicable to benzene derivatives containing side chains and requires accurate measurement of the long-range coupling constant, 6J , between a nucleus in the *para* ring position and a nucleus bonded to the carbon in the α position of the side chain.

Conformational equilibria of benzylic esters have not been studied. However, Schaefer *et al.*⁶⁰ have determined the preferred conformers for the benzyl alkyl ethers, $X = OR$ ($R = CH_3, CH_2CH_3, CH(CH_3)_2, C(CH_3)_3$). The difference in energy between the two conformers, **15** and **16**, is quite small, < 8.4 kJ/mol (< 2 kcal/mol). The lower energy conformer has the CH_2-O bond perpendicular to the plane of the aromatic ring. However, because the energy difference between the two conformers is quite small the stability of the two conformers can easily be reversed by changing

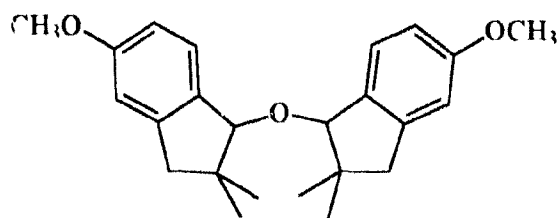
the solvent or adding substituents to the aromatic ring. When chlorine substituents are added to the *meta* position the in-plane conformer becomes more stable. Substituent and solvent effects can only be important when the energy difference between the two conformers is small. For instance, Schaefer's results on benzyl chlorides using the J-method, indicate that the energy difference between the two conformers is larger, >8.4 kJ/mol (>2 kcal/mol), and the stable conformer is always the out-of-plane one, independent of solvent or substituent.

If the energy difference between the two conformers of benzylic esters is small and substituent dependent, as with the benzylic ethers, then it is possible that the enhanced reactivity of the *meta* substrates is due to an increased population of the reactive conformer. To test this possibility, indanyl esters, **3** and **4**, with a rigid homo-conjugated C-X bond were prepared and their photochemistry in methanol was



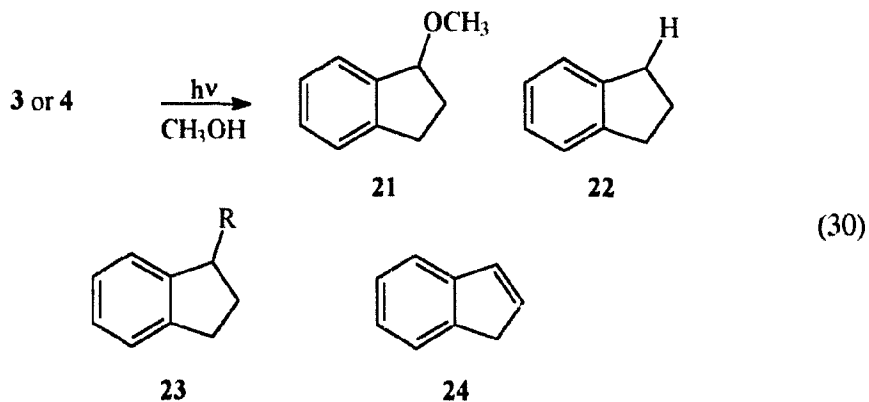
studied. The photochemistry of esters **3** and **4** was more complicated than expected. Therefore, the photochemistry and photophysics of esters **5a-c** and **6a-c**, the dimethyl analogues of esters **3** and **4**, were also examined. The C-O bond in the indanyl esters are rigid and therefore, allow the electronic effect of substituents to be evaluated independently of conformational effects.

yielded only one product that was tentatively identified as the ether, **20**, on the basis of ^1H and ^{13}C NMR data. It is not obvious why the acetate ester could not be prepared by reaction of acetyl chloride with the alcohol since this procedure worked

**20**

well for the pivalate ester. The ester **5c**, was successfully synthesised from the alcohol using *N,N*-carbonyldiimidazole and acetic acid. Complete details are given in the experimental section.

Esters **3** and **4** were photolysed in methanol using low-pressure mercury lamps in a Rayonet reactor. Four products were formed as shown in eq 30. In the previous



photochemical studies of esters **1** and **2**, products could be isolated if a large amount (>500 mg) of ester was photolysed to a high percent conversion. However, this was not possible for esters **3** and **4** because one product was indene. As the concentration of indene increased, significant product formation was observed from the photochemistry of indene. However, the primary products could be identified by GC/MS. The identity of products **21**, **22**, and **24** was confirmed by comparing the retention times and mass spectra of authentic samples to the retention times and mass spectra of products in the photolysis mixture. No authentic sample of product **23** was available but based on the mass spectral fragmentation pattern and GC/MS retention time this is the most probable structure. Using the authentic samples, standards were prepared and the products were quantified by GC/FID. The yield of product **23** was estimated using indan, **22**, after correction for the difference in the number of carbon atoms. The yields obtained in this way are given in Table 9.

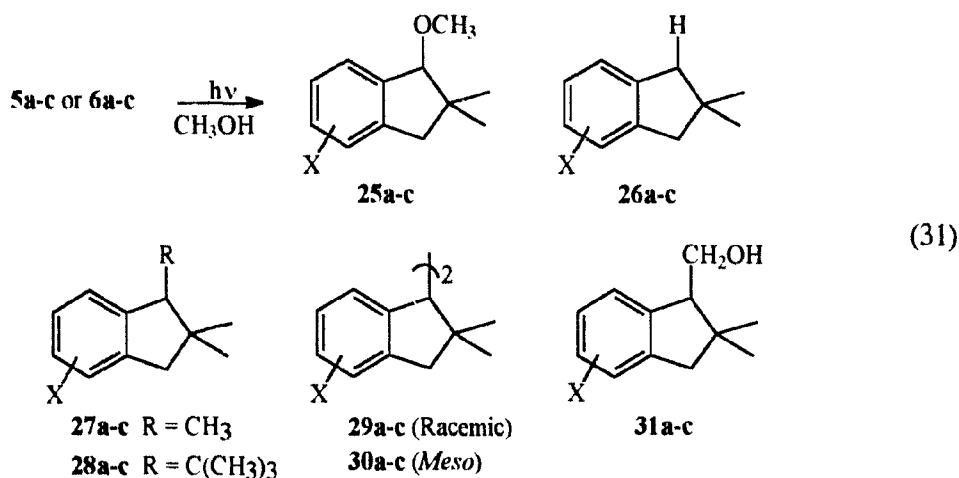
Table 9. Product Yields for the Photolysis of Esters **3** and **4** in Methanol.

Ester	% 21 ether	% 22 indan	% 23 coupled	% 24 indene	Total %
3 , R = CH ₃	23	1	9	39	72
4 , R = C(CH ₃) ₃	5	14	34	31	84

The mechanism, shown in Scheme 5 (p 30), which was used to rationalize product formation for the benzylic esters, **1** and **2**, can also be used to explain product

formation for esters **3** and **4**. The ether, **21**, is formed by trapping of the indanyl cation by methanol. Indan, **22**, and the coupling product, **23**, are formed from the indanyl radical. These products must be formed in-cage because no out-of-cage products were detected indicating that diffusional separation of the radical pair is not efficient. The origin of indene, **22**, is uncertain because it could be formed by loss of hydrogen from the indanyl radical, the indanyl cation or both. Determining the mechanism for formation of indene was not possible. Therefore, rate constants could not be calculated making comparisons with the kinetic results for esters **1a-f** and **2a-f** impossible. To eliminate the problem of indene formation esters **5** and **6** with two methyl groups at carbon 2 were prepared.

When esters **5a-c** and **6a-c** were photolysed in methanol, the five major indanyl products shown in eq 31 were formed. The products were isolated by column chromatography and identified by spectroscopic methods. Again, product formation



can be rationalized using Scheme 5 (p 30). The methyl ethers, **25a-c**, are formed by trapping of the indanyl cation by methanol. The remaining products are radical derived. For these esters, out-of-cage radical products are also formed. The indanyl radical, in-cage or out-of-cage, abstracts a hydrogen atom to form indan. The indanyl radical also couples with the R group to give the coupling product. Whether the coupling occurs in-cage or out-of-cage depends on the rate of decarboxylation of the acyloxy radical relative to the rate of separation of the radical pairs. The alcohol products, **31a-c**, result from coupling of the out-of-cage indanyl radicals with the solvent derived $\cdot\text{CH}_2\text{OH}$ radicals. Once the indanyl radical is out-of-cage it can also couple with itself to form dimers. Two diastomeric dimers are possible because these compounds have two identical stereogenic centers. Both the racemic (*R,R* : *S,S*) **29a-c** and *meso* (*R,S*) **30a-c** dimers were formed and isolated. These dimers have interesting temperature dependent NMR spectra that are discussed in detail in Chapter 3.

The products were quantified by HPLC or GC/FID by comparison with standard samples and the yields are given in Table 10. The yields of the products are highly dependent on the substituent. The yield of ether varies from 60% for the 6-methoxy substituted acetate ester to 9% for the corresponding 5-methoxy substituted acetate. The product yields are also highly dependent on the R group. For instance, the yield of ether is 52% for the unsubstituted acetate but only 14% for the unsubstituted pivalate. Independent of the fact that the C-O bond that is cleaving is homo-conjugated to the aromatic ring, the R group still affects product ratios. As

before, the pathways controlling product distribution occur after the excited-state cleavage and rationalizing product ratios using Scheme 5 is valid.

Speculation on the mechanism for indene formation in the photolysis of the non-methylated esters **3** and **4** discussed previously is now possible based on the results from esters **5a** and **6a**. For ester **5a** the ion pair accounted for ~50% of the reactivity in comparison with only ~14% of the reactivity for ester **6a**. The yield of ether from ester **3** was 23% and the yield of indene was 39%. The sum, 62%, is

Table 10. Product Yields for the Photolysis of Esters **5a-c** and **6a-c** in Methanol.

Ester	% 25 ether	% 26 indan	% 27/28 ^a coupled	% 29 dimer	% 30 dimer	% 31 alcohol	%
5a , X = H	52	nd	12	5	9	11	89
6a	14	11	33	8	16	rd	82
5b , X = 6-OCH ₃	60	1	6	6	6	7	86
6b	13	14	19	9	9	nd	64
5c , X = 5-OCH ₃	9	nd	18	12	18	41	98
6c	nd	11	34	23	32	nd	100

^aFor esters **1** the product is **27**, R = CH₃. For esters **2** the product is **28**, R = C(CH₃)₃.

nd, Not determined, <0.5%.

larger than the yield of the ion-derived product (50%) from **5a**. For the pivalate ester **4**, the ether yield (5%) and the indene yield (31%) are again larger than the yield of ion-derived product from **6a** (14%). These results strongly suggest that, in the photolysis of **3** and **4**, indene is being formed from both the radical pair and the ion

pair.

In the next section the rate constants calculated for the benzylic esters **1** and **2** in Chapter 1.2 will be compared with the rate constants calculated for the indanyl esters **5a-c** and **6a-c**.

1.4.3 Quantitative Mechanistic Scheme for Esters **5a-c** and **6a-c**

Examination of Table 10 reveals that the products for the pivalates, **6a-c**, are predominantly radical-derived and again will serve as probes for the reactivity of the radical pair. As before, the rate constants for decarboxylation of the pivaloyloxy radical and the product yields given in Table 10 can be used to calculate k_D (eq 15 p 32). The calculated values of k_D , given in Table 11, are comparable to the average value of $2 \times 10^{10} \text{ s}^{-1}$ that was obtained for the benzylic esters **2a-f**.

Table 11. Calculated Values of k_D for Esters **6a-c** and k_{I1} for Esters **5a-c**.

Ester	$k_D^a \times 10^{10} \text{ s}^{-1}$	$k_{I1}^{b,c} \times 10^9 \text{ s}^{-1}$
X = H	1.1	7.3 (1.8)
X = 6-OCH ₃	1.1	10.6 (2.0)
X = 5-OCH ₃	2.4	1.2 (0.1)

^aCalculated from eq 15.

^bCalculated from eq 17.

^cValues in brackets are for the benzylic esters, **1**.

To determine the rate constants of electron transfer, k_{ET} , for the acetate esters it will again be assumed that the total yield of the methyl ether formed from photolysis of the pivalate esters results from direct heterolytic cleavage of the C-O bond in the excited state. Heterolytic cleavage is therefore assumed to be maximized for the unsubstituted and the 6-methoxy substituted pivalate esters with efficiencies of 14% and 13%, respectively. No ether was detected for the 5-methoxy substituted pivalate ester. These observations are consistent with the prediction⁵ of the "*meta* effect" for enhanced heterolytic cleavage in the excited state when electron-donating substituents are in the *meta* position. Again, it is important to emphasize that this is the maximum efficiency of heterolytic cleavage for these substrates and that, even then, it is only a minor pathway for photochemical reactivity.

The yield of ether formed exclusively from the electron-transfer pathway in the acetate photochemistry is equal to the total yield of ether minus the yield of ether from the corresponding pivalate ester. The rate constants of diffusion should be very similar for the acetate and pivalate esters. Thus, the values of k_D in Table 11 and eq 17 (p 33) can be used to calculate the rate constants of electron transfer for the acetate esters, corrected for the assumed heterolytic cleavage. These values of k_{ET} are also listed in Table 11. The trends are the same as those observed for the benzylic esters. For the benzylic esters, the largest calculated rate constant was for the 3-OCH₃ substituted ester ($2.0 \times 10^9 \text{ s}^{-1}$), followed by the unsubstituted ester ($1.8 \times 10^9 \text{ s}^{-1}$), and the 4-OCH₃ substituted ester ($0.12 \times 10^9 \text{ s}^{-1}$). The obvious difference between the benzylic and indanyl esters is the absolute magnitude of the rate constants. The

rate constants of electron transfer for the indanyl esters are, on average, six times those for the benzylic esters. Electron transfer must be kinetically more favorable for the indanyl radicals. Without knowing the oxidation potentials of the indanyl radicals and the reorganization energies for the electron-transfer process converting the indanyl radicals to the indanyl cations, the reason for this observation cannot be determined.

The products isolated from the indanyl esters are analogous to those formed from the benzylic esters. As well, the same substituent effects on product ratios have been observed. This confirms that these rigid esters will serve as good probes for the importance of conformational mobility in benzylic ester cleavage reactions.

1.4.4 Photophysical Data for Esters **5a-c** and **6a-c**

The singlet lifetimes, fluorescence and reaction quantum yields measured for the indanyl esters **5a-c** and **6a-c** are given in Table 12. An important point to note from Table 12 is that these values are quite dependent on the substituents but independent of R, acetate versus pivalate. This reemphasizes the conclusion that changes in product yields for **5** versus **6** are not excited-state effects but are a result of changes in a ground-state process, decarboxylation, which occurs after homolytic bond cleavage.

A comparison of the singlet lifetimes and fluorescence quantum yields for the esters **5** and **6** with the unreactive indanyl alcohols **19a-c** shows that the esters have different reactivities. The C-O bonds in the alcohols **19a-c** are not photolabile and the fluorescence quantum yields and lifetimes of the alcohols when compared to the

Table 12. Emission Properties of the Substituted Indanyl Alcohols **13a-c** and Esters **5a-c** and **6a-c** in Methanol.

Alcohol X or Ester	τ_s (ns)	ϕ_f^a	Φ_{RXN}^b	$k_R \times 10^8 \text{ s}^{-1}$	
19a	H	21	0.41	nd	nd
5a		5	0.08	0.14 ± 0.02	0.28 ± 0.03
6a		5	0.09	0.16 ± 0.02	0.32 ± 0.04
19b	6-OCH ₃	6	0.24	nd	nd
5b	(<i>meta</i>)	^c	$<0.005^d$	nd	nd
6b		^e	$<0.007^d$	0.19 ± 0.02	$>1.9^c \pm 0.2$
19c	5-OCH ₃	7	0.28	nd	nd
5c	(<i>para</i>)	7	0.29	0.08 ± 0.02	0.13 ± 0.03
6c		7	0.28	0.08 ± 0.02	0.13 ± 0.03

^aQuantum yields of fluorescence were determined by comparison with a value of 0.13 for toluene in methanol.²⁷

^bUsing 3-methoxybenzyl acetate ($\Phi_{RXN} = 0.13$) in aqueous dioxane as an actinometer.

^cThese lifetimes are too short (<1 ns) to be measured by our single photon counting equipment.

^dThese values are maximums because the esters could be contaminated with a small amount of the precursor alcohol, which is highly fluorescent.

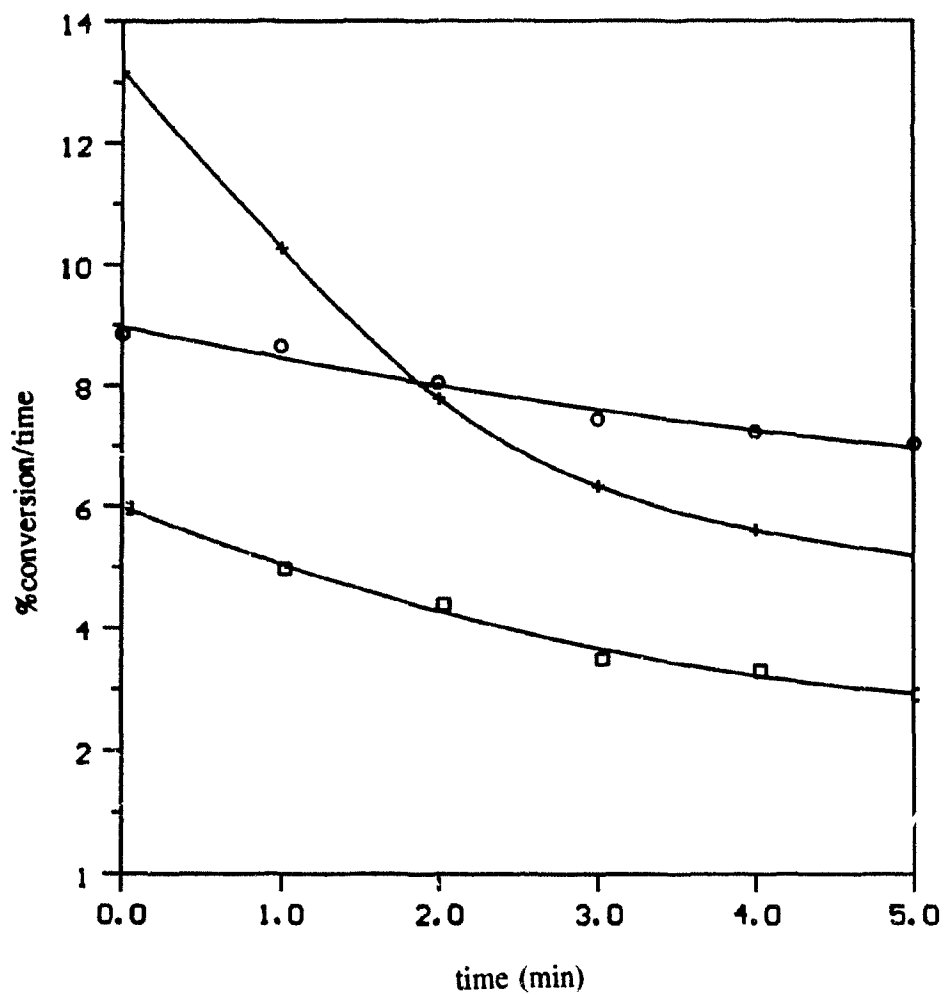
^eBased on a maximum lifetime of 1ns.

nd, Not determined.

fluorescence quantum yields and lifetimes for the esters provide a reasonable measurement of reactivity of the esters. The quantum yields of fluorescence and the singlet lifetimes are diminished for the unsubstituted and *meta* substituted esters relative to the alcohol. However, the quantum yields of fluorescence and lifetimes of the *para* substituted esters do not significantly differ from those of the alcohol. These changes indicate that the unsubstituted esters, **5a** and **6a**, and the *meta* methoxy substituted esters, **5b** and **6b**, are quite reactive whereas the *para* substituted esters, **5c** and **6c**, are much less reactive. The largest difference between the benzylic (Table 3) and indanyl esters is that the fluorescence quantum yields are slightly higher for the indanyl compounds. This is presumably due to loss of free rotor type decay⁶¹ in the rigid indanyl compounds.

The differing reactivity of these esters was quantified by measuring the quantum yields of reaction using 3-methoxybenzyl acetate in aqueous dioxane as the actinometer.⁵ The esters were irradiated simultaneously with the actinometer and plots were made of % conversion/time versus time. Typical plots are shown in Figure 4. These plots are curved because the products have the same chromophore as the starting material and as the % conversion increases more of the incident light is being absorbed by the products. This problem in quantum yield determinations has been discussed in detail.⁶² These plots were extrapolated to zero time and the intercepts were used to measure quantum yields based on the reported value of 0.13 for the 3-methoxybenzyl acetate in aqueous dioxane.⁵ Details are given in the experimental section, 1.5.10. Using the quantum yields of reaction, the rate constants for bond

Figure 4. A plot of % conversion vs. time for the photolysis of the indanyl esters **6b,c** and 3-methoxy benzyl acetate in aqueous dioxane. The circles are for 3-methoxybenzyl acetate, the crosses for 6-methoxy-2,2-dimethyl-1-indanyl pivalate (**6b**), and the squares are for 5-methoxy-2,2-dimethyl-1-indanyl pivalate (**6c**).



cleavage, k_R , were calculated. These are also given in Table 12. These values allow the enhanced reactivity of the unsubstituted and *meta* methoxy substituted relative to the *para* methoxy substituted esters to be expressed quantitatively. The *meta* methoxy substituted esters have the largest rate constants for cleavage followed by the unsubstituted and the *para* methoxy substituted esters. The relative ratio of the rate constants is $> 15:1:2.5$ for *meta:para:unsubstituted*

The indanyl esters are restricted to a conformation that is ideal for bond cleavage yet the unsubstituted and *meta* methoxy substituted esters are still more reactive than the *para* substituted esters. At least one factor controlling cleavage efficiencies must be independent of conformation. This factor could be the *meta* effect. However, instead of increasing the efficiency of heterolytic cleavage, the mechanistic step that must be enhanced is homolytic cleavage because the results in the previous sections have shown that heterolytic cleavage is not an important reaction pathway. Substituent rate enhancements in the ground state are generally small for reactions producing a benzylic radical intermediate. For example, in the free radical hydrogen abstraction reaction of toluene by bromine atoms, the reaction rates correlate with σ^+ giving $\rho^+ = -1.4$.^{63,64,65} This corresponds to relative rates of 10:0.9:1 for *para:meta:unsubstituted*.

Quantum yields of reaction for 3-methoxybenzyl acetate and 4-methoxybenzyl acetate in aqueous dioxane have been reported by Zimmerman and Sandel.⁶ The values are 0.13 and 0.016 respectively. Rate constants for reaction can be calculated using these quantum yields and the singlet lifetimes in Table 3. The ratio of rate

constants for *meta:para* is 48:1. The authors did not study the unsubstituted ester.⁵ This ratio is much greater than the *meta:para* ratio of 15:1 calculated for the indanyl esters. The greater reactivity difference for the conformationally free benzylic esters cannot be attributed to an enhanced reactivity of the *meta* isomer because the indanyl esters are locked into the reactive conformer. Therefore, the *para* isomer must be less reactive than expected in the benzylic system. This suggestion is confirmed by a calculation of $k_R = 0.027 \times 10^8 \text{ s}^{-1}$ for 4-methoxybenzyl acetate, **1a**, from the quantum yield of reaction (0.016) and the singlet lifetime (6 ns). This value of k_R is lower by a factor of five than that obtained ($0.13 \times 10^8 \text{ s}^{-1}$) for 4-methoxy-2,2-dimethyl-1-indanyl acetate, **5c**. The obvious difference between the indanyl system and the benzylic system is loss of conformational motion. The likely reason for the lower reaction rate for the *para* methoxy substituted benzylic ester is that the *para* methoxy substituent is increasing the population of the unreactive conformer and thus causing the rate of cleavage to decrease.

To confirm that the differences between the indanyl and benzylic esters are not due to the different solvents used for the quantum yield determinations, quantum yields of reaction for 3-methoxybenzyl acetate and 4-methoxybenzyl acetate in methanol were also measured. The values determined were 0.18 and 0.02 which gives relative rate constants of cleavage for *meta:para* of 55:1. This ratio is not significantly different from the value of 48:1 measured in aqueous dioxane. Therefore, the differences in reactivity must be conformational and cannot be attributed to solvent differences.

In addition to determining the importance of conformationally mobility, the

data in Table 12 can also be used to calculate rate constants for internal conversion, k_{IC} . The singlet excited state of esters **5** and **6** has four pathways of decay; fluorescence (k_F), reaction (k_R), intersystem crossing (k_{ISC}) and internal conversion (k_{IC}). Therefore, the total decay of the singlet excited state, k , is given by eq 32.

$$k = k_F + k_R + k_{ISC} + k_{IC} = 1/\tau_s \quad (32)$$

The value of k is the reciprocal of the singlet lifetime, τ_s . Values for k_I and k_R have been calculated from the lifetimes and the quantum yields of fluorescence and reaction, respectively (Table 12). Values of k_{ISC} can be estimated by assuming that the values for toluene and anisole will be good models for the unsubstituted and methoxy substituted esters, respectively. The quantum yield of intersystem crossing, singlet lifetime and the calculated k_{ISC} for toluene are 0.53,²⁷ 35 ns,²⁷ and 1.4×10^7 s⁻¹, respectively. For anisole, the corresponding values are 0.64,⁶⁶ 7.5 ns,⁶⁶ and 8.9×10^7 s⁻¹, respectively.

Using the k_{ISC} values for toluene and anisole, k_{IC} can be calculated from eq 32. This is only possible for the unsubstituted and the *para* methoxy substituted indanyl esters for which reliable measurements of the lifetime and fluorescence quantum yield can be made. For these rigid indanyl esters the only reasonable pathway for internal conversion is homolytic cleavage of the C-O bond and reformation of that bond before conversion to product occurs. This internal return process will result in oxygen scrambling.

Using eq 32, along with the values for the experimental (k , k_R , k_F) and

estimated (k_{isc}) rate constants, the value of k_{ic} for the unsubstituted indanyl ester is $13.6 \times 10^7 \text{ s}^{-1}$. Therefore, this pathway is accounting for 68% of the reactivity of the singlet excited state (k_{isc}/k). For the *para* methoxy substituted ester, k_{ic} is $2.0 \times 10^7 \text{ s}^{-1}$. The internal return/internal conversion pathway is now accounting for only 14% of the reactivity of the excited state. Recently, efficiencies of internal return from ^{18}O scrambling experiments, as a function of substituent, have been determined for 1-naphthylethyl esters.³³ The efficiency of internal return was also greatly diminished by the presence of a *para* methoxy substituent on the aromatic ring. However, as was mentioned previously the internal return pathway has only a small perturbation on calculated rate constants.

1.4.5 Conclusions

This work has shown that the influence of substituents on photochemical benzylic reactivity is three-fold. First, substituents control the oxidation potential of the benzylic radical and thus the rate of electron transfer. This is the major effect that controls the yield of the ion-pair product. Second, substituents also exert a strong electronic effect on the rate of the homolytic cleavage step which is fastest for a *meta* methoxy substituted case. Finally, if the esters are conformationally unrestricted, the substituents also alter the populations of the two possible conformers. The results suggest that a methoxy group in the *para* position increases the population of the unreactive parallel conformer, **15**, and this leads to a decrease in the rate of cleavage. Confirmation of this would require extensive NMR studies and *ab initio* MO

calculations.

This work also provides rate constants for internal return as a function of substituents. The internal return pathway accounts for 68% of the excited singlet state reactivity for the unsubstituted ester and only 14% for the *para* methoxy substituted ester.

1.5 Experimental

1.5.1 General Procedures

Proton (^1H) and carbon (^{13}C) nuclear magnetic resonance (NMR) spectra were obtained in CDCl_3 on a Bruker AC 250 F NMR spectrometer in automation mode. Chemical shifts are reported in parts per million (δ) relative to tetramethylsilane (0.00) as an internal standard. Multiplicities are abbreviated as follows: s = singlet, d = doublet, t = triplet, q = quartet, m = multiplet. Infrared spectra were obtained on a Nicolet 205 FTIR spectrophotometer and frequencies are reported in wavenumbers (cm^{-1}). Ultraviolet (UV) spectra were obtained in methanol solution in 1 cm quartz cuvettes on a Varian Cary 219 spectrometer. Wavelength maxima (λ_{max}) are reported in nanometers. GC/MS analyses were done on a Hewlett Packard 5890 A GC 5970 with a mass selective detector. The column used was a 25 m x 0.2 mm 5% phenylmethyl silicone on fused silica with a film thickness of 0.25 μm . Masses are reported in units of mass over charge (m/z). Intensities are reported as a percent of the base peak intensity. The molecular ion is indicated by M^+ . GC/FID analyses were obtained on either a Hewlett Packard 5890 A gas chromatograph (column: 1 m glass column, 10% Fluorad FC-431 and 1% H_3PO_4 on Chromosorb W HP 80/100 mesh) using a Hewlett Packard 7673 automatic injector with a Hewlett Packard 7673 A controller and a Hewlett Packard 3396 A integrator or a Perkin Elmer autosystem GC/FID (column: 12 m \times 0.22 mm 100% polymethylsilicone on fused silica, film thickness of 0.23 μm). HPLC analyses were obtained with a Waters 6000 solvent delivery system and a Waters U6K injector under isocratic conditions with a flow rate

of 2 mL/min using a Brownlee Lab Spheri-10 10 μ l reverse phase column (25 x 0.46 cm) with a Waters Model 450 variable wavelength detector. UV detection for monitoring the reactions was at 254 nm. Combustion analyses were carried out by Canadian Microanalytical Service Ltd., Delta, BC, Canada. Silica gel F 6145 plates from Sigma were used for thin layer chromatography (TLC). Silica gel 60 Å (70-230 mesh), purchased from the Aldrich Chemical Company, was used for normal column chromatography.

1.5.2 Fluorescence Measurements

Fluorescence measurements were done using a Perkin Elmer MPF 66 fluorescence spectrometer at 25 °C. Corrected spectra were obtained. All samples were degassed by three freeze-pump-thaw cycles. Fluorescence quantum yields were determined by comparison with a fluorescence quantum yield of 0.13 for toluene in methanol.²⁷ Singlet-state energies were determined by the position of the 0,0 band using the overlap between the emission and excitation spectra. Singlet lifetimes were measured using a PRA single photon counting apparatus with a hydrogen flash lamp of pulse width about 1 ns.

1.5.3 Syntheses of the Benzyl Alcohols 7a-l and the Indanyl Alcohols 19a-c Syntheses of the Benzylic Alcohols (7a-l).

The preparation of the esters **1a-l** and **2a-l** required the corresponding benzyl alcohols. The alcohols **7a,c,d,e,j,l** were purchased from the Aldrich Chemical Company. The alcohols **7b,f** have been prepared and characterized elsewhere.¹⁷

3,5-Dimethoxybenzyl Alcohol (7h): This alcohol was prepared by reducing 3,5-dimethoxybenzoic acid with 1M borane/THF solution in dry THF. Upon completion of the reaction, water was added to the reaction mixture and extracted with dichloromethane. Rotary evaporation of the organic layer gave 8.5 g (51 mmol, 89%) of the crude alcohol. The alcohol was purified by bulb to bulb distillation. The ¹H NMR agreed with the literature⁶⁷ spectrum: ¹H NMR δ 6.6 (s, 2H), 6.45 (s, 1H), 4.72 (s, 2H), 3.85 (s, 6H), 2.0 (s, 1H).

Preparation of Alcohols 7g, 7i, 7k

To a solution of 0.024 mol of the aldehyde in 40 mL of ethanol was slowly added 0.008 mol of sodium borohydride. The solution was kept at room temperature, and the reaction was stirred for 3 h. Water (50 mL) was then added and the aqueous layer was extracted twice with CH₂Cl₂ (2 × 40 mL), the organic layers were combined and dried with MgSO₄, and the solvent was removed under reduced pressure to give the impure alcohol. The alcohols were purified by bulb-to-bulb distillation. The ¹H NMR spectra of the pure alcohols were consistent with the previously reported spectra: 3,4-dimethoxybenzyl alcohol,⁶⁸ 3,4,5-trimethoxybenzyl alcohol,⁶⁹ 3-cyanobenzyl alcohol.⁷⁰

Synthesis of the Indanyl Alcohols 19a-c

Synthesis of the 2,2-dimethyl-1-indanols, **19a-c**, required preparation of the corresponding indanones, **18a-c**, which were then reduced to the alcohols as

described above

Dimethylation of Indanones 17a-c The indanones, purchased from Aldrich Chemical Co., were dimethylated using the procedure of Lissel *et al.*⁷¹ Powdered KOH, 0.34 mol (19 g), was mixed with 100 mL of toluene and 0.1 mmol of 18-crown-6. The ketone, 50 mmol, was added and the mixture was heated to 70 °C. To this heated mixture was added 0.32 mol of iodomethane. The solution was refluxed overnight. After cooling, water was added and the two layers were separated. The aqueous layer was washed with ether and the combined organic layers were washed with saturated sodium bisulphite and dried over magnesium sulphate. The ketones were purified by column chromatography on silica gel.

2,2-Dimethyl-1-Indanone (18a): This compound has been previously prepared by Orliac-Le Moing *et al.*⁷² The spectral data for this compound are provided below because the authors reported only a partial ¹H NMR spectrum. ¹H NMR δ 7.75 (d, 1H, J = 7.6 Hz), 7.59 (t, 1H, J = 7.5 Hz), 7.42 (d, 1H, J = 7.3 Hz), 7.36 (t, 1H, J = 7.5 Hz), 3.00 (s, 2H), 1.24 (s, 6H); ¹³C NMR δ 211.4 (C=O), 152.2 (C), 135.3 (C), 134.8 (CH), 127.4 (CH), 126.7 (CH), 124.4 (CH), 45.5 (C), 42.9 (CH₂), 25.3 (CH₃); GC/MS *m/z*: 160 (M⁺, 40), 146 (10), 145 (100), 142 (13), 117 (26), 116 (10), 115 (35), 91 (24), 90 (12), 89 (13), 77 (10), 65 (13), 63 (14), 51 (13).

6-Methoxy-2,2-Dimethyl-1-Indanone (18b): $^1\text{H NMR } \delta$ 7.32 (d, 1H, $J = 9.2$ Hz), 7.21-7.18 (m, 2H), 3.84 (s, 3H), 2.93 (s, 2H), 1.24 (s, 6H); $^{13}\text{C NMR } \delta$ 211.5 (C=O), 159.4 (C), 145.0 (C), 136.4 (C), 127.3 (CH), 124.3 (CH), 105.5 (CH), 55.6 (CH₃-O), 46.3 (C), 42.2 (CH₂), 25.3 (CH₃); GC/MS m/z 190 (M⁺, 51), 176 (13), 175 (100), 172 (21), 161 (13), 147 (21), 131 (12), 129 (10), 121 (13), 117 (10), 115 (22), 103 (19), 91 (43), 89 (12), 78 (19), 77 (40), 65 (12), 63 (25), 53 (10), 51 (38).

5-Methoxy-2,2-Dimethyl-1-Indanone (18c): $^1\text{H NMR } \delta$ 7.69 (d, 1H, $J = 8.4$ Hz), 6.88 (m, 2H), 3.88 (s, 3H), 2.95 (s, 2H), 1.22 (s, 6H); $^{13}\text{C NMR } \delta$ 209.6 (C=O), 165.5 (C), 155.13 (C), 128.5 (C), 126.1 (CH), 115.4 (CH), 109.7 (CH), 55.6 (CH₃-O), 45.6 (C), 42.9 (CH₂), 25.4 (CH₃); GC/MS m/z 190 (M⁺, 29), 176 (12), 175 (100), 115 (12), 91 (23), 77 (17), 63 (15), 51 (16).

Preparation of the Indanyl Alcohols (19a-c)

The alcohols were prepared by sodium borohydride reduction of the ketones **18a-c** in methanol, except for 1-indanol which was purchased from the Aldrich Chemical Co.

2,2-Dimethyl-1-Indanol (19a): This compound has been prepared previously by Orliac-Le Moing *et al.*⁷² The spectral data for this compound are provided below because the authors reported only a partial $^1\text{H NMR}$ spectrum. $^1\text{H NMR } \delta$ 7.39-7.33 (m, 1H), 7.25-7.16 (m, 3H), 4.67 (d, 1H, $J = 5.03$ Hz), 2.78 (d, 1H, $J = 15.5$ Hz).

2.57 (d, 1H, $J = 15.5$ Hz), 1.97 (d, 1H, $J = 5.8$ Hz), 1.19 (s, 3H), 1.04 (s, 3H);
 ^{13}C NMR δ 144.5 (C), 141.9 (C), 128.0 (CH), 126.6 (CH), 125.0 (CH), 124.5 (CH),
83.5 (CH-O), 44.9 (CH₂), 44.6 (C), 26.8 (CH₃), 21.5 (CH₃); GC/MS m/z 162 (M⁺,
43), 161 (21), 147 (13), 144 (17), 143 (12), 130 (12), 129 (100), 128 (25), 127 (10),
120 (19), 119 (51), 115 (21), 91 (50), 89 (10), 77 (21), 65 (21), 63 (13), 51 (19).

6-Methoxy-2,2-Dimethyl-1-Indanol (19b): ^1H NMR δ 7.06 (d, 1H, $J = 8.1$ Hz),
6.91 (d, 1H, $J = 2.0$ Hz), 6.76 (dd, 1H, $J_1 = 8.2$ Hz, $J_2 = 2.4$ Hz), 4.63 (s, 1H),
3.78 (s, 3H), 2.68 (d, 1H, $J = 15.1$ Hz), 2.59 (d, 1H, $J = 15.1$ Hz), 1.85 (brs, 1H),
1.17 (s, 3H), 1.00 (s, 3H); ^{13}C NMR δ 158.9 (C), 145.9 (C), 133.6 (C), 125.7
(CH), 114.3 (CH), 109.4 (CH), 83.7 (CH-O), 55.4 (CH₃-O), 45.1 (C), 44.1 (CH₂),
26.8 (CH₃), 21.4 (CH₃); GC/MS m/z 192 (M⁺, 7), 177 (15), 174 (21), 159 (47), 150
(16), 149 (100), 131 (10), 121 (94), 116 (13), 115 (28), 105 (10), 103 (12), 91 (50),
89 (12), 79 (13), 78 (20), 77 (50), 65 (18), 63 (16), 55 (12), 53 (13), 52 (10), 51
(30).

5-Methoxy-2,2-Dimethyl-1-Indanol (19c): ^1H NMR δ 7.27 (d, 1H, $J = 7.9$ Hz),
6.78-6.74 (m, 2H), 4.59 (s, 1H), 3.79 (s, 3H), 2.76 (d, 1H, $J = 15.7$ Hz), 2.61 (d,
1H, $J = 15.7$ Hz), 1.59 (s, 1H), 1.14 (s, 3H), 1.06 (s, 3H); ^{13}C NMR δ 160.0 (C),
143.9 (C), 136.8 (C), 125.4 (CH), 112.4 (CH), 110.5 (CH), 82.1 (CH-O), 55.4
(CH₃-O), 45.0 (CH₂), 44.7 (C), 27.0 (CH₃), 21.7 (CH₃); GC/MS m/z 192 (M⁺, 66),
191 (100), 177 (32), 176 (11), 175 (34), 174 (16), 173 (16), 162 (11), 161 (50), 159

(59), 158 (16), 150 (13), 149 (53), 145 (11), 144 (25), 135 (16), 131 (16), 129 (12), 128 (15), 121 (25), 116 (16), 115 (32), 105 (12), 103 (13), 91 (50), 89 (13), 79 (15), 78 (21), 77 (50), 65 (25), 63 (25), 55 (12), 53 (12), 51 (27).

1.5.4 Preparation and Characterization of the Benzyl and Indanyl Esters 1-6

The corresponding acid chloride (0.02 mol) in 30 ml of dry benzene was added to a solution of the benzyl or indanyl alcohol (0.02 mol) and 1 ml of pyridine in 50 ml of dry benzene. The solution was stirred overnight at room temperature. Then 50 ml of water was added and the two layers were separated. The benzene layer was washed twice with 10% aqueous HCl, once with 5% aqueous NaOH and finally with water. The organic layer was dried (MgSO_4), filtered, and evaporated under reduced pressure to give the crude ester. The esters were purified by column chromatography followed by distillation. Unless otherwise noted the ester is an oil. The yields were 40-80%. Benzyl acetate (1c) was purchased from the Aldrich Chemical Company. The esters **1a,b,d,f** and **2a,b,d,f** were prepared and characterized previously.¹⁷

4-(Trifluoromethyl)benzyl Acetate (1e): bp 75-78 °C at 2 mm Hg (lit.¹⁷ 126-127 °C at 30 mmHg); ^1H NMR δ 7.63 (d, 2H, $J = 8.2$ Hz), 7.47 (d, 2H, $J = 8.2$ Hz), 5.16 (s, 2H), 2.13 (s, 3H); ^{13}C NMR δ 170.7 (C=O), 140.0 (C), 130.0 (q, C, J_{CF} = 37.0 Hz), 128.2 (CH), 125.6 (q, CH, J_{CF} = 3.82 Hz), 124.0 (q, CF_3 , J_{CF} = 272 Hz), 65.3 ($\text{CH}_2\text{-O}$), 20.9 (CH_3); IR (neat) 2950, 1740 (C=O), 1617, 1450, 1375, 1360, 1320, 1220, 1160, 1120, 1060, 1040, 1012, 830, 820 cm^{-1} ; GC/MS 218 m/z (M^+ , 25), 199

(15), 176 (100), 159 (94), 158 (30), 145 (23), 127 (47), 119 (14), 109 (47), 108 (13), 107 (96), 95 (10), 89 (18), 77 (13), 75 (15), 63 (16), 51 (16); UV (CH₃OH) λ_{\max} (ϵ) 254 (411), 259 (490), 265 (379);

3,4-Dimethoxybenzyl Acetate (1g): ¹H NMR 6.96-6.83 (m, 3H), 5.04 (s, 2H), 3.89 (s, 3H), 3.88 (s, 3H), 2.09 (s, 3H); ¹³C NMR δ 170.9 (C=O), 149.1 (C), 149.0 (C), 128.4 (C), 121.3 (CH), 111.8 (CH), 111.0 (CH), 66.4 (CH₂-O), 55.88 (CH₃-O), 55.86 (CH₃-O), 21.1 (CH₃); IR (neat) 3000, 2946, 2833, 1736, 1518, 1263, 1237, 1161, 1140, 1028 cm⁻¹; GC/MS *m/z* 210 (M⁺, 58), 168 (31), 152 (12), 151 (100), 137 (14), 135 (12), 107 (23), 79 (12), 77 (12), 65 (12), 51 (12); UV (CH₃OH) λ_{\max} (ϵ) 276 (2400). Anal. Calcd for C₁₁H₁₄O₄: C, 62.85; H, 6.71. Found: C, 62.36; H, 6.75.

3,5-Dimethoxybenzyl Acetate (1h): ¹H NMR δ 6.50 (s, 2H), 6.41 (s, 1H), 5.04 (s, 2H), 3.79 (s, 6H), 2.11 (s, 3H); ¹³C NMR δ 170.7 (C=O), 160.9 (C), 138.2 (C), 106.0 (CH), 100.1 (CH₂), 66.2 (CH₂-O), 55.3 (CH₃-O), 20.9 (CH₃); IR (neat) 2910, 2904, 2840, 1769, 1609, 1465, 1242, 1154, 1070, 834 cm⁻¹; GC/MS *m/z* 210 (M⁺, 49), 169 (11), 168 (100), 167 (40), 151 (24), 139 (98), 124 (18), 108 (12), 107 (12), 91 (24), 79 (19), 78 (21), 77 (39), 65 (25), 63 (19); UV (CH₃OH) λ_{\max} (ϵ) 278 (2100). Anal. Calcd for C₁₁H₁₄O₄: C, 62.85; H, 6.71. Found: C, 62.57; H, 6.65.

3,4,5-Trimethoxybenzyl Acetate (1i): ¹H NMR δ 6.47 (s, 2H), 4.89 (s, 2H), 3.73

(s, 6H), 3.69 (s, 3H), 1.97 (s, 3H); ^{13}C NMR δ 170.7 (C=O), 153.3 (C), 137.9 (C), 131.6 (C), 105.6 (CH), 66.5 (CH₂-O), 60.7 (CH₁-O), 56.1 (CH-O), 21.0 (CH₃); IR (neat) 2998, 2841, 1739, 1592, 1508, 1462, 1423, 1236, 1128, 1009 cm⁻¹; GC/MS m/z 240 (M⁺, 86), 198 (52), 155 (13), 138 (13), 123 (25), 95 (25), 77 (18), 52 (13); UV (CH₃OH) λ_{max} (ϵ) 265 (730). Anal. Calcd for C₁₇H₁₆O₄: C, 59.99; H, 6.71. Found: C, 59.94; H, 6.68.

3-Methylbenzyl Acetate (1j): ^1H NMR δ 7.24-7.08 (m, 4H), 5.04 (s, 2H), 2.32 (s, 3H), 2.06 (s, 3H); ^{13}C NMR δ 170.8 (C=O), 138.2 (C), 136.0 (C), 129.06 (CH), 129.03 (CH), 128.5 (CH), 125.4 (CH), 66.4 (CH₂-O), 21.3 (CH₃), 21.0 (CH₃); IR (neat) 3026, 2954-2923, 1740, 1490, 1460, 1360, 1229, 1028 cm⁻¹; GC/MS m/z 164 (M⁺, 41), 123 (10), 122 (100), 107 (50), 106 (10), 105 (76), 104 (38), 103 (38), 93 (25), 91 (40), 79 (32), 78 (47), 77 (49), 65 (24), 63 (19), 51 (20); UV (CH₃OH) λ_{max} (ϵ) 261 (260).

3-Cyanobenzyl Acetate (1k): ^1H NMR δ 7.67-7.46 (m, 4H), 5.14 (s, 2H), 2.14 (s, 3H); ^{13}C NMR δ 170.5 (C=O), 137.6 (C), 132.6 (CH), 131.8 (CH), 131.4 (CH), 129.5 (CH), 118.5 (CN), 112.7 (C), 64.8 (CH₂), 20.9 (CH₃); IR (neat) 3075, 2950, 2232, 1746, 1380, 1227, 688 cm⁻¹; GC/MS m/z 175 (M⁺, 28), 134 (10), 133 (100), 132 (24), 116 (81), 115 (25), 104 (38), 102 (15), 89 (40), 77 (13), 76 (17), 75 (16), 63 (23), 62 (10), 51 (21); UV (CH₃OH) λ_{max} (ϵ) 269 (630). Anal. Calcd for C₁₀H₉NO₂: C, 68.56; H, 5.18; N, 8.00; Found: C, 68.07; H, 5.16; N, 7.81.

3-Trifluoromethylbenzyl Acetate (11): ^1H NMR δ 7.62-7.44 (m, 4H), 5.15 (s, 2H), 2.12 (s, 3H); ^{13}C NMR δ 170.6 (C=O), 137.0 (C), 131.4 (CH), 129.0 (CH), 124.9 (CH), 124.8 (CH), 65.3 (CH₂), 20.8 (CH₃); IR (neat) 3080, 2960, 1751, 1450, 1390, 1331, 1239, 1165, 1125, 1075, 1050, 800, 710 cm^{-1} ; GC/MS m/z 218 (M^+ , 16), 176 (100), 159 (75), 158 (31), 145 (25), 137 (11), 127 (49), 119 (15), 109 (38), 107 (38), 89 (19), 77 (15), 75 (17), 69 (16), 51 (19); UV (CH₃OH) λ_{max} (ϵ) 259 (500).

1-Indanyl Acetate (3): This compound has been prepared previously by Groenewold *et al.*⁷⁴ Because only a partial 70 eV mass spectrum was reported, spectral characterization of this ester is provided below. ^1H NMR δ 7.42-7.39 (d, 1H, $J = 7.0$ Hz), 7.29-7.20 (m, 3H), 6.19 (dd, 1H, $J_1 = 6.9$ Hz, $J_2 = 3.7$ Hz), 3.18-3.05 (m, 1H), 2.95-2.80 (m, 1H), 2.56-2.42 (m, 1H), 2.18-2.05 (m, 1H), 2.07 (s, 3H); ^{13}C NMR δ 171.1 (C=O), 144.4 (C), 141.0 (C), 128.9 (CH), 126.7 (CH), 125.4 (CH), 124.8 (CH), 78.3 (CH-O), 32.3 (CH₂), 30.2 (CH₂), 21.3 (CH₃); GC/MS m/z 176 (M^+ , 0.1), 134 (12), 133 (24), 117 (73), 116 (100), 115 (96), 91 (23), 89 (12), 77 (21), 65 (11), 63 (18), 51 (20); Anal. Calcd for C₁₁H₁₂O₂: C, 74.98; H, 5.86; Found: C, 75.19; H, 6.61.

2,2-Dimethyl-1-Indanyl Acetate (5a): ^1H NMR δ 7.35- 7.32 (m, 1H), 7.29-7.16 (m, 3H), 5.81 (s, 1H), 2.92 (d, 1H, $J = 15.6$ Hz), 2.66 (d, 1H, $J = 15.6$ Hz), 2.08 (s, 3H), 1.12 (s, 6H); ^{13}C NMR δ 171.1 (C=O), 143.6 (C), 141.1 (C), 128.8 (CH), 126.7 (CH), 126.1 (CH), 125.1 (CH), 84.1 (CH-O), 45.6 (CH₂), 43.3 (C), 27.3

(CH₃), 22.5 (CH₃), 21.2 (CH₃); GC/MS *m/z* (No M⁺ observed), 152 (20), 161 (13), 145 (25), 144 (97), 143 (28), 130 (19), 129 (100), 128 (48), 127 (13), 119 (17), 117 (12), 115 (38), 91 (38), 89 (11), 77 (19), 65 (17), 63 (12), 51 (14); UV (CH₃OH) λ_{max} (ε) 262 (818); Calcd Exact Mass for C₁₁H₁₆O₂: 204.115, Found: 204.115.

6-Methoxy-2,2-Dimethyl-1-Indanyl Acetate (5b): ¹H NMR δ 7.09 (d, 1H, J = 7.9 Hz), 6.88-6.81 (m, 2H), 5.77 (s, 1H), 3.78 (s, 3H), 2.84 (d, 1H, J = 15.1 Hz), 2.59 (d, 1H, J = 15.1 Hz), 2.09 (s, 3H), 1.12 (s, 6H); ¹³C NMR δ 171.1 (C=O), 158.8 (C), 142.3 (C), 135.5 (C), 125.7 (CH), 115.3 (CH), 110.8 (CH), 84.2 (CH-O), 55.5 (CH₃-O), 44.7 (CH₂), 43.8 (C), 27.4 (CH₃), 22.5 (CH₃), 21.2 (CH₃); GC/MS *m/z* 234 (M⁺, 10), 175 (21), 174 (100), 159 (36), 43 (15); UV (CH₃OH) λ_{max} (ε) 279 (2800); Calcd Exact Mass for C₁₁H₁₈O₃: 234.126; Found: 234.127.

4-(Trifluoromethyl)benzyl Pivalate (2e). bp 84-86 °C at 22 mm Hg; ¹H NMR δ 7.61 (d, 2H, J = 8.1 Hz), 7.45 (d, 2H, J = 8.1 Hz), 5.16 (s, 2H), 1.25 (s, 9H); ¹³C NMR δ 178.2 (C=O), 140.6 (C), 130.0 (q, C, J_{C-F} = 34 Hz), 127.7 (CH), 125.5 (q, CH, J_{C-F} = 3.82 Hz), 124.0 (q, CF₃, J_{C-F} = 272 Hz), 65.1 (CH₂), 38.9 (C), 27.2 (CH₃); IR (neat) 2970, 2865, 1730 (C=O), 1618, 1478, 1458, 1418, 1396, 1365, 1322, 1280, 1140, 1062, 1015, 820 cm⁻¹; GC/MS *m/z* 260 (M⁺, 3), 159 (47), 109 (18), 85 (12), 57 (100). UV (CH₃OH) λ_{max} (ε) 253 (419), 259 (503), 265 (398).

3,4-Dimethoxybenzyl Pivalate (2g): ¹H NMR δ 6.93-6.82 (m, 3H), 5.05 (s, 2H),

3.88 (s, 3H), 3.87 (s, 3H), 1.22 (s, 9H); ^{13}C NMR δ 178.3 (C=O), 148.88 (C), 148.81 (C), 129.0 (C), 120.6 (CH), 111.2 (CH), 110.9 (CH), 66.0 (CH₂-O), 55.84 (CH₃-O), 55.80 (CH₃-O), 38.8 (C), 27.2 (CH₃); IR (neat) 2976-2875 (C-H), 2838 (O-CH₃), 1727 (C=O), 1519, 1464, 1278, 1268, 1239, 1159, 1148. 1030 cm⁻¹; GC/MS *m/z* 252 (M⁺, 15), 151 (100); UV (CH₃OH) λ_{max} (ϵ) 276 (2900). Anal. Calcd for C₁₄H₂₀O₄: C, 66.65; H, 7.99. Found: C, 66.57; H, 7.95.

3,5-Dimethoxybenzyl Pivalate (2h): ^1H NMR δ 6.47 (s, 2H), 6.39 (s, 1H), 5.05 (s, 2H), 3.78 (s, 6H), 1.24 (s, 9H); ^{13}C NMR δ 178.2 (C=O) 161.0 (C), 138.8 (C), 105.3 (CH), 99.8 (CH), 65.8 (CH₂-O), 55.3 (CH₃-O), 38.8 (C), 27.2 (CH₃); IR (neat) 2938, 2840, 1729 (C=O), 1610, 1478, 1343, 1035, 833 cm⁻¹; GC/MS *m/z* 252 (M⁺, 41), 168 (24), 167 (100), 151 (79), 91 (22), 78 (19), 77 (24), 65 (19), 57 (98); UV (CH₃OH) λ_{max} (ϵ) 278 (1500). Anal. Calcd for C₁₄H₂₀O₄: C, 66.65; H, 7.99. Found: C, 66.65; H, 7.93.

3,4,5-Trimethoxybenzyl Pivalate (2i): ^1H NMR δ 6.58 (s, 2H), 5.05 (s, 2H), 3.84 (s, 6H), 3.83 (s, 3H), 1.24 (s, 9H); ^{13}C NMR δ 177.4 (C=O), 152.7 (C), 137.1 (C), 131.7 (C), 104.0 (CH), 65.4 (CH₂-O), 60.4 (CH₃-O), 55.3 (CH₃-O), 38.1 (C), 26.6 (CH₃); IR (neat) 2970-2908, 2640 (O-CH₃), 1728 (C=O), 1592, 1509, 1462, 1239, 1152, 1128 (C-O) cm⁻¹; GC/MS *m/z* 282 (M⁺, 27), 197 (13), 182 (8), 181 (100), 57 (27); UV (CH₃OH) λ_{max} (ϵ) 264 (710). Anal. Calcd for C₁₅H₂₂O₅: C, 63.81; H, 7.85. Found: C, 64.05; H, 7.93.

3-Methylbenzyl Pivalate (2j): $^1\text{H NMR}$ δ 7.19-7.10 (m, 4H), 5.05 (s, 2H), 2.33 (s, 3H), 1.24 (s, 9H); $^{13}\text{C NMR}$ δ 178.2 (C=O), 138.0 (C), 136.4 (C), 128.7 (CH), 128.48 (CH), 128.45 (CH), 66.0 (CH₂-O), 38.7 (CH₃), 27.2 (CH₃), 21.3 (CH₃); IR (neat) 3028, 2973-2872, 1735, 1490, 1459, 1395, 1282, 1148 cm⁻¹; GC/MS m/z 206 (M⁺, 12), 106 (12), 105 (98), 103 (11), 91 (12), 79 (12), 78 (11), 57 (100); UV (CH₃OH) λ_{max} (ϵ) 268 (130). Anal. Calcd for C₁₄H₁₈O₂: C, 75.69; H, 8.80. Found: C, 75.60; H, 8.64.

1-Indanyl Pivalate (4): $^1\text{H NMR}$ δ 7.35 (d, 1H, $J = 7.0$ Hz), 7.28-7.19 (m, 2H), 6.18 (dd, 1H, $J_1 = 7.0$ Hz, $J_2 = 4.7$ Hz), 3.14-3.02 (m, 1H), 2.93-2.81 (m, 1H), 2.60-2.46 (m, 1H), 2.08-1.95 (m, 1H), 1.20 (s, 9H); $^{13}\text{C NMR}$ δ 178.6 (C=O), 144.1 (C), 141.4 (C), 128.7 (CH), 126.7 (CH), 125.2 (CH), 124.8 (CH), 78.0 (CH-O), 38.7 (C), 32.3 (CH₂), 30.1 (CH₂), 27.1 (CH₃); GC/MS m/z 218 (M⁺, 0.1), 117 (100), 116 (49), 115 (30), 57 (18); Calcd Exact Mass for C₁₄H₁₈O₂: 218.131; Found: 218.128.

2,2-Dimethyl-1-Indanyl Pivalate (6a): $^1\text{H NMR}$ δ 7.25-7.17 (m, 4H), 5.82 (s, 1H), 2.87 (d, 1H, $J = 15.6$ Hz), 2.70 (d, 1H, $J = 15.6$ Hz), 1.22 (s, 9H), 1.16 (s, 3H), 1.10 (s, 3H); $^{13}\text{C NMR}$ δ 178.4 (C=O), 143.0 (C), 141.4 (C), 128.4 (CH), 126.6 (CH), 125.6 (CH), 124.9 (CH), 83.7 (CH-O), 45.7 (CH₂), 43.7 (C), 39.0 (C), 27.3 (CH₃), 22.6 (CH₃); GC/MS m/z 246 (M⁺, 0.05), 146 (11), 145 (92), 144 (68), 143 (21), 130 (13), 129 (41), 128 (25), 117 (13), 115 (21), 91 (21), 57 (100); UV

(CH₃OH) λ_{\max} (ϵ) 262 (829); Calcd Exact Mass for C₁₆H₂₅O₇: 246.162; Found: 246.161

6-Methoxy-2,2-Dimethyl-1-Indanyl Pivalate (6b): recrystallized from hexanes: mp 73-74 °C; ¹H NMR δ 7.09 (d, 1H, J = 9.0 Hz), 6.82-6.79 (m, 2H), 5.78 (s, 1H), 3.77 (s, 3H), 2.80 (d, 1H, J = 15.2 Hz), 2.63 (d, 1H, J = 15.2 Hz), 1.22 (s, 9H), 1.16 (s, 3H), 1.08 (s, 3H); ¹³C NMR δ 178.4 (C=O), 158.7 (C), 142.7 (C), 134.9 (C), 125.5 (CH), 114.7 (CH), 110.5 (CH), 83.7 (CH-O), 55.4 (CH₃-O), 44.8 (CH₂), 44.2 (C), 39.1 (C), 27.3 (CH₃), 22.6 (CH₃); GC/MS *m/z* 276 (M⁺, 0.2), 175 (37), 174 (100), 160 (16), 159 (37), 115 (15), 91 (11), 57 (61); UV (CH₃OH) λ_{\max} (ϵ) 279 (3020); Anal Calcd for C₁₇H₂₄O₃: C, 73.87; H, 8.76; Found: C, 73.87; H, 8.22.

5-Methoxy-2,2-Dimethyl-1-Indanyl Pivalate (6c): ¹H NMR δ 7.20 (d, 1H, J = 9.0 Hz), 6.73-6.71 (m, 2H), 5.70 (s, 1H), 3.79 (s, 3H), 2.88 (d, 1H, J = 15.6 Hz), 2.63 (d, 1H, J = 15.6 Hz), 1.19 (s, 9H), 1.13 (s, 3H), 1.11 (s, 3H); ¹³C NMR δ 178.5 (C=O), 160.3 (C), 145.2 (C), 133.6 (C), 126.8 (CH), 112.4 (CH), 110.1 (CH), 83.5 (CH-O), 55.3 (CH₃-O), 45.8 (CH₂), 43.8 (C), 31.6 (C), 27.2 (CH₃), 22.7 (CH₃); GC/MS *m/z* 276 (M⁺, 1), 176 (13), 175 (100), 174 (27), 160 (10), 159 (10), 115 (11), 91 (10), 57 (43); UV (CH₃OH) λ_{\max} (ϵ) 273 (2200); Calcd Exact Mass for C₁₇H₂₄O₃: 276.173; Found: 276.174.

Preparation of 5-Methoxy-2,2-Dimethyl-1-Indanyl Acetate (5c)

Several attempts to prepare this ester using the above method were unsuccessful. The procedure used was a combination from papers by Staab and Rohr⁷⁵ and Carpenter and Moore.⁷⁶ Acetic acid (24 mmol, 1.5 g) in 60 mL of THF was added to a stirring solution of N,N-carbonyldiimidazole (21 mmol, 3.32 g) in 60 mL of THF. After the solution was stirred for 1 h at room temperature, 5-methoxy-2,2-dimethyl-1-indanol (5.2 mmol, 1 g) in 40 mL of THF and a small piece of sodium metal was added. The reaction was monitored by HPLC. After 44 h of refluxing most of the alcohol was converted to ester. The reaction was stopped and the solvent was removed. Water was added to the residue (50 mL) and the product was extracted into ether (3 × 25 mL). The combined organic layers were washed with 1M Na₂CO₃, water, and then dried over magnesium sulphate. The ester was purified by column chromatography on silica gel followed by bulb-to-bulb distillation: Yield (0.62 g, 50%); ¹H NMR δ 7.27 (d, 1H, J = 9.3 Hz), 6.75-6.72 (m, 2H), 5.71 (s, 1H), 3.79 (s, 3H), 2.92 (d, 1H, J = 15.7 Hz), 2.60 (d, 1H, J = 15.7 Hz), 2.06 (s, 3H), 1.14 (s, 3H), 1.10 (s, 3H); ¹³C NMR δ 171.1 (C=O), 160.5 (C), 145.8 (C), 133.3 (C), 127.2 (CH), 112.5 (CH), 110.2 (CH), 83.8 (CH-O), 55.3 (CH₃-O), 47.5 (CH₃), 43.5 (C), 27.5 (CH₃), 22.6 (CH₃), 21.3 (CH₃); GC/MS *m/z* 234 (M⁺, 7), 191 (13), 176 (11), 175 (66), 174 (100), 173 (13), 161 (16), 160 (16), 159 (53), 158 (13), 121 (12), 115 (25), 91 (25), 77 (16); UV (CH₃OH) λ_{max} (ε) 273 (1790); Anal. Calcd for C₁₄H₁₈O₃: C, 71.76; H, 7.75; Found: C, 71.71; H, 7.30.

1.5.5 Preparative Photolyses

For each ester, a solution of 1-2 g in 100 mL of methanol was purged with nitrogen and then irradiated in a Rayonet photochemical reactor using 16 lamps (75 W 253.7 nm). The progress of the reaction was monitored by HPLC, and the reaction was stopped when the ester was >90% consumed. The products of the photolysis were separated by column chromatography and identified by spectroscopic methods.

1.5.6 Characterization and Preparation of the Photoproducts 8-13 and 21-31.

Some of the products were commercially available. Those that were not available were either isolated from the photolysis mixture by chromatography or synthesized by a literature procedure.

The Methyl Ethers 8a-j, 21, and 25a-c In addition to isolating the methyl ethers from the photolysis mixture they were also prepared from the corresponding benzyl alcohols using the following general procedure: To a well stirred solution of 0.015 mol of the alcohol in 30 mL of DMSO was added 0.6 g (0.025 mol) of sodium hydride. The hydride was washed with hexane and then dried in the oven for 2 min. The solution was stirred for 10 min then 5.7 mL (0.092 mol) of iodomethane was added, and the mixture was stirred for 2 h. Water (50 mL) was added, and the aqueous layer was then extracted twice with CH_2Cl_2 (2×25 mL). The organic layer was washed with water (NaCl sat) and dried with MgSO_4 . The solvent was removed under reduced pressure to give the crude ethers which were further purified by

distillation. The ^1H NMR spectra of **8a-d,f** (prepared by J. Hilborn)¹⁷ were identical to those in the literature.⁷⁷

4-(Trifluoromethyl)benzyl Methyl Ether (8e): bp 65 °C at 2 mm Hg; ^1H NMR δ 7.61 (d, 2H, J = 8.3 Hz), 7.44 (d, 2H, J = 8.1 Hz), 4.51 (s, 2H, $\text{CH}_2\text{-O}$), 3.41 (s, 3H, $\text{CH}_3\text{-O}$); ^{13}C NMR δ 143.9 (C), 127.6 (CH), 125.3 (q, CH, $J_{\text{C1}} = 3.82$ Hz), 73.9 ($\text{CH}_2\text{-O}$), 58.4 ($\text{CH}_3\text{-O}$); GC/MS m/z 190 (M^+ , 34), 189 (33), 171 (19), 160 (32), 159 (77), 145 (17), 141 (28), 121 (100), 119 (14), 109 (38), 91 (30), 89 (16), 77 (19), 75 (15), 68 (16), 63 (19), 51 (18).

3,4-Dimethoxybenzyl Methyl Ether (8g): ^1H NMR δ 6.89-6.78 (m, 3H), 4.38 (s, 2H), 3.89 (s, 3H), 3.88 (s, 3H), 3.35 (s, 3H); ^{13}C NMR δ 149.0 (C), 148.6 (C), 130.7 (C), 120.3 (CH), 111.0 (CH), 110.8 (CH), 74.6 (CH_2), 57.9 ($\text{CH}_3\text{-O}$), 55.9 ($\text{CH}_3\text{-O}$), 55.8 ($\text{CH}_3\text{-O}$); GC/MS m/z 182 (M^+ , 43), 181 (11), 152 (13), 151 (100), 108 (11), 107 (13), 77 (11), 65 (12), 51 (11).

3,5-Dimethoxybenzyl Methyl Ether (8h): ^1H NMR δ 6.49 (s, 2H), 6.38 (s, 1H), 4.39 (s, 2H), 3.77 (s, 6H), 3.37 (s, 3H); ^{13}C NMR δ 160.9 (C), 140.6 (C), 105.3 (CH), 99.7 (CH), 74.6 (CH_2), 58.0 ($\text{CH}_3\text{-O}$), 55.3 ($\text{CH}_3\text{-O}$); GC/MS m/z 182 (M^+ , 25), 152 (100), 91 (20), 77 (24).

3,4,5-Trimethoxybenzyl Methyl Ether (8i): $^1\text{H NMR } \delta$ 6.57 (s, 2H), 4.39 (s, 2H), 3.86 (s, 6H), 3.33 (s, 3H), 3.40 (s, 3H); $^{13}\text{C NMR } \delta$ 153.3 (C), 137.3 (C), 133.9 (C), 104.5 (CH), 74.9 (CH_2), 60.9 ($\text{CH}_3\text{-O}$), 58.2 ($\text{CH}_3\text{-O}$), 56.1 ($\text{CH}_3\text{-O}$); GC/MS m/z 212 (M^+ , 90), 197 (11), 182 (42), 181 (100), 169 (22), 167 (14), 154 (13), 151 (14), 148 (14).

Methyl 3-Methylbenzyl Ether (8j): $^1\text{H NMR } \delta$ 7.22-7.04 (m, 4H), 4.37 (s, 2H), 3.34 (s, 3H), 3.30 (s, 3H); $^{13}\text{C NMR } \delta$ 138.3 (C), 138.0 (C), 128.6 (CH), 128.5 (CH), 128.4 (CH), 124.9 (CH), 74.8 ($\text{CH}_2\text{-O}$), 58.0 ($\text{CH}_3\text{-O}$), 21.4 (CH_3); GC/MS m/z 136 (M^+ , 42), 135 (36), 121 (76), 106 (37), 105 (100), 104 (43), 103 (22), 91 (87), 79 (39), 78 (25), 65 (35), 63 (25), 51 (35).

1-Indanyl Methyl Ether (21): $^1\text{H NMR } \delta$ 7.41-7.38 (m, 1H), 7.26-7.19 (m, 3H), 4.84-4.79 (m, 1H), 3.40 (s, 3H), 3.14-3.02 (m, 1H), 2.87-2.75 (m, 1H), 2.37-2.26 (m, 1H), 2.14-2.02 (m, 1H); $^{13}\text{C NMR } \delta$ 144.0 (C), 142.5 (C), 128.4 (CH), 126.2 (CH), 125.1 (CH), 125.0 (CH), 84.5 (CH-O), 56.1 ($\text{CH}_3\text{-O}$), 31.9 (CH_2), 30.2 (CH_2); GC/MS m/z 148 (M^+ , 32), 147 (46), 118 (18), 117 (100), 116 (42), 115 (88), 105 (12), 103 (12), 91 (28), 89 (19), 79 (12), 77 (24), 65 (12), 63 (24), 51 (24).

2,2-Dimethyl-1-Indanyl Methyl Ether (25a): $^1\text{H NMR } \delta$ 7.36-7.24 (m, 1H), 7.23-7.20 (m, 3H), 4.20 (s, 1H), 3.52 (s, 3H), 2.86 (d, 1H, $J = 15.5$ Hz), 2.62 (d, 1H, $J = 15.5$ Hz), 1.17 (s, 3H), 1.16 (s, 3H); $^{13}\text{C NMR } \delta$ 142.9 (C), 128.1 (CH), 126.0

(CH), 125.4 (CH), 125.2 (CH), 92.1 (CH-O), 58.1 (CH₃-O), 45.6 (CH₂), 44.6 (C), 27.9 (CH₃), 22.0 (CH₃); GC/MS *m/z* 176 (M⁺, 19), 145 (25), 144 (23), 143 (13), 131 (11), 130 (13), 129 (100), 128 (30), 127 (10), 117 (12), 115 (24), 91 (25), 77 (11), 65 (12), 63 (11), 51 (13).

6-Methoxy-2,2-Dimethyl-1-Indanyl Methyl Ether (25b): ¹H NMR δ 7.07 (d, 1H, J = 8.1 Hz), 6.89 (d, 1H, J = 2.30 Hz), 6.77 (dd, 1H, J₁ = 8.3 Hz, J₂ = 2.4 Hz), 4.15 (s, 1H), 3.80 (s, 3H), 3.51 (s, 3H), 2.72 (d, 1H, J = 15.1 Hz), 2.53 (d, 1H, J = 15.1 Hz), 1.16 (s, 3H), 1.09 (s, 3H); ¹³C NMR δ 158.5 (C), 144.3 (C), 134.4 (C), 125.7 (CH), 114.0 (CH), 110.5 (CH), 92.2 (CH-O), 58.4 (CH₃-O), 55.4 (CH₃-O), 45.1 (C), 44.8 (CH₂), 28.0 (CH₃), 21.9 (CH₃); GC/MS *m/z* 206 (M⁺, 206), 191 (11), 175 (29), 174 (49), 173 (14), 161 (16), 160 (16), 159 (100), 158 (16), 145 (12), 144 (16), 131 (13), 128 (13), 121 (16), 116 (13), 115 (32), 91 (32), 78 (12), 77 (25), 65 (11), 63 (13), 51 (16).

5-Methoxy-2,2-Dimethyl-1-Indanyl Methyl Ether (25c): ¹H NMR δ 7.26 (d, 1H, J = 7.92 Hz), 6.74 (m, 2H), 4.10 (s, 1H), 3.79 (s, 3H), 3.45 (s, 3H), 2.85 (d, 1H, J = 15.6 Hz), 2.55 (d, 1H, J = 15.6 Hz), 1.16 (s, 3H), 1.11 (s, 3H); ¹³C NMR δ 160.0 (C), 145.0 (C), 135.0 (C), 126.4 (CH), 111.7 (CH), 110.6 (CH), 91.4 (CH-O), 57.4 (CH₃-O), 55.3 (CH₃-O), 45.8 (CH₂), 44.7 (C), 28.0 (CH₃), 22.2 (CH₃); GC/MS *m/z* 206 (M⁺, 18), 176 (15), 175 (100), 160 (13), 159 (25), 115 (21), 91 (19), 77 (15).

The Toluenes, 9a-j, 22 and 26a-c Toluenes **9a-f,j** and **22** were obtained from the Aldrich Chemical Company. Toluenes **26a-c** were isolated from preparative photolysis mixtures by chromatography on silica gel. Toluenes **9g-i** were prepared by reduction of the aldehyde by the Huang-Minlon modification⁷⁸ of the Wolff-Kishner reaction. The crude products were purified by silica gel chromatography or by bulb-to-bulb distillation.

3,4-Dimethoxytoluene (9g): ¹H NMR δ 6.78-6.68 (m, 3H), 3.90 (s, 3H), 3.88 (s, 3H), 2.29 (s, 3H); ¹³C NMR δ 148.7 (C), 146.8 (C), 130.4 (C), 120.8 (CH), 112.4 (CH), 111.2 (CH), 55.9 (CH₃-O), 21.0 (CH₃); GC/MS *m/z* 152 (M⁺, 100), 109 (49), 107 (13), 94 (22), 91 (33), 81 (25), 79 (33), 78 (13), 77 (44), 66 (32), 65 (32), 63 (14), 53 (16), 52 (12), 51 (25).

3,5-Dimethoxytoluene (9h): ¹H NMR δ 6.34 (d, 2H, J = 2.60 Hz), 6.29 (t, 1H, J = 2.2 Hz), 3.78 (s, 6H) 2.30 (s, 3H); ¹³C NMR δ 160.7 (C), 140.2 (C), 107.1 (CH), 97.6 (CH), 55.2 (CH₃-O), 21.8 (CH₃); GC/MS *m/z* 152 (M⁺, 100), 123 (75), 121 (16), 109 (24), 92 (19), 91 (38), 77 (512), 66 (19), 65 (19).

3,4,5-Trimethoxytoluene (9i): ¹H NMR δ 6.42 (s, 2H), 3.88 (s, 9H), 2.22 (s, 3H); ¹³C NMR δ 153.0 (C), 135.8 (C), 133.6 (C), 106.0 (CH), 60.8 (CH₃), 55.9 (CH₃-O), 21.8 (CH₃-O); GC/MS *m/z* 182 (M⁺, 82), 167 (100), 139 (59), 124 (44), 121 (10), 108 (48), 106 (48), 91 (12), 79 (30), 77 (21), 66 (11), 65 (26), 53 (82), 52 (19).

2,2-Dimethylindan (26a): $^1\text{H NMR}$ δ 7.21-7.12 (m, 4H), 2.75 (s, 4H), 1.18 (s, 6H); $^{13}\text{C NMR}$ δ 143.6 (C), 126.0 (CH), 124.8 (CH), 47.8 (CH₂), 43.12 (C), 28.9 (CH₃); GC/MS m/z 146 (M⁺, 39), 132 (12), 131 (100), 129 (13), 128 (11), 116 (13), 115 (25), 91 (39), 77 (12), 64 (11), 63 (13), 51 (13).

6-Methoxy-2,2-Dimethylindan (26b): $^1\text{H NMR}$ δ 7.04 (d, 1H, J = 8.1 Hz), 6.72 (s, 1H), 6.67 (d, 1H, J = 8.1 Hz), 3.77 (s, 3H), 2.69 (s, 2H), 2.65 (s, 2H), 1.14 (s, 6H); $^{13}\text{C NMR}$ δ 158.5 (C), 145.0 (C), 135.6 (C), 125.1 (CH), 111.7 (CH), 110.4 (CH), 55.4 (CH₃-O), 48.0 (CH₂), 46.9 (CH₂), 40.6 (C), 28.9 (CH₃); GC/MS m/z 176 (M⁺, 76), 162 (11), 161 (100), 146 (19), 145 (29), 135 (13), 131 (15), 129 (11), 128 (11), 121 (11), 117 (17), 115 (33), 105 (18), 103 (17), 91 (43), 77 (21), 65 (17), 63 (11), 51 (19).

5-Methoxy-2,2-Dimethylindan (26c): $^1\text{H NMR}$ δ 7.04 (d, 1H, J = 8.1 Hz), 6.72 (s, 1H), 6.67 (d, 1H, J = 8.2 Hz), 3.77 (s, 3H), 2.69 (s, 2H), 2.65 (s, 2H), 1.14 (s, 6H); $^{13}\text{C NMR}$ δ 158.5 (C), 138.2 (C), 134.9 (C), 125.1 (CH), 111.7 (CH), 110.4 (CH), 55.4 (CH₃-O), 48.0 (CH₂), 46.9 (CH₂), 40.5 (C), 28.9 (CH₃); GC/MS m/z 176 (M⁺, 77), 175 (12), 162 (12), 161 (100), 146 (19), 145 (25), 135 (12), 131 (12), 129 (11), 128 (10), 121 (11), 117 (12), 115 (25), 105 (19), 103 (12), 91 (39), 77 (20), 65 (13), 63 (12), 51 (19).

The Radical Coupling Products 10a-j, 11a-j, 27a-c and 28a-c

The coupling product **10c** (ethylbenzene) was obtained from the Aldrich Chemical Company. The coupling products (**10a,d,e**) were prepared by a Wolff-Kishner reduction of the corresponding acetophenone obtained from Aldrich Chemical Company. A mixture of 0.009 mol of the appropriate acetophenone, 1 mL of anhydrous hydrazine, and 40 mL of diethylene glycol was heated until the ketone had dissolved. Heating was continued for 5 min. To this solution was then added 6 g of KOH, and the solution was refluxed for 1 h. After the solution was cooled, water was added and the mixture was extracted with CH₂Cl₂. The CH₂Cl₂ layer was washed with 10% HCl, then with water several times, and dried over MgSO₄. The solvent was removed, and the compounds were purified by distillation or chromatography. The coupling products **10b,f** were not synthesized. For quantitative purposes in these cases, the response of the FID detector was assumed to be the same as for the unsubstituted compound **10c** with a correction factor of 9/8 for the relative carbon content.

(4-Methoxyphenyl)ethane (10a): ¹H NMR δ 7.11 (d, 2H, J = 8.4 Hz), 6.83 (d, 2H, J = 8.6 Hz), 3.78 (s, 3H, CH₃-O), 2.59 (q, 2H, J = 7.6 Hz), 1.20 (t, 3H, J = 7.6 Hz); ¹³C NMR δ 159.5 (C), 136.4 (C), 128.7 (CH), 113.7 (CH), 55.3 (CH₃-O), 28.0 (CH₂), 15.9 (CH₃); GC/MS *m/z* 242 (M⁺, 14), 122 (12), 121 (100), 91 (12), 78 (24), 77 (20).

(3-Methoxyphenyl)ethane (10d): ^1H NMR δ 7.19 (t, 1H, $J = 7.8$ Hz), 6.80-6.63 (m, 3H), 3.77 (s, 3H, $\text{CH}_3\text{-O}$), 2.61 (q, 2H, $J = 7.6$ Hz), 1.22 (t, 3H, $J = 7.5$ Hz); ^{13}C NMR δ 159.7 (C), 146.0 (C), 129.4 (CH), 120.5 (CH), 113.8 (CH), 111.0 (CH), 55.3 ($\text{CH}_3\text{-O}$), 29.0 (CH_2), 15.6 (CH_3).

(4-(Trifluoromethyl)phenyl)ethane (10e): ^1H NMR δ 7.53 (d, 2H, $J = 8.1$ Hz), 7.30 (d, 2H, $J = 7.9$ Hz), 2.71 (q, 2H, $J = 7.5$ Hz), 1.26 (t, 3H, $J = 7.6$ Hz); ^{13}C NMR δ 143.9 (C), 128.1 (CH), 125.2 (q, CH, $J_{\text{CF}} = 3.82$ Hz), 28.8 (CH_2), 15.3 (CH_3); GC/MS m/z 174 (M^+ , 39), 159 (100), 155 (12), 105 (67), 51 (10).

4-Ethyl-1,2-Dimethoxybenzene (10g, R = CH_3): GC/MS m/z 166 (M^+ , 51), 152 (10), 151 (100), 108 (12), 107 (10), 95 (20), 91 (20), 79 (12), 77 (17), 65 (10), 51 (12).

1-Ethyl-3,5-Dimethoxybenzene (10h, R = CH_3): ^1H NMR δ 6.38 (2H, d, $J = 2.1$ Hz), 6.32 (1H, t, $J = 2.1$ Hz), 3.80 (s, 6H), 2.61 (q, 2H, $J = 7.6$ Hz), 1.24 (t, 3H, $J = 7.6$ Hz); ^{13}C NMR δ 160.8 (C), 146.7 (C), 105.9 (CH), 97.6 (CH), 55.2 ($\text{CH}_3\text{-O}$), 29.2 (CH_2), 15.4 (CH_3); GC/MS m/z 166 (M^+ , 100), 165 (17), 137 (16), 121 (32), 109 (32), 108 (16), 105 (13), 91 (44), 79 (22), 78 (16), 77 (33), 65 (26), 63 (15), 53 (13), 51 (17).

5-Ethyl-1,2,3-Trimethoxybenzene (10i, R = CH₃): ¹H NMR δ 6.42 (s, 2H), 3.85 (s, 6H), 3.82 (s, 3H), 2.60 (q, 2H, J = 7.63 Hz), 1.24 (t, 3H, J = 7.63 Hz); ¹³C NMR δ 153.0 (C), 140.0 (C), 135.9 (C), 105.9 (CH), 60.8 (CH₃-O), 56.0 (CH₃-O), 29.3 (CH₂), 15.7 (CH₃); GC/MS *m/z* 196 (M⁺, 74), 181 (100), 153 (25), 138 (22), 123 (15), 121 (19), 93 (12), 91 (14), 79 (13), 77 (18), 67 (18), 65 (13), 53 (12).

1-Methoxy-4-Neopentylbenzene (11a) This coupling product was synthesized by a Friedel-Crafts acylation followed by a Clemmenson reduction. To a solution of 14 g (0.009 mol) of anhydrous aluminum chloride in 25 mL of CH₂Cl₂ was added 8.0 g (0.067 mol) of pivaloyl chloride in 15 mL of CH₂Cl₂. To this mixture was slowly added 8.1 g (0.075 mol) of anisole in 10 mL of CH₂Cl₂. The reaction was kept at room temperature for 30 min and then was poured into a mixture consisting of 50 g of ice in 25 mL of concentrated hydrochloric acid. The aqueous layer was extracted with CH₂Cl₂ (30 mL). The organic layer was washed with sodium bicarbonate (50 mL) and dried over MgSO₄. The CH₂Cl₂ was removed by rotary evaporation and the remaining liquid was distilled under vacuum.

The ketone was reduced by a Clemmenson reduction. To 2.89 g (0.01 mol) of the ketone was added amalgamated zinc (4.19 g in 19 mL of concentrated HCl). The mixture was refluxed for 18 h and filtered, and the filtrate was extracted with ether. The ether layer was washed with water and saturated sodium bicarbonate and then dried over MgSO₄. Purification of the product was accomplished by chromatography. The product structure was confirmed by ¹H NMR: ¹H NMR δ 7.03 (d, 2H, J = 8.7

Hz), 6.80 (d, 2H, $J = 8.9$ Hz), 3.78 (s, 3H), 2.43 (s, 2H), 0.88 (s, 9H). This compound was previously synthesized and characterized by Jaxa-Chamiec *et al.*⁷⁹.

4-Trifluoromethyl-1-Neopentylbenzene (11e) This coupling product was isolated from the photolysis mixture. The crude reaction mixture (0.6 g) was chromatographed on a column packed with 60 g of silica gel and eluted with 1:9 ethyl acetate:hexane. One 50 mL fraction followed by 20 mL fractions was collected. Fractions 4-6 were combined, and the solvent was removed to give **11e**: $^1\text{H NMR } \delta$ 7.52 (d, 2H, $J = 7.9$ Hz), 7.22 (d, 2H, $J = 7.9$ Hz), 2.55 (s, 2H) 0.91 (s, 9H); GC/MS m/z 216 (M^+ , 2), 159 (25), 109 (11), 57 (100).

The remaining coupling products (**11b-d,f**) were quantified by GC/FID using **11e** as a standard and correcting for carbon content.

1,2-Dimethoxy-4-Neopentylbenzene (11g, $\text{R} = \text{C}(\text{CH}_3)_3$): $^1\text{H NMR } \delta$ 6.79-6.76 (m, 4H), 3.86 (s, 3H), 3.85 (s, 3H), 2.43 (s, 2H), 0.90 (s, 9H); $^{13}\text{C NMR } \delta$ 148.2 (C), 147.3 (C), 132.4 (C), 122.5 (CH), 114.0 (CH), 110.7 (CH), 55.8 ($\text{CH}_3\text{-O}$), 49.9 (CH_2), 31.8 (C), 29.4 (CH_3); GC/MS m/z 208 (M^+ , 25), 152 (16), 151 (100).

1,3-Dimethoxy-5-Neopentylbenzene (11h, $\text{R} = \text{C}(\text{CH}_3)_3$): $^1\text{H NMR } \delta$ 6.33 (t, 1H, $J = 2.25$ Hz), 6.29 (d, 2H, $J = 2.27$ Hz), 3.77 (s, 6H), 2.43 (s, 2H), 0.92 (s, 9H); $^{13}\text{C NMR } \delta$ 160.1 (C), 142.1 (C), 108.8 (CH), 97.7 (CH), 55.2 ($\text{CH}_3\text{-O}$), 50.6

(CH₂), 29.6 (CH₃); GC/MS *m/z* 268 (M⁺, 27), 152 (100), 137 (6), 121 (6), 91 (8), 77 (8), 57.2 (31).

1,2,3-Trimethoxy-5-Neopentylbenzene (11i, R = C(CH₃)₃): ¹H NMR δ 6.33 (s, 2H), 3.84 (s, 9H), 2.44 (s, 2H), 0.93 (s, 9H); ¹³C NMR δ 152.4 (C), 136.2 (C), 135.5 (C), 107.5 (CH), 60.8 (CH₃-O), 56.0 (CH₃-O), 31.8 (C), 29.5 (CH₃); GC/MS *m/z* 238 (M⁺, 15), 182 (14), 181 (100), 57 (50).

1-Methyl-3-Neopentylbenzene (11j, R = C(CH₃)₃): ¹H NMR δ 7.24-6.91 (m, 4H), 2.45 (s, 2H), 2.33 (s, 3H), 0.90 (s, 9H); ¹³C NMR δ 139.7 (C), 137.0 (C), 131.3 (CH), 127.45 (2 × CH), 126.4 (CH), 50.1 (CH₂), 31.7 (C), 29.4 (CH₃), 21.5 (CH₃); GC/MS *m/z* 162 (M⁺, 13), 106 (98), 105 (47), 103 (10), 91 (42), 79 (13), 78 (10), 77 (21), 57 (100).

The products **27a-c** and **28a-c** were isolated from preparative photolysis mixtures by chromatography on silica gel.

1,2,2-Trimethylindan (27a, R = CH₃): ¹H NMR δ 7.16-7.10 (m, 4H), 2.81 (q, 1H, J = 7.2 Hz), 2.72 (d, 1H, J = 15.5 Hz), 2.64 (d, 1H, J = 15.5 Hz), 1.17 (s, 3H), 1.15 (d, 3H, J = 7.2 Hz), 0.84 (s, 3H); ¹³C NMR δ 148.2 (C), 142.6 (C), 126.0 (CH), 124.4 (CH), 123.3 (CH), 48.9 (CH), 47.2 (CH₂), 44.0 (C), 27.6 (CH₃), 22.4 (CH₃), 13.0 (CH₃); GC/MS *m/z* 160 (M⁺, 27), 146 (12), 145 (100), 131 (13), 130

(10), 129 (13), 128 (15), 117 (29), 115 (24), 91 (20).

6-Methoxy-1,2,2-Trimethylindan (27b, R = CH₃): This compound was not isolated from the preparative photolysis mixture. It was quantified using product **26b**, correcting for the difference in carbon atoms.

5-Methoxy-1,2,2-Trimethylindan (27c, R = CH₃): A preparative photolysis was not done for ester **5c** because of difficulties encountered in making a sufficient quantity of the ester. This product was quantified using product **26c**, correcting for the difference in carbon atoms.

1-tert-Butyl-2,2-Dimethylindan (28a, R = C(CH₃)₃): ¹H NMR δ 7.28-7.26 (m, 1H), 7.15-7.05 (m, 3H), 2.93 (d, 1H, J = 15.4 Hz), 2.49 (s, 1H), 2.41 (d, 1H, J = 15.4 Hz), 1.33 (s, 3H), 1.04 (s, 9H), 1.02 (s, 3H); ¹³C NMR δ 147.5 (C), 143.9 (C), 127.9 (CH), 125.9 (CH), 124.7 (CH), 124.5 (CH), 64.8 (CH), 48.1 (C''), 44.8 (C), 35.3 (C), 33.0 (CH₃), 29.4 (CH₃), 25.9 (CH₃); GC/MS *m/z* 202 (M⁺, 0.8), 146 (27), 145 (100), 131 (11), 130 (11), 129 (13), 128 (15), 117 (20), 115 (20), 91 (12), 57 (13).

6-Methoxy-1-tert-Butyl-2,2-Dimethylindan (28b, R = C(CH₃)₃): ¹H NMR δ 7.04 (d, 1H, J = 8.1 Hz), 6.84 (d, 1H, J = 2.3 Hz), 6.69 (dd, 1H, J₁ = 8.1 Hz, J₂ = 2.4 Hz), 3.79 (s, 3H), 2.86 (d, 1H, J = 15.0 Hz), 2.44 (s, 1H), 2.33 (d, 1H, J = 15.0

Hz), 1.32 (s, 3H), 1.04 (s, 9H), 1.00 (s, 3H); ^{13}C NMR δ 157.3 (C), 147.8 (C), 136.1 (C), 124.7 (CH), 114.4 (CH), 111.0 (CH), 65.0 (CH), 55.4 (CH₃-O), 47.2 (CH₂), 45.3 (C), 35.3 (C), 33.0 (CH₃), 29.4 (CH₃), 25.9 (CH₃); GC/MS m/z 232 (M^+ , 6), 176 (20), 175 (100), 160 (13), 115 (13), 57 (13).

5-Methoxy-1-*tert*-Butyl-2,2-Dimethylindan (28c, R = C(CH₃)₃): ^1H NMR δ 7.14 (d, 1H, $J = 8.2$ Hz), 6.71 (s, 1H), 6.64 (d, 1H, $J = 8.4$ Hz), 3.78 (s, 3H), 2.89 (d, 1H, $J = 15.4$ Hz), 2.41 (s, 1H), 2.36 (d, 1H, $J = 15.4$ Hz), 1.31 (s, 3H), 1.00 (s, 12H); ^{13}C NMR δ 158.3 (C), 145.4 (C), 138.3 (C), 128.4 (CH), 110.4 (CH), 109.9 (CH), 64.1 (CH), 55.2 (CH₃-O), 48.3 (CH₂), 45.1 (C), 35.3 (C), 33.0 (CH₃), 29.3 (CH₃), 25.9 (CH₃); GC/MS m/z 232 (M^+ , 2), 176 (13), 175 (100).

5-*tert*-Butyl-6-Methoxyindan This compound was isolated from a preparative photolysis of ester **6b**. It results from coupling of an out-of-cage *tert*-butyl radical with the aromatic ring of the indanyl radical. It was formed in less than 1% yield and was not quantified. ^1H NMR δ 7.05 (s, 1H), 6.71 (s, 1H), 3.80 (s, 3H), 2.68 (s, 2H), 2.65 (s, 2H), 1.35 (s, 9H), 1.14 (s, 6H); ^{13}C NMR δ 157.5 (C), 141.8 (C), 136.1 (C), 134.6 (C), 122.6 (CH), 108.4 (CH), 55.2 (CH₃-O), 48.0 (CH₂), 47.5 (CH₂), 40.3 (C), 34.7 (C), 30.0 (CH₃), 29.2 (CH₃); GC/MS m/z 232 (M^+ , 16), 218 (16), 217 (100).

The Dimers **12a-j**, **28a-c** and **29a-c** 1,2-diphenylethane (**12c**), was obtained from the

Aldrich Chemical Company. Dimers **12a,b,d,f** were quantified using the corresponding toluene as an equivalent on the basis of the expected identical UV detection response in HPLC detection. The remaining dimers were isolated from preparative photolysis solutions by chromatography on silica gel. The characterization for dimers **29a-c** and **30a-c** is in the experimental section of Chapter 3.

4,4'-bis(trifluoromethyl)bibenzyl (12e): $^1\text{H NMR}$ δ 7.53 (d, 2H, $J = 7.9$ Hz), 7.25 (d, 2H, $J = 7.9$ Hz), 2.98 (s, 2H); $^{13}\text{C NMR}$ δ 145.0 (C), 128.7 (CH), 127.0 (q, C, $J_{\text{CT}} = 272$ Hz), 125.4 (q, CH, $J_{\text{CT}} = 3.82$ Hz); GC/MS m/z 318 (M^+ , 42), 299 (19), 160 (9), 159 (100), 109 (18).

3,3',4,4'-Tetramethoxybibenzyl (12g): $^1\text{H NMR}$ δ 6.76-6.65 (m, 3H), 3.84 (s, 3H), 3.82 (s, 3H), 2.83 (s, 2H); $^{13}\text{C NMR}$ δ 148.7 (C), 147.2 (C), 134.4 (C), 120.3 (CH), 111.9 (CH), 111.1 (CH), 55.9 ($\text{CH}_3\text{-O}$), 55.7 ($\text{CH}_3\text{-O}$), 37.7 (CH_2); GC/MS m/z 302 (M^+ , 47), 152 (11), 151 (100).

3,3',5,5'-Tetramethoxybibenzyl (12h): $^1\text{H NMR}$ δ 6.35 (s, 2H), 6.32 (s, 1H), 3.76 (s, 6H), 2.84 (s, 2H); $^{13}\text{C NMR}$ δ 160.7 (C), 144.1 (C), 106.4 (CH), 97.9 (CH), 55.2 ($\text{CH}_3\text{-O}$), 38.0 (CH_2); GC/MS m/z 302 (M^+ , 99), 152 (13), 151 (100), 91 (10), 77 (12).

3,3',4,4',5,5'-Hexamethoxybibenzyl (12i): $^1\text{H NMR}$ δ 6.37 (s, 2H), 3.82 (s, 9H),

2.85 (s, 2H); ^{13}C NMR δ 153.0 (C), 137.4 (C), 136.1 (C), 105.4 (CH), 60.9 (CH₃-O), 56.0 (CH₃-O), 38.5 (CH₂); GC/MS m/z 362 (M⁺, 37), 181 (100).

3,3'-Dimethylbibenzyl (12j): ^1H NMR δ 7.24-7.00 (m, 4H), 2.86 (s, 2H), 2.33 (s, 3H); ^{13}C NMR δ 141.9 (C), 137.9 (C), 129.2 (CH), 128.2 (CH), 126.6 (CH), 125.4 (CH), 38.0 (CH₂), 21.4 (CH₃); GC/MS m/z 210 (M⁺, 23), 106 (11), 105 (100), 79 (20), 77 (23).

The Arylmethanol Products 31a-c These products were isolated from a preparative photolysis mixture by chromatography on silica gel.

2,2-Dimethyl-1-Indanylmethanol (31a): ^1H NMR δ 7.32-7.28 (m, 1H), 7.19-7.15 (m, 3H), 3.90 (q, 1H, $J_1 = 10.8$ Hz, $J_2 = 5.6$ Hz), 3.81 (q, 1H, $J_1 = 10.8$ Hz, $J_2 = 6.6$ Hz), 2.86 (t, 1H, $J_1 = 6.6$ Hz, $J_2 = 5.6$ Hz), 2.79 (d, 1H, $J = 15.4$ Hz), 2.68 (d, 1H, $J = 15.4$ Hz), 1.52 (brs, 1H), 1.17 (s, 3H), 1.10 (s, 3H); ^{13}C NMR δ 144.2 (C), 143.4 (C), 126.8 (CH), 126.2 (CH), 124.9 (CH), 124.8 (CH), 63.6 (CH₂-O), 56.7 (CH), 47.4 (CH₂), 42.3 (C), 29.7 (CH₃), 23.3 (CH₃); GC/MS m/z 176 (M⁺, 14), 146 (13), 145 (100), 143 (10), 130 (13), 129 (19), 128 (21), 117 (24), 115 (21), 105 (10), 91 (19).

6-Methoxy-2,2-Dimethyl-1-Indanylmethanol (31b): ^1H NMR δ 7.08 (d, 1H, $J = 8.1$ Hz), 6.87 (brs, 1H), 6.72 (dd, 1H, $J_1 = 8.2$ Hz, $J_2 = 2.4$ Hz), 3.92-3.67 (m,

2H), 3.79 (s, 3H), 2.81 (t, 1H, $J = 6.0$ Hz), 2.70 (d, 1H, $J = 15.1$ Hz), 2.60 (d, 1H, $J = 15.1$ Hz), 1.15 (s, 3H), 1.08 (s, 3H); ^{13}C NMR δ 158.6 (C), 145.8 (C), 135.3 (C), 125.4 (CH), 112.3 (CH), 110.6 (CH), 63.5 (CH₂-O), 57.0 (CH), 55.4 (CH₃-O), 46.5 (CH₂), 42.7 (C), 29.7 (CH₃), 23.3 (CH₃); GC/MS m/z 206 (M^+ , 21), 176 (13), 175 (100), 160 (13), 145 (11), 128 (10), 115 (14), 91 (13).

5-Methoxy-2,2-Dimethyl-1-Indanylmethanol (31c): A preparative photolysis was not done for ester **5c** because of difficulties encountered in making sufficient quantity of the ester. This product was quantified using the isomer **31b**.

1.5.7 Quantitative Photolyses

The procedure followed was the same as that described in the preparative photolysis section, except the solutions contained only 100-200 mg of the ester in 100 mL of methanol and analyses were done with less than 50% of the ester consumed. At conversions below 50%, product yields were shown to be independent of percent conversion. At very high conversions, the mass balance dropped to 75-80% because of slow photodegradation of the products. This is not surprising because the ester and the products have the same chromophore at high conversions most of the light is being absorbed by the products. Dark samples of the esters in methanol showed no significant conversion to products.

Standard solutions of each of the products were prepared to determine the yields of the products for the photolysis reaction. The photolysis samples and the

standards were analyzed by GC/FID and the integrated areas for the standards containing a known amount of photoproduct were compared to the integrated areas of the photoproducts. The dimers, **12a-f**, were not volatile enough for an GC analysis and thus were analyzed by HPLC. Quenched irradiations (Table 4) were done as described above except that 2,3-dimethyl-1,3-butadiene ($(1-6) \times 10^{-3}$ M) was added to the solution.

1.5.8 Analytical Determination of the Ether Yields **8a,e,f**

As can be seen from Table 2 the yields of photoproducts **8a,e,f** are low. These yields are important because they are necessary to determine the rate constant for electron transfer. To ensure that these numbers are accurate, the analyses were done more carefully. Two separate photolyses on each of the corresponding acetate esters and two separate standards were analysed. Each photolysis and standard sample was injected twice on the GC/FID.

1.5.9 Oxidation Potential Measurements

Oxidation potentials for the 3,5-dimethoxybenzyl radical and the 3,4,5-trimethoxybenzyl radical were measured. This required the corresponding substituted toluene. The oxidation potentials were measured by modulated photolysis cyclic voltammetry. The details of this technique have been previously reported by Sim *et al.*³⁵ The measured potentials are given in Table 3.

1.5.10 Quantum Yield Measurements

The quantum yield of reaction for the esters **5** and **6** in methanol were determined using the photolysis of 3-methoxybenzyl acetate in aqueous dioxane as the actinometer. The quantum yield of reaction for 3-methoxybenzyl acetate is 0.13.⁵ The esters, as well as the standard, were irradiated in a merry-go-round apparatus using a Hanovia reactor with five 75 W 253.7 nm lamps. Samples were taken every minute for five minutes. Each sample was run in duplicate. A plot of percent conversion of the ester divided by time versus time was extrapolated to zero time (Figure 4). The ratio of the zero time values for the % conversion of the ester and the standard multiplied by 0.13 provided the quantum yield of reaction.

Chapter 2

The Photochemistry of 1-Naphthylmethyl Carbonates and Carbamates

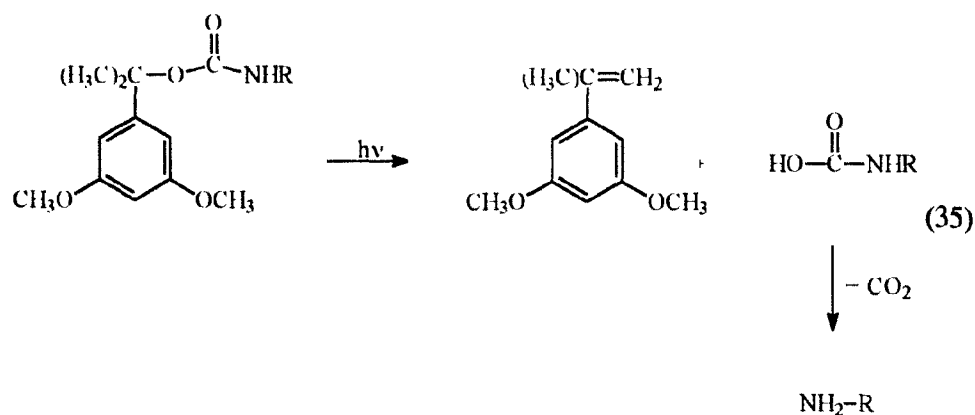
2.1 Introduction

The photochemistry of substituted benzylic esters of acetic and pivalic acid was discussed in Chapter 1. The photochemistry of 1-naphthylmethyl esters of phenylacetic acid has been discussed elsewhere.¹² In both cases, excitation of the aromatic group resulted in loss of the ester functionality by homolytic cleavage of the C-O bond to give a radical pair. The radical pair formed the ion pair by electron transfer in competition with forming products. The substituents on the aromatic ring influenced product ratios (radical vs. ionic) by altering the oxidation potential of the arylmethyl radical and thus the rate constants of electron transfer. The acid group (acetic vs. pivalic) altered product ratios by changing the rate constant for decarboxylation of the acyloxy radical. This chapter explores the generality of the proposed reaction mechanism by changing the "leaving group" from an ester to a carbonate and a carbamate.

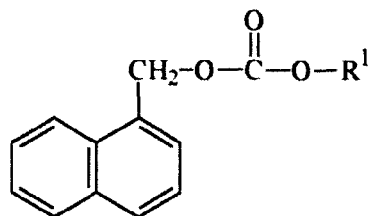
There are only a few reports in the literature on the photochemistry of aromatic compounds conjugated to carbonates ($R^1O-CO-OR^2$) and carbamates ($R^1NH-CO-OR^2$). In most cases the carbonate or carbamate is directly conjugated to the aromatic chromophore, R^1 is phenyl and R^2 is alkyl. In these cases homolytic cleavage of the carbonyl carbon-oxygen, eq 33,⁸⁰ or carbonyl carbon-nitrogen bond, eq 34,⁸¹ dominates and a radical pair is formed. The resulting radical pair recombines to give starting material and products isomeric with the starting material. This reaction is

called a photo-Fries reaction and the products are called photo-Fries products. The first two products shown in eqs 33 and 34 are the photo-Fries products. The 2-methoxyphenol in eq 33 and aniline in eq 34 are formed by the out-of-cage radical pair abstracting a hydrogen atom from the solvent. The photo-Fries reaction is also dominant when an ester functionality is directly conjugated to the aromatic group.^{82,83,84}

The carbamate shown in eq 35 is structurally similar to the compounds studied in this chapter. The carbamate functional group is homo-conjugated to the aromatic ring and products result from cleavage of the CH-O bond. The methoxy substituents were chosen to enhance heterolytic cleavage. The only products observed were 3,5-dimethoxystyrene and the carbamic acid with the latter readily losing carbon dioxide to give an amine.⁸⁵

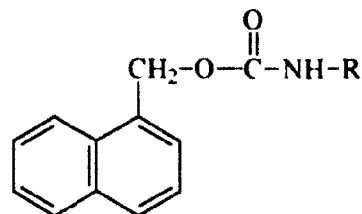


The compounds studied in this chapter are the carbonates **31** and **32** and the carbamates **33** and **34**. These compounds should also react photochemically by



31, $R^1 = \text{CH}_2\text{Ph}$

32, $R^1 = \text{Ph}$



33, $R^1 = \text{CH}_2\text{Ph}$

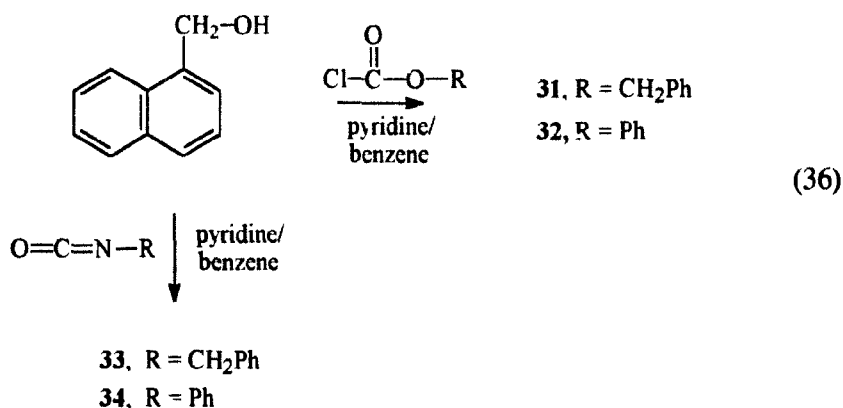
34, $R^1 = \text{Ph}$

cleaving the $\text{CH}_2\text{-O}$ bond. If the reaction mechanism for compounds 31-34 is the same as that shown in Scheme 5 (p 30) for the esters, the singlet excited state will cleave homolytically to give a radical pair. The product ratios should be very different from those observed for the esters because the rates of decarboxylation for the phenoxyacyloxy radicals ($\dot{\text{O}}_2\text{C-O-R}$) and the carbamoyloxy radicals ($\dot{\text{O}}_2\text{C-NH-R}$) should be very different from those for the acyloxy radicals ($\dot{\text{O}}_2\text{CR}$).¹⁸ Both the phenyl ($R^1 = \text{Ph}$) and benzyl ($R^1 = \text{CH}_2\text{Ph}$) carbonates and carbamates were chosen for study because changing R from phenyl to benzyl will change the rate constant of decarboxylation. When $R^1 = \text{Ph}$, decarboxylation should be rapid because the resulting radical is stabilized by resonance delocalization. In contrast, when $R^1 = \text{CH}_2\text{Ph}$, the decarboxylation will be much slower because the resulting radical is now insulated from the benzene ring by a methylene group and cannot be stabilized by resonance.

2.2 Results and Discussion

2.2.1 Synthesis of the 1-Naphthylmethyl Carbonates and Carbamates

The carbonates were prepared by reaction of 1-naphthylmethanol with benzyl chloroformate for **31** and phenyl chloroformate for **32**, eq 36. The carbamates were prepared by reaction of 1-naphthylmethanol with benzyl isocyanate for **33** and phenyl isocyanate for **34**, eq 36. Details and data for characterization are in the experimental section, 2.3.2.



2.2.2 Excited-State Properties of the Carbonates and Carbamates

The fluorescence quantum yields (ϕ_f), singlet lifetimes (τ_s), and singlet energies ($E_{0,0}$) for the carbonates and carbamates were measured and are given in Table 13. For comparison, the values for 1-naphthylmethylphenyl acetate and naphthalene are also given. The excited-state properties for the carbonates, carbamates, and 1-naphthylmethylphenyl acetate are very similar. Inclusion of nitrogen or oxygen into the functional group does not change the excited-state

Table 13. Photophysical Data for the Carbonates and Carbamates.

Compounds ^a	ϕ_f^b	τ_s (ns)	$E_{0,0}$ kJ/mol (kcal/mol)	λ_{max} (nm) [ϵ]
31, NM Benzyl Carbonate	0.14	36.0	385 (92)	276 [6815]
32, NM Phenyl Carbonate	0.11	31.0	389 (93)	276 [7054]
33, NM N-Benzyl Carbamate	0.14	38.5	389 (93)	276 [5977]
34, NM N-Phenyl Carbamate	0.12	38.5	389 (93)	276 [7327]
1-Naphthylmethyl Phenylacetate	0.14	49.0	385 (92)	275 [7400]
Naphthalene	0.20	90.0	385 (92)	270 [4918]

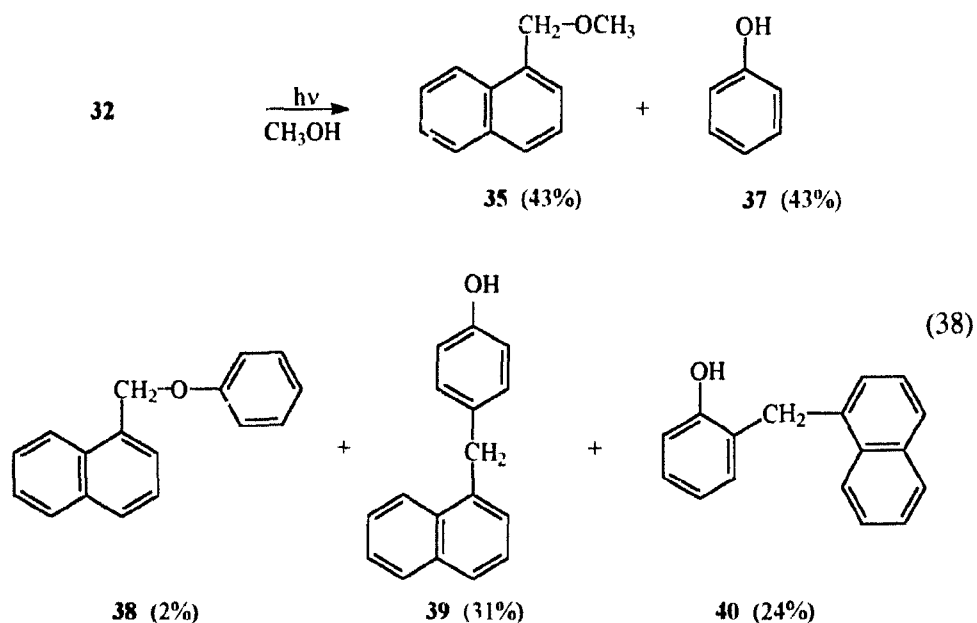
^aNM = 1-Naphthylmethyl

^b ϕ_f were determined by comparing the emission spectrum of the compound to the emission spectrum of naphthalene

Decomposition, by loss of carbon dioxide, has not been studied for aryl monocarbonates but has been studied for alkyl monocarbonates.⁸⁶ The reaction is base catalysed and the rate levels off at high pH where carbonic acid is completely ionized. Based on the pK_a of the alcohol/phenol and a Bronsted plot, rate constants, for decomposition in water of about 10^3 s^{-1} for $\text{PhCH}_2\text{O-CO}_2^-$ and about 10^1 s^{-1} for PhOCO_2^- can be estimated. The values in methanol should not be much different. Since these alkyl carbonates are also reasonably strong acids ($pK_a \sim 3$);⁸⁷ they will be greater than 50% ionized in neutral solvents so that the rate of loss of CO_2 will be fast relative to the photolysis times.

The product yields for 1-naphthylmethylbenzyl carbonate, **31**, suggest that if the mechanism shown in Scheme 5 is correct $k_{\text{IT}} \gg k_{\text{CO}_2}$. A value for the rate constant of decarboxylation of acyloxy radicals of this type (RO-CO-O^\bullet) has been estimated, by laser flash photolysis studies,⁸⁸ to be less than 10^6 s^{-1} . Since electron transfer rates in these radical pairs can be expected to be greater than 10^9 s^{-1} (*vide supra*), the mechanism is reasonable.

Photolysis of 1-naphthylmethyl phenyl carbonate, **32**, gave the five products shown in eq 38. The products were isolated by chromatography and identified by spectroscopic methods. Identification of compounds **35-38** was trivial. Assignment of **39** and **40** was based on the coupling pattern of the aromatic hydrogens in the ^1H NMR spectrum and carbon count in the ^{13}C NMR spectrum. Compound **39** was assigned as the *para* substituted phenol based on only 14 signals in the aromatic region of the ^{13}C NMR spectrum and two doublets, each integrating for 2 protons, in



the aromatic region of the ^1H NMR spectrum. The assignment of **40** as *ortho* was based on the observation that the hydrogen *para* to the OH at δ 6.80 (calcd⁸⁹ 6.76) showed two *ortho* couplings. The *meta* isomer, which was not detected, would have had a hydrogen *para* to the OH at δ 6.68 (calcd) with only one *ortho* coupling. The yields given in eq 38 were determined by quantitative HPLC analyses. Further details are given in the experimental section.

The methyl ether, **35**, is formed by trapping of the 1-naphthylmethyl cation by methanol. Again, decomposition of the monocarbonate anion (PhO-CO-O^-) is fast (*vide supra*) and phenol, **37**, is formed. The yield of methyl ether, **35**, is much lower than that from the photolysis of 1-naphthylmethylbenzyl carbonate, **31**. The remainder

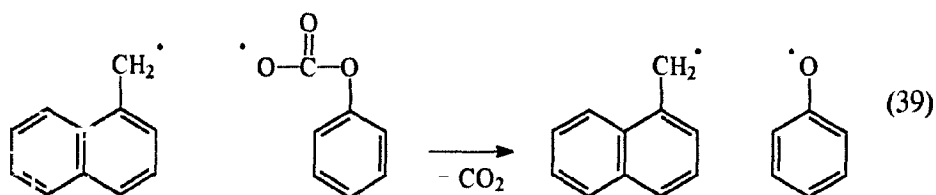
of the products can be formed from either the ion pair or the radical pair. The ether **38** is most likely formed from the radical pair. To be formed from the ion pair a phenoxide anion would have to couple with the 1-naphthylmethyl cation. Trapping of the monocarbonate anion by solvent would occur more rapidly than decarboxylation ($k = 10^3 \text{ s}^{-1}$) to form phenoxide anion.

The phenols **39** and **40** could be formed by a Friedel-Crafts reaction of the 1-naphthylmethyl cation with the monocarbonate anion (PhOCO_2^-) followed by loss of CO_2 . The oxygen on the phenyl ring would be *ortho-para* directing and only the *ortho* and *para* substituted phenols are formed. To test this possibility a ground-state solvolysis was done. In the ground state only ion pairs will be formed. The ground-state solvolysis of **32** in methanol at 50°C gave only the methyl ether, **35**, and phenol, **37**. This indicates that the phenols **39** and **40** are formed from the radical pair.

The above conclusion is true only if the ground-state solvolysis occurs by an $\text{S}_{\text{N}}1$ mechanism, *i.e.*, an ion pair intermediate is formed. The mechanism ($\text{S}_{\text{N}}1$ vs. $\text{S}_{\text{N}}2$) of a benzylic solvolysis is dependent upon the substituents on the benzene ring. There is no available literature on the solvolysis of arylmethyl carbonates. However, a detailed study of substituent effects on solvolysis rates of benzyl tosylates in 80% acetone-water has been reported.⁹⁰ Carbonic acids and sulfonic acids should be comparable leaving groups based on the similarity of their pK_{a} values. For the tosylates the change in mechanism was found to occur for the unsubstituted compound, $\sigma^+ = 0$, with better electron-donating groups ($\rho^+ = -5.8$) favoring an $\text{S}_{\text{N}}1$

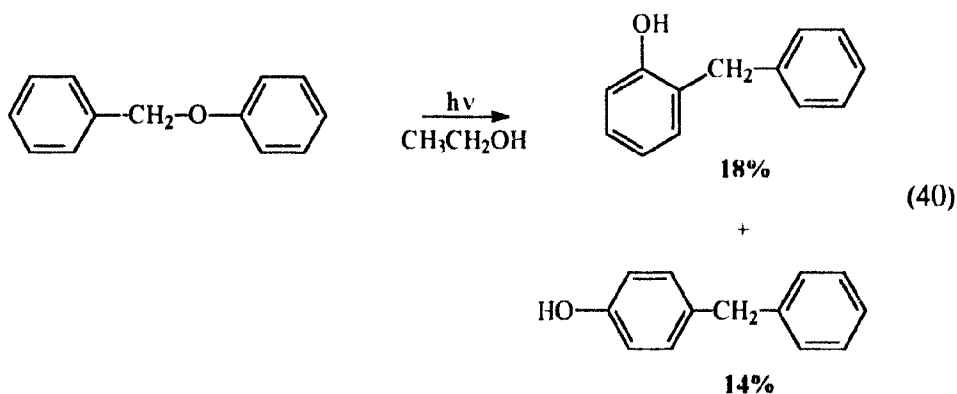
mechanism. A similar conclusion was reached when the solvolysis of benzyl tosylates was studied in a variety of solvents, including methanol.⁹¹ Fitting solvolysis rates to the Grunwald-Winstein equation indicated that sensitivity to solvent nucleophilicity (l) dropped and the solvent ionizing power (m) exceeded unity as the substituent changed from H to 4-CH₃. Methyl substitution enhances the solvolysis rate by a factor of 20. The carbonates studied are unsubstituted however, they are 1-naphthylmethyl rather than benzylic. Changing from phenyl to 1-naphthylmethyl is known to increase the rate of solvolysis by a factor of 20.⁹² Thus the rate of solvolysis of an unsubstituted 1-naphthylmethyl carbonate should be similar to a 4-methyl substituted benzylic tosylate and probably proceeds by a rate-determining S_N1 ionization to give a short-lived ion pair. Therefore, the conclusion that products **39** and **40** are formed from the radical pair is reasonable.

The ether, **38**, must be formed by coupling after decarboxylation of the radical pair. However, the phenols **39** and **40** can be formed either before or after decarboxylation. The rate constant for decarboxylation, eq 39, is not known. However, the rate constant for decarboxylation must be greater than that for the alkyl monocarbonate radicals (RO-CO-O[•], R = alkyl) where $k_{\text{CO}_2} < 10^6 \text{ s}^{-1}$ because the



more stable phenoxy radical is formed. If products **38-40** are formed after decarboxylation the product ratios should reflect the spin density of the phenoxy radical. Estimates of these values from ESR measurements⁹¹ are approximately 20% at oxygen, 40% at the *para*, and 20% at the two *ortho* carbons. Clearly, the product ratios in eq 38 do not reflect the spin densities. The yield of the ether **38** is far lower than expected.

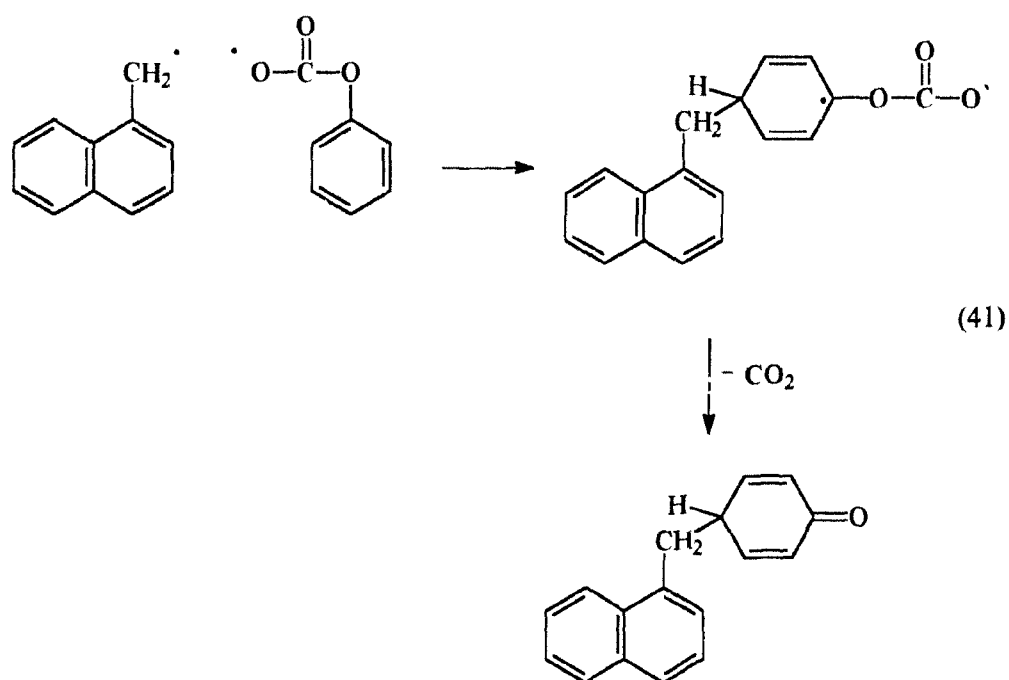
The reason for the low yield of ether **38** is that it is photolabile. Photolysis of the ether **38** in methanol resulted in efficient formation of the phenols **39** and **40** in a ratio of 47:53. There is literature precedence for photoreactivity of phenyl aryl ethers. Photolysis of benzyl phenyl ether in ethanol has been shown to give phenolic products analogous to products **39** and **40**, eq 40.⁹⁴ The yield of ether **38** is low



because it has the same chromophore as the carbonate and thus does not build up in the solution. Because of this complication it is difficult to know the primary product distribution from the radical pair.

The other possibility for forming the phenol products is coupling of the radical

pair before decarboxylation, as shown in eq 41. The intermediate should rapidly lose CO_2 and the resulting ketone would then tautomerize to form the phenol. The decision as to when the phenol products are formed, before or after decarboxylation, can only be made if the rate constant for decarboxylation was known.

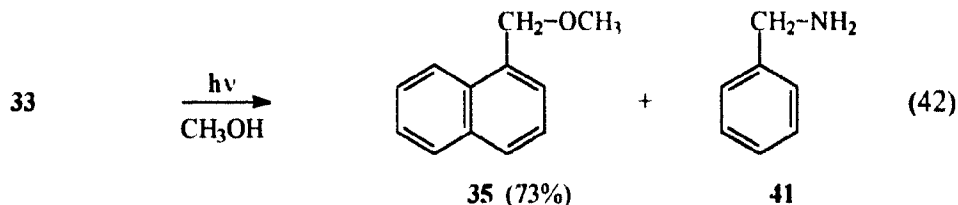


The photochemistry of 1-naphthylmethyl carbonates, **31** and **32**, can be explained by the general mechanism shown in Scheme 5. The photophysical properties of the phenyl and benzyl carbonate are identical yet the product ratios are quite different. The ratio of products derived from the ion pair versus the radical pair are 43:57 for the phenyl carbonate and $>20:1$ for the benzyl carbonate. The difference in product ratios is due to the different rates of decarboxylation. For 1-

naphthylmethylphenyl carbonate decarboxylation is fast and competitive with electron transfer resulting in the formation of products from both the radical pair and the ion pair. However, for 1-naphthylmethylbenzyl carbonate decarboxylation is much slower and is not competitive with electron transfer. Thus, only products from the ion pair are formed.

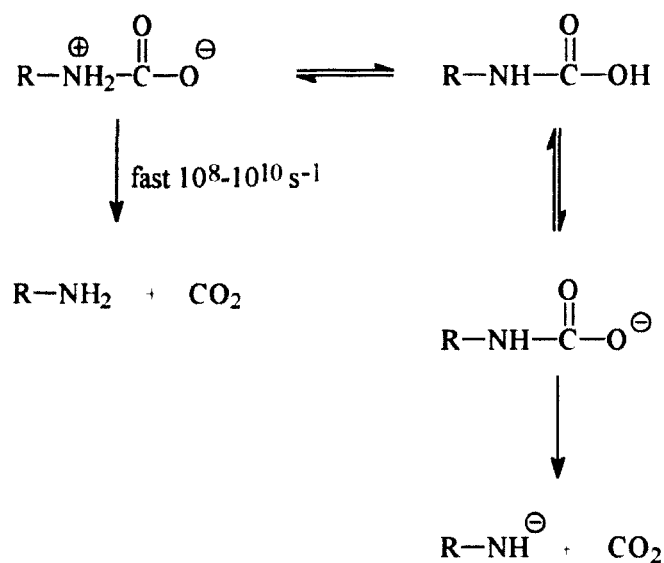
2.2.4 Photolysis of the Carbamates 33 and 34

Photolysis of 1-naphthylmethyl N-benzyl carbamate, **33**, gave only products from the ion pair, eq 42, analogous to the photoreaction of 1-naphthylmethylbenzyl



carbonate. The mass balance is lower for the carbamate. The solutions went green and murky as the photolysis proceeded. No carbamic acid products were observed. As shown in Scheme 6, at high pH decarboxylation of carbamic acids is slow because instability of R-NH⁻ makes it a poor leaving group. However, at lower pH values a zwitterion is formed and the rate constant for decarboxylation has been estimated between 10⁸ - 10¹⁰ s⁻¹ depending on the nature of R.^{95,96} Decomposition of the carbamic acid is faster than the photolysis times and benzylamine is isolated.

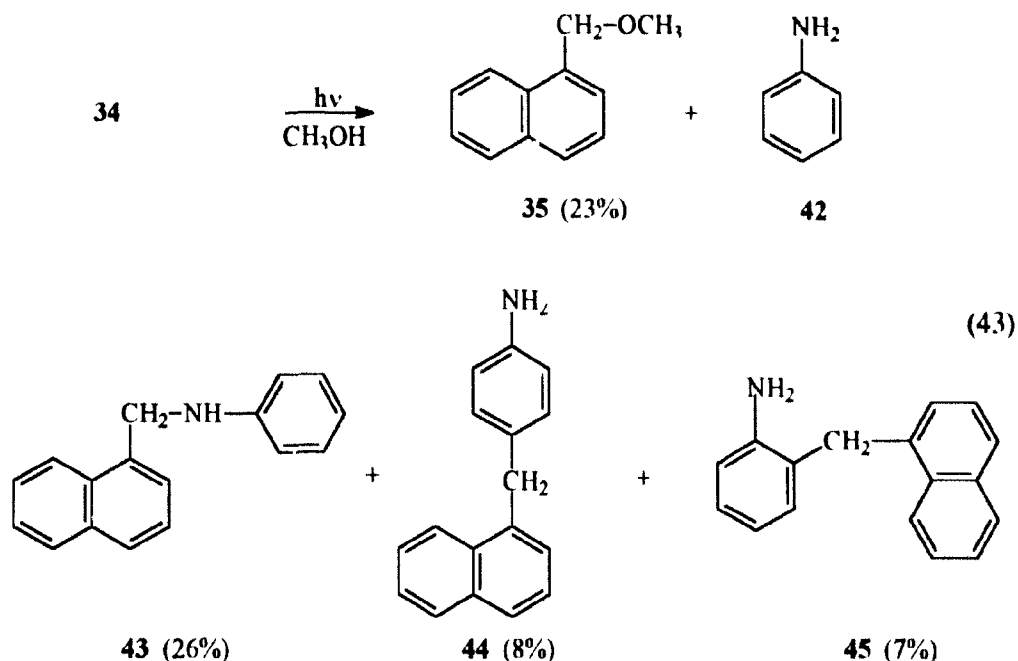
Photolysis of 1-naphthylmethyl N-phenyl carbamate gave products from both

Scheme 6. Pathways for the Decarboxylation of Carbamic Acids.

the ion pair and the radical pair, eq 43. The methyl ether is formed by trapping of the 1-naphthylmethyl cation by methanol and aniline is formed by thermal decomposition of the carbamic acid. The products formed from the radical pair are the secondary amine, **43**, and the substituted anilines, **44** and **45**. ^1H and ^{13}C NMR spectroscopy was used to assign **44** as *para* and **45** as *ortho*.

The secondary amine, **43**, would have to be formed after decarboxylation. It is difficult to determine whether the substituted anilines **44** and **45** are formed before or after decarboxylation because there is no information available on the rate constants of decarboxylation of the carbamoyloxy radicals ($\text{R}-\text{NH}-\overset{\cdot}{\text{C}}-\text{O}^{\ominus}$).

The yield of the secondary amine, **43**, (26%) is much greater than that for the corresponding ether **38** (2%) from the photolysis of 1-naphthylmethylphenyl carbonate.



Also, the yields of the substituted anilines **44** and **45** (8% and 7%) are much lower than the yields of the substituted phenols **39** and **40** (31% and 24%). The reason for the difference in product yields is that all of the products formed from photolysis of 1-naphthylmethyl N-phenyl carbamate, **34**, are primary photoproducts. Photolysis of the secondary amine, **43**, that is analogous to the ether **38** resulted in no product formation after prolonged periods of irradiation in methanol. An explanation for this observation is the different bond strengths of the amine and the ether. The bond strength for the ether $\text{CH}_3\text{-OPh}$ is 277 kJ/mol (66.2 kcal/mol) versus a bond strength of 298 kJ/mol (71.2 kcal/mol) for the amine $\text{CH}_3\text{-NH-Ph}$.¹⁵

As expected, based on their photophysical properties, the photochemistry of the 1-naphthylmethyl carbamates is similar to that of the 1-naphthylmethyl carbonates. Products result from cleavage of the $\text{CH}_2\text{-O}$ bond. For 1-naphthylmethyl N-phenyl carbamate, decarboxylation is fast and products are formed from both the radical and ion pairs. However, for the 1-naphthylmethyl N-benzyl carbamate decarboxylation is slower and only ion pair products are observed.

2.2.5 Conclusion

The study of the photochemistry of the 1-naphthylmethyl carbonates, **31** and **32**, and the 1-naphthylmethyl carbamates, **33** and **34**, showed that the mechanism for photolysis of the benzylic esters and 1-naphthylmethyl esters can also be used to rationalize the photoreactivity of 1-naphthylmethyl carbonates and carbamates. The important competing pathways are decarboxylation and electron transfer. For the benzyl compounds decarboxylation is slow and only ion pair products are observed. For the phenyl compounds decarboxylation is faster and products are formed from both the ion pair and the radical pair. Heterolytic cleavage is not necessary to explain the results.

2.3 Experimental

2.3.1 General Experimental

See Chapter 1.5.1

2.3.2 Synthesis of the Carbonates 31 and 32 and Carbamates 33 and 34

Synthesis of the 1-Naphthylmethyl Carbonates (31, 32)

The appropriate chloroformate (0.044 mol, 5.5 mL) in 40 mL of benzene was slowly added to a well-stirred solution of 6.33 g (0.04 mol) of 1-naphthylmethanol and 4 mL of pyridine in 150 mL of benzene. The reaction mixture was stirred for 6 h and then poured into 50 mL of water and the organic layer was separated. This layer was washed with 80 mL of 10% HCl, 80 mL of 5% NaOH and 80 mL of water, dried with MgSO₄ and evaporated to give an oil.

(1-Naphthylmethyl) Benzyl Carbonate (31): The crude oil was purified by column chromatography using 400 g of silica gel and eluting with 25% ethyl acetate/75% hexane. Fractions were collected every 30 mL. Fractions 18-30 were combined and the solvent removed to give 8.8 g (80% yield) of the purified carbonate. For the quantitative photolysis and spectroscopy the carbonate was further purified by bulb-to-bulb distillation: bp 99 °C at 0.15 mm Hg; ¹H NMR δ 7.98 (d, 1H, J = 7.6 Hz), 7.78 (m, 2H), 7.52-7.26 (m, 9H), 5.59 (s, 2H), 5.13 (s, 2H); ¹³C NMR δ 155.1 (C=O), 135.2 (C), 133.7 (C), 131.5 (C), 130.7 (C), 129.5 (CH), 128.7 (CH), 128.53 (CH), 128.47 (CH), 128.3 (CH), 127.6 (CH), 126.7 (CH), 125.9 (CH), 125.2 (CH),

123.5 (CH), 69.7 (CH₂), 67.2 (CH₂); IR (neat) 3063, 2961, 1744 (C=O), 1600, 1513, 1498, 1456, 1391, 1258 (C-O), 1245 (C-O), 952, 936, 909, 801, 792, 777 cm⁻¹; GC/MS *m/z* 292 (M⁺, 38), 201 (51), 141 (62), 129 (100), 128 (25), 127 (27), 115 (32), 91 (66), 77 (17), 65 (17), 51 (13); Anal. Calcd for C₁₉H₁₆O₃: C, 78.06; H, 5.52. Found: C, 78.11; H, 5.52.

(1-Naphthylmethyl) Phenyl Carbonate (32): The crude oil was distilled under vacuum to give a solid product. The solid was recrystallized from hexane: mp 56-57 °C; ¹H NMR δ 8.09 (d, 1H, J = 8.4 Hz), 7.88 (d, 2H, J = 8.4 Hz), 7.63-7.33 (m, 6H), 7.24-7.15 (m, 3H), 5.74 (s, 2H); ¹³C NMR δ 153.8 (C=O), 151.3 (C), 133.7 (C), 131.5 (C), 130.2 (C), 129.7 (CH), 129.3 (CH), 128.7 (CH), 128.0 (CH), 126.7 (CH), 126.0 (CH), 125.9 (CH), 125.1 (CH), 123.3 (CH), 120.9 (CH), 68.5 (CH₂); IR (Nujol) 1745 (C=O), 1580, 1440, 1240 (C-O), 1200, 1050 (C-O), 730, 790, 675 cm⁻¹; GC/MS *m/z* 278 (M⁺, 3), 142 (12), 141 (100), 140 (3), 139 (6), 115 (15); Anal. Calcd for C₁₈H₁₄O₃: C, 77.68; H, 5.07. Found: C, 77.45; H, 5.12.

Synthesis of the 1-naphthylmethyl carbamates (33, 34):

The appropriate isocyanate (2.5 mL, 0.023 mol) was slowly added to 3.0 g (0.019 mol) of 1-naphthylmethanol. The reaction mixture was heated with stirring on a hot water bath for 10 minutes. The viscous liquid solidified upon cooling to give the crude carbamate.

(1-Naphthylmethyl) Benzyl Carbamate (33): The crude carbamate was purified by column chromatography using silica gel and eluting with dichloromethane. The carbamate was further purified by recrystallization from hexane/dichloromethane to constant melting point: mp 118-119 °C; ^1H NMR δ 8.06 (d, 1H, $J = 7.8$ Hz), 7.86 (m, 2H), 7.47 (m, 4H), 7.29 (s, 5H), 5.61 (s, 2H), 5.05 (brs, 1H), 4.40 (d, 2H, $J = 5.8$ Hz); ^{13}C NMR δ 156.4 (C=O), 138.4 (C), 133.6 (C), 131.9 (C), 131.6 (C), 129.1 (CH), 128.6 (CH), 128.5 (CH), 127.4 (CH), 127.3 (CH), 126.4 (CH), 125.8 (CH), 125.2 (CH), 123.6 (CH), 65.0 (CH₂), 45.0 (CH₂); IR (Nujol) 3310 (NH), 2953, 2854, 1680 (C=O), 1545, 1456, 1264, 777, 700 cm⁻¹; GC/MS m/z 291 (M⁺, 29), 158 (76), 150 (19), 142 (14), 141 (100), 140 (18), 140 (18), 139 (18), 129 (37), 128 (14), 127 (13), 115 (37), 106 (11), 91 (19), 77 (14), 51 (14); Calcd Exact Mass for C₁₉H₁₇NO₂: 291.1259; Found: 291.1256.

(1-Naphthylmethyl) N-Phenyl Carbamate (34): The crude carbamate was purified by chromatography on silica gel eluting with 70% dichloromethane/30% hexane and was purified further by recrystallization from hexane to a constant melting point: mp 89-90 °C; ^1H NMR δ 8.09 (d, 1H, $J = 7.9$ Hz), 7.89 (t, 2H, $J = 7.7$ Hz), 7.61-7.26 (m, 8H), 7.06 (t, 1H, $J = 7.2$ Hz), 6.65 (brs, 1H), 5.67 (s, 2H); ^{13}C NMR δ 148.0 (C=O), 136.2 (C), 133.3 (C), 131.7 (C), 130.6 (C), 129.5 (CH), 129.1 (CH), 128.8 (CH), 127.8 (CH), 126.7 (CH), 126.0 (CH), 125.3 (CH), 123.6 (CH), 123.5 (CH), 118.6 (CH), 65.4 (CH₂); IR (Nujol) 3330 (NH), 1680 (C=O), 1585, 1520, 1300, 1230 (C-O), 1050, 790, 755, 730 cm⁻¹; GC/MS m/z 277 (M⁺, 12), 141 (100),

116 (10); Calcd Exact Mass for $C_{18}H_{15}NO_2$: 277.1103; Found: 277.1095.

2.3.3 Fluorescence Measurements

A Perkin-Elmer MPF 66 fluorescence spectrometer was used for the fluorescence studies. The samples were degassed by three freeze-pump-thaw cycles. Fluorescence quantum yields were determined by comparison with a fluorescence quantum yield of 0.24 for naphthalene in methanol.⁹⁷ Singlet-state energies were determined by the position of the 0,0 band using the overlap between the excitation and emission spectra. Fluorescence lifetimes were measured using a PRA single photon counting apparatus using a H_2 lamp with a pulse width of about 1 ns.

2.3.4 Preparative Photolysis

A solution of ~1 g of the 1-naphthylmethyl carbonate or carbamate in 420 mL of distilled methanol was placed in an immersion well and degassed with nitrogen for 15 minutes before irradiation, degassing was continued during the irradiation. The light source was a Pyrex-filtered 200 W medium-pressure Hanovia mercury lamp. Irradiation was continued until the starting material was greater than 90% consumed. The photolysis solution was concentrated under vacuum to give an oil. The products were separated on a column packed with silica gel. The products isolated in this manner were further purified if necessary.

2.3.5 Characterization of the Photoproducts

Benzyl alcohol (**36**), phenol (**37**), benzyl amine (**41**) and aniline (**42**) were purchased from the Aldrich Chemical Company and purified if necessary. The (1-naphthylmethyl) methyl ether, **35**, was available in the laboratory and has been previously characterized.¹²

1-Naphthylmethyl Phenyl Ether (38): An insufficient quantity of pure compound was isolated from the photolysis mixture of the carbonate for the study of its photochemistry. This compound was synthesized using the following procedure. Sodium phenoxide was prepared by adding 1.0 g (0.044 mol) of sodium to 30 mL of methanol, followed by the addition of 4.0 g (0.043 mol) of phenol. The sodium phenoxide solution was slowly added to 4.6 mL (0.031 mol) of 1-(chloromethyl)naphthalene in 20 mL of methanol. The reaction mixture was stirred overnight and then concentrated by rotary evaporation to 10 mL. Water (40 mL) was added and the water layer was washed with dichloromethane (3 × 20 mL). The organic layers were combined and dried over MgSO₄. The crude product was recrystallized from ethanol: mp 68-68.5 °C (lit.^{9k} 66-67 °C); ¹H NMR δ 8.05 (m, 1H), 7.90 (d, 1H, J = 5.7 Hz), 7.85 (d, 1H, J = 9.3 Hz), 7.60 (1H, d, J = 5.9 Hz), 7.55-7.43 (m, 3H), 7.32 (t, 2H, J = 7.3 Hz), 7.07 (d, 2H, J = 7.8 Hz), 6.99 (t, 1H, J = 7.3 Hz), 5.49 (s, 2H); ¹³C NMR δ 158.9 (C), 133.8 (C), 132.4 (C), 131.6 (C), 129.6 (CH), 129.0 (CH), 128.7 (CH), 126.6 (CH), 126.5 (CH), 125.9 (CH), 125.4 (CH), 123.7 (CH), 121.1 (CH), 114.9 (CH), 68.6 (CH₂); GC/MS *m/z* 234 (M⁺, 5),

142 (12), 141 (100), 115 (37) 65 (11).

4-(1-Naphthylmethyl)phenol (39): $^1\text{H NMR}$ δ 7.97 (m, 1H), 7.84 (m, 1H), 7.73 (d, 2H, $J = 8.4$ Hz), 7.48-7.30 (m, 4H), 7.03 (d, 2H, $J = 8.2$ Hz), 6.71 (d, 2H, $J = 8.4$ Hz), 4.36 (s, 2H); $^{13}\text{C NMR}$ δ 153.2 (C), 140.6 (C), 133.9 (C), 131.3 (C), 129.8 (CH), 128.6 (CH), 127.1 (CH), 127.0 (CH), 125.9 (CH), 125.6 (CH), 125.5 (CH), 124.2 (CH), 115.2 (CH), 38.2 (CH₂); IR (neat) 3380 (br) 3075, 2990, 2924, 1620, 1511, 1440, 1260, 792 cm⁻¹; GC/MS m/z 234 (M⁺, 100), 233 (44), 217 (16), 215 (32), 203 (11), 202 (20), 189 (9), 141 (16), 128 (32), 107 (14), 77 (11).

2-(1-Naphthylmethyl)phenol (40): $^1\text{H NMR}$ δ 8.03 (m, 1H), 7.85 (m, 1H), 7.75 (d, 1H, $J = 8.4$ Hz), 7.49-7.36 (m, 4H), 7.11 (t, 1H, $J = 7.7$ Hz), 6.95 (d, 1H, $J = 6.3$ Hz) 6.80 (m, 2H), 4.44 (s, 2H); $^{13}\text{C NMR}$ δ 153.6 (C), 135.6 (C), 133.9 (C), 132.8 (C), 132.2 (C), 130.8 (CH), 128.7 (CH), 127.7 (CH), 127.3 (CH), 126.6 (CH), 126.1 (CH), 125.7 (CH), 125.6 (CH), 124.1 (CH), 121.0 (CH), 115.5 (CH), 32.8 (CH₂); IR (neat) 3400 (br), 3025, 2950, 2900, 1580, 1500, 1455, 1260, 760 cm⁻¹; GC/MS m/z 234 (M⁺, 51), 215 (13), 202 (10), 128 (100).

N-(1-Naphthylmethyl)aniline (43): This compound was isolated from the photolysis mixture and was also synthesised because more compound was needed for further analyses. Aniline (2.2 mL, 0.024 mol) was added to a solution of 3.75 g (0.024 mol) of 1-naphthaldehyde in 80 mL of methanol. The solution was refluxed overnight.

After cooling the solvent was removed to give the crude imine. The crude imine was purified by column chromatography using 250 g of silica gel and eluting with 90% hexane/10% ethyl acetate. Fractions were collected every 20 mL and fractions 9-19 were found to contain the imine. The fractions were combined and the solvent removed to give 3.9 g (0.017 mol) of the imine (yield 70%). The imine was dissolved in 200 mL of methanol and 0.63 g (0.017 mol) of sodium borohydride was added slowly. The solution was refluxed for 20 min then cooled. Excess sodium borohydride was added to ensure that all of the imine had been reduced (as indicated by the disappearance of the yellow color). The amine was liberated by addition of an equal amount of water to the flask. The amine precipitated and was collected. It was purified by recrystallization from methanol/water to give 0.60 g of the amine (15% yield) which was identical by spectroscopy to that isolated from the photolysis mixture of carbamate **33**: mp 63.4-64 °C (lit.⁹⁹ 64 °C); ¹H NMR δ 7.89-7.77 (m, 4H), 7.51-7.40 (m, 2H), 6.77-6.65 (m, 4H), 4.70 (s, 2H), 3.97 (brs, 1H); ¹³C NMR δ 148.2 (C), 134.3 (C), 133.8 (C), 131.5 (C), 129.3 (CH), 128.7 (CH), 128.2 (CH), 126.3 (CH), 126.0 (CH), 125.8 (CH), 125.5 (CH), 123.6 (CH), 117.5 (CH), 112.7 (CH), 47.2 (CH₂); GC/MS *m/z* 233 (M⁺, 31), 142 (40), 141 (100), 115 (29), 77 (12), 65 (19).

4-(1-Naphthylmethyl)aniline (44): ¹H NMR δ 7.99 (m, 1H), 7.84 (m, 1H), 7.73 (d, 1H, J = 8.1 Hz), 7.46-7.37 (m, 3H), 7.26 (d, 1H, J = 6.6 Hz), 7.00 (d, 2H, 8.1 Hz), 6.66 (d, 2H, 8.1 Hz), 4.36 (s, 2H), 3.60 (br s, 2H); ¹³C NMR δ 143.0 (C),

137.2 (C), 133.9 (C), 132.1 (C), 129.6 (C), 128.6 (CH), 127.1 (CH), 127.0 (CH), 125.9 (CH), 125.53 (CH), 125.50 (CH), 124.3 (CH), 116.0 (CH), 38.2 (CH₂); GC/MS *m/z* 233 (M⁺, 100), 232 (59), 217 (13), 215 (17), 115 (11), 106 (25).

2-(1-Naphthylmethyl)aniline (45): ¹H NMR δ 8.08 (m, 1H), 7.88 (m, 1H), 7.76 (d, 1H, J = 8.2 Hz), 7.52-7.48 (m, 2H), 7.37 (t, 1H, J = 8.2 Hz), 7.15-7.08 (m, 2H), 6.92 (d, 1H, J = 7.5 Hz), 6.76-6.70 (m, 2H), 4.31 (s, 2H), 3.57 (brs, 2H); ¹³C NMR δ 144.6 (C), 134.7 (C), 133.8 (C), 132.2 (C), 130.7 (CH), 128.8 (CH), 127.6 (CH), 127.2 (CH), 126.1 (CH), 125.9 (CH), 125.7 (CH), 125.68 (CH), 124.3 (C), 123.8 (CH), 118.9 (CH), 115.7 (CH), 34.5 (CH₂); GC/MS *m/z* 233 (M⁺, 100), 232 (57), 215 (28), 128 (13), 115 (14), 106 (11).

2.3.6 Quantitative Photolysis

Compounds **31-34** were irradiated in the same manner as was described under the preparative photolysis section except only 100 mg of the substrate was used. Analyses were done with less than 50% of the starting material consumed. The product yields were calculated at various percent conversions and no change in product ratio as a function of time was indicated. Dark reactions were negligibly slow. Standard solutions were prepared which contained a known amount of the photoproducts. These standards were used to determine the yields of photoproducts for the photolysis by HPLC. The peak heights of the products in the sample were measured and compared with the peak heights of a standard solution of the

corresponding product.

2.3.7 Photolysis of 1-Naphthylmethyl Phenyl Ether 38

A solution of 173 mg of the ether in 300 mL of methanol was irradiated until >90% of the ether had reacted. There were two photoproducts formed from this reaction. They were separated on a 30 × 2.2 cm column packed with 25 g of silica gel. One 100 mL fraction was collected, followed by ten 10 mL fractions and then ten 30 mL fractions. The fractions were analyzed by HPLC. Fractions 9-13 were combined. The solvent was removed giving 47 mg of photoproduct. This product was identified as 2-(1-naphthylmethyl)phenol, **40**, by comparison with previously recorded spectra. Fractions 17-19 were combined and the solvent was removed to give 18 mg of photoproduct. By comparison with previously recorded spectra this photoproduct was identified as 4-(1-naphthylmethyl)phenol, **39**).

2.3.8 Photolysis of N-(1-Naphthylmethyl)aniline, 43

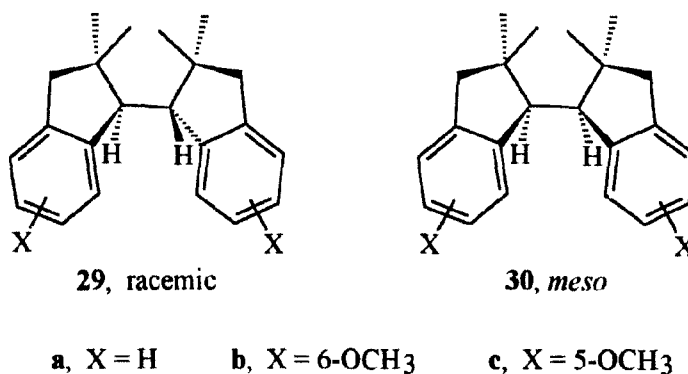
This compound was photolysed analogously to that described above. After 48 h of irradiation no product formation was detected.

Chapter 3

Conformational Behaviour of Highly Hindered Ethanes: *Meso* and *dl* Dimers of 2,2,2',2'-Tetramethyl-1-1'-biindanyl

3.1 Introduction

Most of the products isolated from the photolyses in Chapters 1 and 2 are structurally simple and their characterization is discussed in one paragraph consisting of the ^1H NMR, ^{13}C NMR and GC/MS data. In contrast, this entire chapter is dedicated to the discussion of the diastereomeric dimers **29a** and **30a** isolated from the photolysis of 2,2-dimethyl-1-indanyl acetate and pivalate (Chapter 1.4). Dimer **29a** is a racemic mixture of compounds having (*R,R*) or (*S,S*) configurations (*R,R* is shown) while the other, **30a**, is a *meso* (*R,S*) compound. The former mixture will be called the racemic dimer.

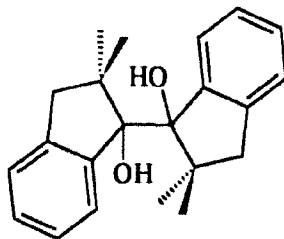


Interest in these dimers started with the observation of broadened signals in the room temperature NMR spectra of the *meso* dimer, **30a**, that were temperature dependent. Sharp signals were observed in the room temperature NMR spectra of the

racemic dimer and these were temperature independent. As will be discussed, the broadened signals in the NMR spectra of the *meso* compound are the result of a barrier of 61.7 kJ/mol (14.7 kcal/mol) for rotation about the central carbon-carbon bond that joins the two halves of the dimer.

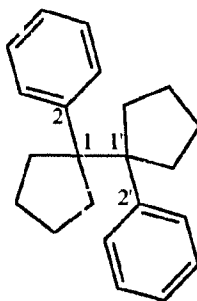
During the photochemical studies, the ring-substituted dimers **29b-c** and **30b-c** were also isolated. Although these compounds were not studied in detail, again, one dimer gave sharp signals in the NMR spectra at room temperature and the other gave broadened NMR signals at room temperature. Low-temperature NMR spectra of the methoxy *meso* dimers were very similar to those of the unsubstituted *meso* dimer.

A survey of the literature indicated that these compounds merited further study. No examples were found of structurally similar compounds having barriers as large as that for dimer **30a**. The barrier to rotation about the bond between the two isopropyl groups in 2,3-dimethylbutane is only 18 kJ/mol (4.3 kcal/mol).¹⁰⁴ In fact, compounds more sterically hindered than dimers **29a** and **30a** have been reported that have free rotation about the central carbon-carbon bond at room temperature. For example, Orliac-Le Moing *et al.*⁷² have reported ¹H NMR spectra for both the racemic and *meso* form of bis 1,1'-(2,2-dimethyl-1-indanol), **46**. Both of the dimers were crystalline. No mention was made of broadened lines in the NMR spectra of either dimer. The spectrum of the racemic dimer was reported to contain a singlet at 0.83 ppm (2 × CH₃), a singlet at 1.72 ppm (2 × CH₃), and a doublet with J = 15 Hz at 2.32 ppm for the methylene group. The other spectrum contained singlets at 1.04 ppm (2 × CH₃) and 1.38 ppm (2 × CH₃). In this latter spectrum, the methylene

46 (racemic and *meso*)

groups appeared as a singlet at 2.47 ppm. The chemical shifts were not reported for the aromatic protons. Unfortunately, the field strength of the spectrometer used was not mentioned because the reported doublet for the methylene group of the former compound must have been the central lines of an AB quartet.

Crystallographic studies have been reported for a series of 1,1-diphenyl-1,1'-bicycloalkyl systems which included 1,1'-diphenyl-1,1'-bicyclopentyl,¹⁰⁰ 47. The



47

major focus of this work was studying bond lengths as a function of steric interactions. The bicyclopentyl compound has a central C(1)-C(1') bond length of 1.575 Å. The energy as a function of the C(2)-C(1)-C(1')-C(2)' torsional angle was determined by MM2 and AM1 calculations. Both methods correctly predicted that the conformation

with the phenyl groups *gauche* would be more stable than the *anti* one. The calculated barrier to interconversion between the two conformers was only ~19 kJ/mol (4.5 kcal/mol). The barrier for eclipsing of C(2) and C(2)', the torsional angle equal to zero, was ~40 kJ/mol (9.6 kcal/mol).

There are examples of compounds having high barriers to rotation about sp^3 - sp^3 single bonds.^{101,102,103,104,105,106} However, the high barriers are usually a result of hindered rotation about a carbon-carbon bond where both carbon atoms are quaternary. Some compounds, such as substituted triptycene or dihydroanthracene derivatives, have high enough barriers that two conformational isomers can be separated and are stable to equilibration at room temperature.¹⁰¹ The barriers to rotation about tertiary carbon-carbon bonds can be large if two bulky groups are present at both ends of the bond. The barriers in these cases often result from the correlated motion of several large groups.^{102,105,107,108,109}

Another reason for the thorough study of dimers **29a** and **30a** is because they can exist in conformations where the aromatic rings are either stacked or distant from each other allowing the importance of aromatic stacking to be evaluated. Recently, the importance of aryl-aryl interactions in the aggregation of compounds containing aromatic rings has been discussed in the literature.^{110,111} Calculations suggest that an



48



49

offset face-to-face stack, **48**, is one of the most favourable geometries, however, an edge-to-face arrangement, **49**, is only 0.8 kJ/mol (0.2 kcal/mol) higher in energy.^{112,113}

The conclusions reached in this section are that the most highly populated conformers of dimers **29a** and **30a** have the two aromatic rings offset face-to-face stacked. Calculations indicate that this stacking of the aromatic rings may be an important interaction. For the *meso* dimer, there are two low energy conformers related by a plane of symmetry and they are thus equally populated. Interconversion between the two conformers occurs by rotation about the central carbon-carbon bond joining the two halves of the dimer. The smallest barrier for this rotation has been measured as 61.7 kJ/mol (14.7 kcal/mol). The barrier slows the exchange on the NMR time scale and results in broadened signals in the room temperature NMR spectra. Only one conformer of the racemic dimer is populated and the NMR spectra are temperature independent.

The remainder of this chapter will highlight some of the evidence (NMR and calculations, MM3, AM1 and STO-3G) for the above conclusions. The study of these dimers has been a collaborative effort and complete details of this work can be found elsewhere.¹¹⁴

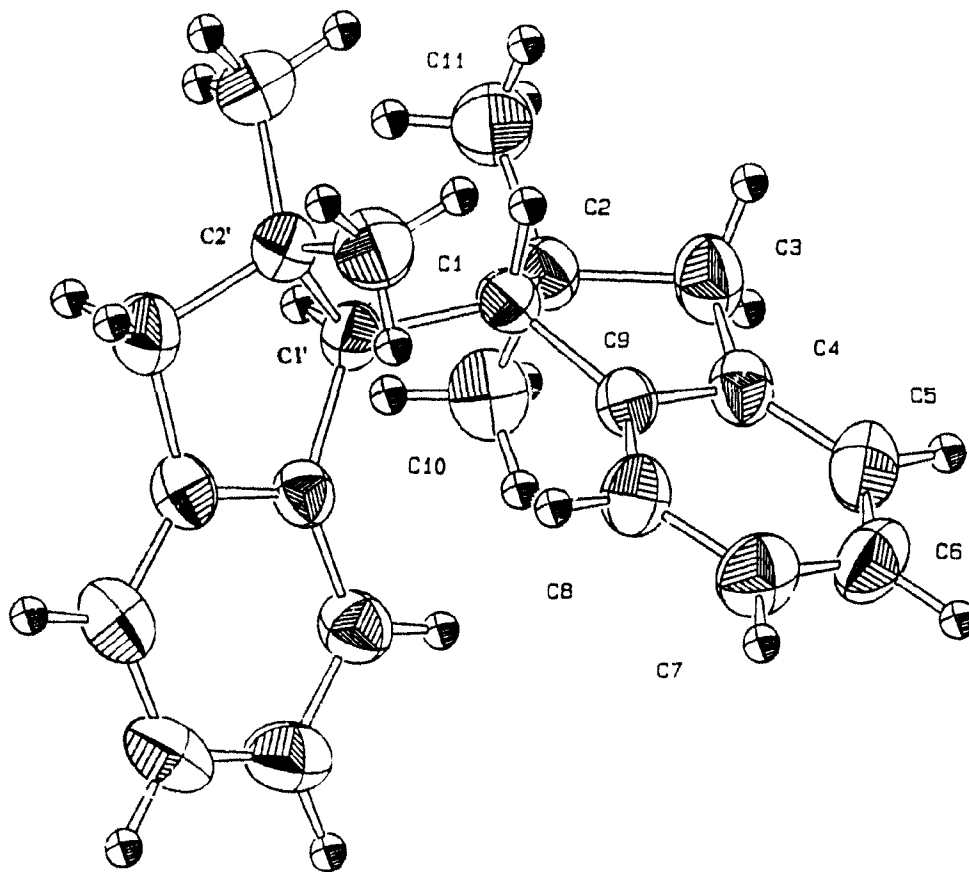
3.2 Results

3.2.1 Crystallography

Dimer **29a** crystallized easily from hexanes whereas **30a** resisted all attempts at crystallization and remained an oil. The crystal structure for **29a** was solved by direct methods^{115,116} and refined to R and R_w values of 3.57 and 3.62%, respectively. The crystals were orthorhombic and belonged to the Pbcn space group. An ORTEP representation of the structure is given in Figure 5. Only the *R,R* form is shown. The *S,S* form makes up the other half of the unit cell. There is a C₂ symmetry axis through the centre of the central C(1) C(1)' bond. The crystal structure establishes that this dimer is the racemic compound, **29a**.

The crystallographic data show several interesting structural features. The bond between the two tertiary carbons, C(1) and C(1)', that connects the two halves of the dimer, is only slightly elongated at 1.554 Å. Each five-membered ring is in an envelope conformation. As expected, the four carbons of each cyclopentane ring that are part of or bonded to the aromatic ring are essentially planar; the torsional angle between the bonds C(1) C(9) and C(4) C(3) is only 0.7°. In contrast, the remaining atom, C(2), is significantly out of the plane with a torsional angle of 32.2° between the C(3) C(2) and C(1) C(9) atoms. The two halves of the molecule are oriented such that the *ortho* hydrogens at C(8) of the aromatic rings are above the plane of the carbon atoms of the other ring; the torsional angle between C(9) C(1) and C(1)' C(9)' is only 23° so that the C(9)'s are close to being eclipsed. For comparison with calculated results, values for some key structural features are given in Table 16.

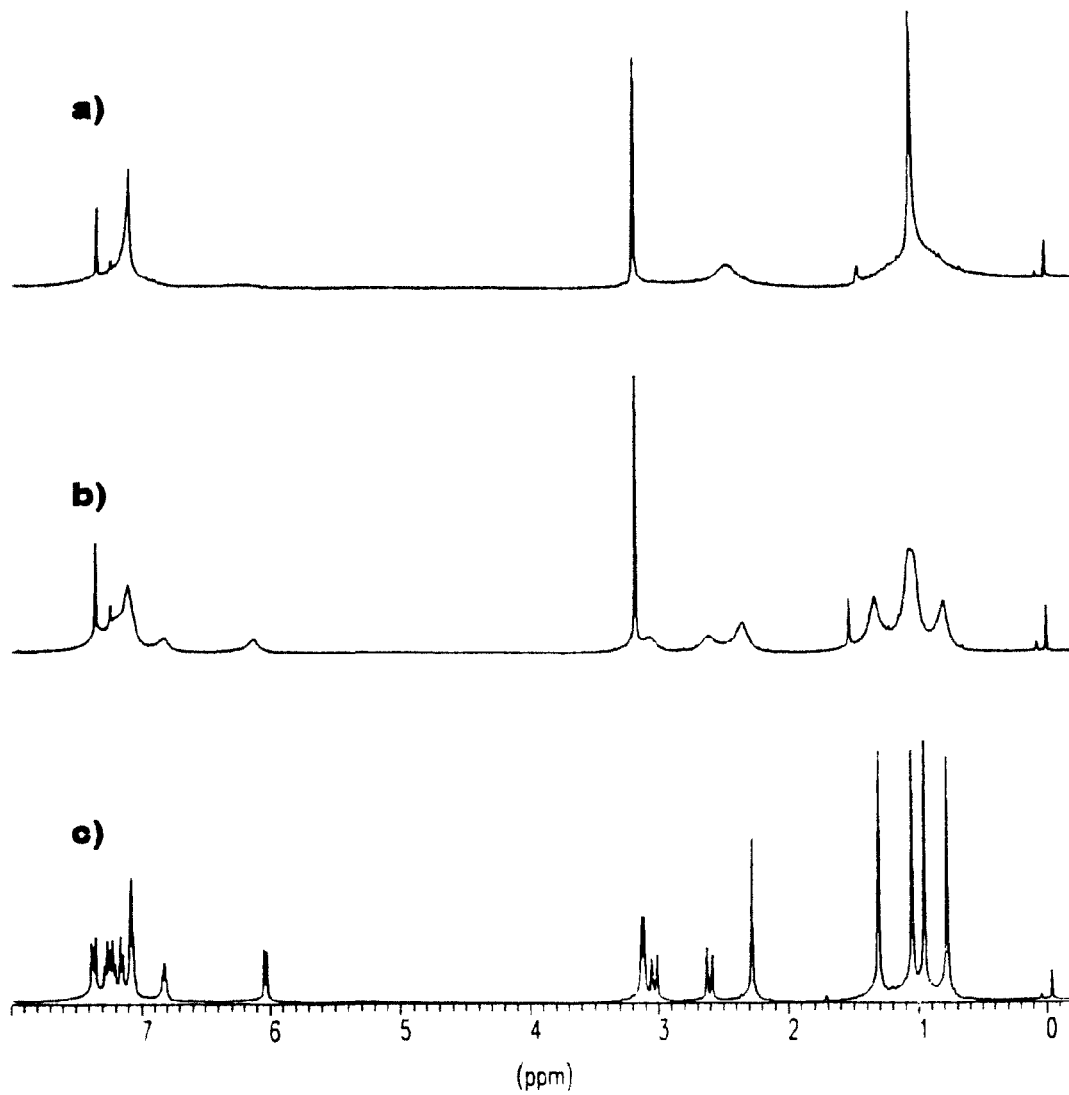
Figure 5. An ORTEP representation of the *R,R* form of the racemic dimer **29a**.



3.2.2 NMR Analysis of the Meso Dimer 30a

Hindered rotation around the C(1) C(1)' bond in the *meso* dimer causes broadened signals in the room temperature ^1H NMR spectrum, Figure 6b. Variable temperature ^1H NMR experiments were performed. Lowering the temperature slows the rate of interconversion between pairs of conformations, resulting in sharp signals in the ^1H NMR spectrum, Figure 6c (-40 °C). The signals were assigned based on integration and a HETCOR experiment at -40 °C. Both the ^1H and ^{13}C NMR spectra of this compound at -40 °C were consistent with a structure that had no symmetry. The four signals at 1.35, 1.09, 1.00, and 0.82 ppm are assigned to the four methyl groups. For comparison, the methyl groups in 2,2-dimethylindan absorb at 1.18 ppm. Therefore, one methyl group is significantly shielded and another somewhat deshielded. The singlet at 2.32 ppm integrates for two protons and is assigned to the methylene group in one of the five-membered rings. The two protons in this methylene group are accidentally isochronous. An AB quartet with $J = -16.1$ Hz is assigned to the methylene group in the other five-membered ring. Unlike the other signals, the resonance at 3.17 ppm due to the two methine protons was sharp at room temperature. It decreased in intensity and slightly broadened upon cooling and then split at about -30 °C into two distinct signals which sharpened into an AB quartet, with $\Delta\nu$ 0.0270 ppm and $J_{A,B}$ 2.0 Hz at -55 °C. The remainder of the signals is assigned to the aromatic protons and, consistent with lack of symmetry, there are more than four environments for aromatic protons in the populated conformer at -40 °C. One interesting feature of the aromatic region is the doublet at 6.07 ppm, a

Figure 6. 400 MHz ^1H NMR spectra of the *meso* dimer **30a** at a) +45 °C; b) +25 °C; and c) -40 °C.



highly shielded *ortho* aromatic proton.

A tentative structure of the populated conformer at $-40\text{ }^{\circ}\text{C}$ can be assigned based on the NMR data. The 2.0 Hz coupling constant measured between the protons on C(1) and C(1)' corresponds to an H-C(1)-C(1)'-H angle of either 65° or 111° using the Altona version¹¹⁷ of the Karplus equation with electronegativities of 2.3 for $\text{C}(\text{Me})_2\text{CH}_2$ and 2.41 for phenyl.¹¹⁸ Other features of the ^1H NMR data indicate that only the value near 65° can be correct. In conformations with the H-C(1)-C(1)'-H torsional angle between 69 and 81° , the two aromatic rings are offset face-to-face stacked and an *ortho* hydrogen on one aromatic ring is in the shielding cone of the other aromatic ring. This is consistent with the observation of a doublet at δ 6.07 ppm. Moreover, in this conformer, the geometrical relationship of the methyl groups and the benzene rings is consistent with the deshielding of one methyl group (1.4 ppm) and the shielding of another (0.82 ppm).

The ^1H NMR spectrum recorded at $45\text{ }^{\circ}\text{C}$ is shown in Figure 6a. By this temperature, the signals of the aromatic protons as well as those of one set of methyl groups have coalesced and the methine signals and the other set of methyl signals are approaching coalescence.

The ^{13}C NMR spectrum of this compound was also run at room temperature and the signals were again broadened. In contrast, at $-40\text{ }^{\circ}\text{C}$, 22 sharp lines were observed, one for each carbon atom in the molecule. The chemical shifts and multiplicities are given in the experimental section, 3.4.

The barrier to conformational motion in the *meso* dimer was estimated by

obtaining ^{13}C NMR (62.5 MHz) spectra at various temperatures. The barrier was obtained from the coalescence temperatures of the aliphatic signals using eq 44. T_c is

$$\Delta G^\ddagger (\text{kJ/mol}) = RT_c \left[2.3 + \ln\left(\frac{T_c}{\Delta\nu}\right) \right] \quad (44)$$

the coalescence temperature of the signals that were separated by $\Delta\nu$ at $-40\text{ }^\circ\text{C}$. At $-40\text{ }^\circ\text{C}$, there are two sets of methyl carbons, one at 23.7 and 25.7 ppm and another 34.1 and 32.9 ppm. The two quaternary carbons resonate at 41.3 and 40.3 ppm, and the methylene carbons and methine carbons at 47.5 and 48.6 ppm, and 56.6 and 62.3 ppm, respectively. The signals for the two methine carbons had the greatest chemical shift difference even though the protons on these carbons atoms were very close in chemical shift. The ^{13}C NMR spectra were recorded from $-40\text{ }^\circ\text{C}$ to $30\text{ }^\circ\text{C}$, increasing the temperature in $5\text{ }^\circ\text{C}$ steps except close to a coalescence point where they were recorded at $2\text{ }^\circ\text{C}$ intervals. The results are shown in Table 14. The average ΔG^\ddagger calculated is $61.7 \pm 0.3\text{ kJ/mol}$ ($14.7 \pm 0.1\text{ kcal/mol}$). Rate constants

Table 14. Coalescence Temperatures and Kinetic Data for the *Meso* Dimer.

signal	$\Delta\nu$ (Hz)	T_c (K)	ΔG^\ddagger (kJ/mol)	k_c (s^{-1})
$2 \times \text{C}$	14.3	288	62.2	32
$2 \times \text{CH}_2$	63.9	303	61.7	142
$2 \times \text{CH}_3$	77.3	307	62.2	172
$2 \times \text{CH}_3$	124.0	311	61.8	274
$2 \times \text{CH}$	370.1	320	60.7	822

of coalescence were calculated using eq 45 and are also given in Table 14.

$$k = \frac{\pi \Delta v}{\sqrt{2}} \quad (45)$$

3.2.3 Calculations for the Meso Dimer, 30a

Coordinates for the *meso* dimer were generated using the software package, PCMODEL. Then the molecular mechanics program, MM3 (94), was used to locate the minima. Five minima, I-V, were found all of which had the two five-membered rings in an envelope conformation, with C(2) and C(2)' significantly out of the plane. The numbering system used will be the same as that in the ORTEP representation of the racemic dimer, Figure 5. The C(1)-C(2)-C(3)-C(4) and C(1)'-C(2)'-C(3)'-C(4)' torsional angles were on the order of $\pm 30^\circ$. The energies of the five minima, relative to the global minima and the C(1)-C(2)-C(3)-C(4) and C(1)'-C(2)'-C(3)'-C(4)' torsional angles are given in Table 15. Also given in Table 15 are the C(2)'-C(1)'-C(1)-C(2) and H-C(1)'-C(1)-H torsional angles. These angles give the orientation of the two halves of the dimer with respect to one another.

The global minimum, IV, had a C(2)'-C(1)'-C(1)-C(2) torsional angle of 81.7° and a H-C(1)'-C(1)-H torsional angle of 72.2° . The conformer that has a C(2)'-C(1)'-C(1)-C(2) torsional angle of 155.1° , II, was only 0.1 kJ/mol (0.02 kcal/mol) higher in energy. The structure at the global minimum, IV, is consistent with the NMR data. The calculated H-C(1)'-C(1)-H angle of 72.2° would give a small coupling constant. The calculated C(2)'-C(1)'-C(1)-C(2) torsional angle of 81.7° places the two aromatic

rings in an offset face-to-face stacked orientation with an *ortho* proton of one aromatic ring in the shielding cone of the other.

MM3 can be used to construct a potential energy surface. To completely describe the potential energy surface for this compound it is necessary to measure the energy as a function of the central torsional angle, C(2)'-C(1)'-C(1)-C(2) and one of the angles in each of the five-membered rings that includes the carbon atom out of the plane, *i.e.*, C(2)' and C(2). The remainder of the molecule is fairly rigid. A potential energy surface was constructed by doing dihedral driver calculations on the C(2)'-C(1)'-C(1)-C(2), C(1)-C(2)-C(3)-C(4) and C(1)'-C(2)'-C(3)'-C(4)' torsional angles. For example, one set of dihedral driver calculations was done holding the torsional angles in both five-membered rings constant and calculating the energy as a function of the C(2)'-C(1)'-C(1)-C(2) torsional angle. Many dihedral driver calculations were done and the resulting surface is very complex with many shallow minima. The surface is complicated because the two five-membered rings can exist in numerous groups of conformations. The C(1)-C(2)-C(3)-C(4) and C(1)'-C(2)'-C(3)'-C(4)' torsional angles can be both positive, both negative or of opposite sign. This is discussed in detail elsewhere.¹¹⁴

The C(1)-C(2)-C(3)-C(4) and C(1)'-C(2)'-C(3)'-C(4)' torsional angles in the structure at the global minimum are of opposite sign. This corresponds to a structure that has each five-membered ring puckered away from the adjacent half of the molecule, minimizing steric interactions arising from interactions of the methyl groups on C(2) and C(2)'. The resulting structure maintains a plane of symmetry and is still

Table 15. Select Geometrical Data for Conformers of the *Meso* Dimer.

Feature	I		II		III	
	MM3	MM3	AM1	STO-3G	MM3	AM1
Relative stability (kJ/mol)	7.0 ^a	0.1 ^a	24.7 ^b	18.0 ^c	23.3 ^a	7.1 ^b
C(2)'-C(1)'-C(1)-C(2)	73.6	155.1	141.0	143.0	268.6	270.3
H-C(1)'-C(1)-H	68.3	158.5	142.1	146.0	- 80.6	-81.4
C(1)-C(2)-C(3)-C(4)	- 36.2	-39.4	- 24.1	- 34.2	- 31.8	-15.2
C(1)'-C(2)'-C(3)'-C(4)'	-32.8	-36.6	-29.2	-34.2	-27.3	-17.5
C(1)-C(1)' (Å)	1.567	1.565	1.525	1.574	1.569	1.526
C(1)-C(2) (Å)	1.580	1.568	1.578	1.587	1.574	1.564

Feature	IV			V
	MM3	AM1	STO-3G	MM3
Relative stability (kJ/mol)	0.0 ^a	0.0 ^b	0.0 ^c	8.87 ^a
C(2)'-C(1)'-C(1)-C(2)	81.7	86.2	84.0	158.9
H-C(1)'-C(1)-H	72.2	80.7	76.9	155.3
C(1)-C(2)-C(3)-C(4)	33.4	11.4	26.4	39.2
C(1)'-C(2)'-C(3)'-C(4)'	- 28.2	-9.0	-21.8	-38.2
C(1)-C(1)' (Å)	1.573	1.528	1.577	1.590
C(1)-C(2) (Å)	1.576	1.564	1.585	1.573

^aWith respect to the global MM3 minimum.

^bWith respect to the global AM1 minimum.

^cWith respect to the global STO-3G minimum.

a *meso* form. This means there are two identical conformers one with a C(2)'-C(1)'-C(1)-C(2) torsional angle of 81.7° and the other with that angle -81.7° . The broadened peaks in the NMR spectra are a result of slow interconversion between these two conformers. The largest barrier to interconverting these two conformers on the calculated potential energy surface is 17.9 kJ/mol (4.3 kcal/mol).¹¹⁴ The smallest barrier for interconversion of the populated conformers was determined experimentally to be 61.7 kJ/mol (14.7 kcal/mol) (*vide infra*). The geometry of the conformation of the MM3 global minimum is consistent with the experimental data. The rest of the potential energy surface is not.

Each of the five MM3 minimized geometries was used as input for AM1 calculations. Only three minima were found by AM1. The structure at the global minimum was very similar to that calculated by MM3. Relative energies and select data for the AM1 minima are given in Table 15.

One significant difference between the results of the MM3 and AM1 calculations is the degree of puckering in the five-membered rings. The MM3 global minimum has a C(1)-C(2)-C(3)-C(4) torsional angle of 33.4° whereas it is only 11.4° in the AM1 global minimum. The *meso* dimer is not crystalline, therefore, crystal structure data is not available. However, the C(1)-C(2)-C(3)-C(4) angle in the crystal structure of the racemic dimer is 31.9° suggesting that MM3 is a better predictor of the geometry in the five-membered rings. It would be possible to calculate a potential energy surface using AM1. However, because the degree of puckering in the five-membered ring is an important parameter and because AM1 flattens out the rings, the

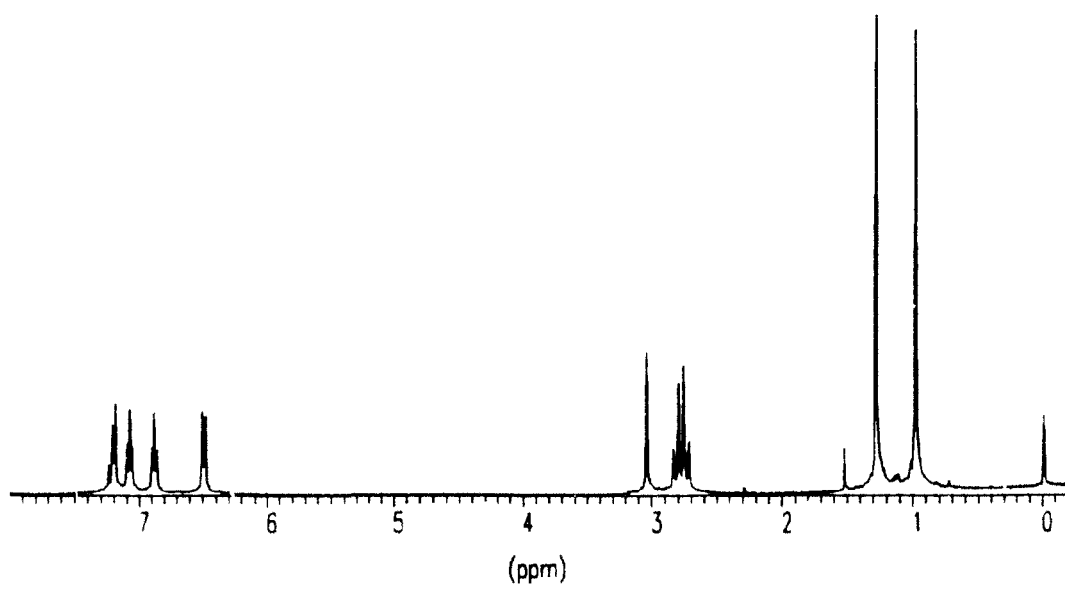
AM1 surface would not likely fit the actual potential energy surface very reliably.

STO-3G optimizations were also performed. Again, the global minimum had a C(2)'-C(1)'-C(1)-C(2) torsional angle in the 80° range and torsional angles in the five-membered rings of opposite sign. The relative energies and select geometrical data for the STO-3G calculations are given in Table 15. The STO-3G geometries at the minima have the five-membered rings puckered by ~30°. These values are similar to the MM3 values and are consistent with the crystal structure data for the racemic dimer. Examining the potential energy surface using STO-3G calculations might therefore be informative, however, the amount of computer time required means this would not be practical.

3.2.4 NMR Analysis of the Racemic Dimer, 29a

The room temperature ¹H NMR spectrum of the racemic dimer is shown in Figure 7. The two halves of the molecule are equivalent by virtue of its C₂ axis. The ¹H NMR spectra were sharp at all temperatures and no significant changes in chemical shift were observed with temperature, the maximum change for any signal from +45 °C to -60 °C being <0.1 ppm. The two methyl groups appear as singlets at 1.00 and 1.30 ppm. The protons of the CH₂ group give rise to an AB quartet (J = -15.0 Hz) centred at 2.80 ppm. The methine protons appear as a singlet at 3.07 ppm. Only one ¹³C satellite of the methine signal was observed 61.0 Hz higher frequency of the main methine singlet. The less shifted satellite was obscured by the methylene

Figure 7. The room temperature 400 MHz ^1H NMR (CDCl_3) spectrum of the racemic dimer, **29a**.

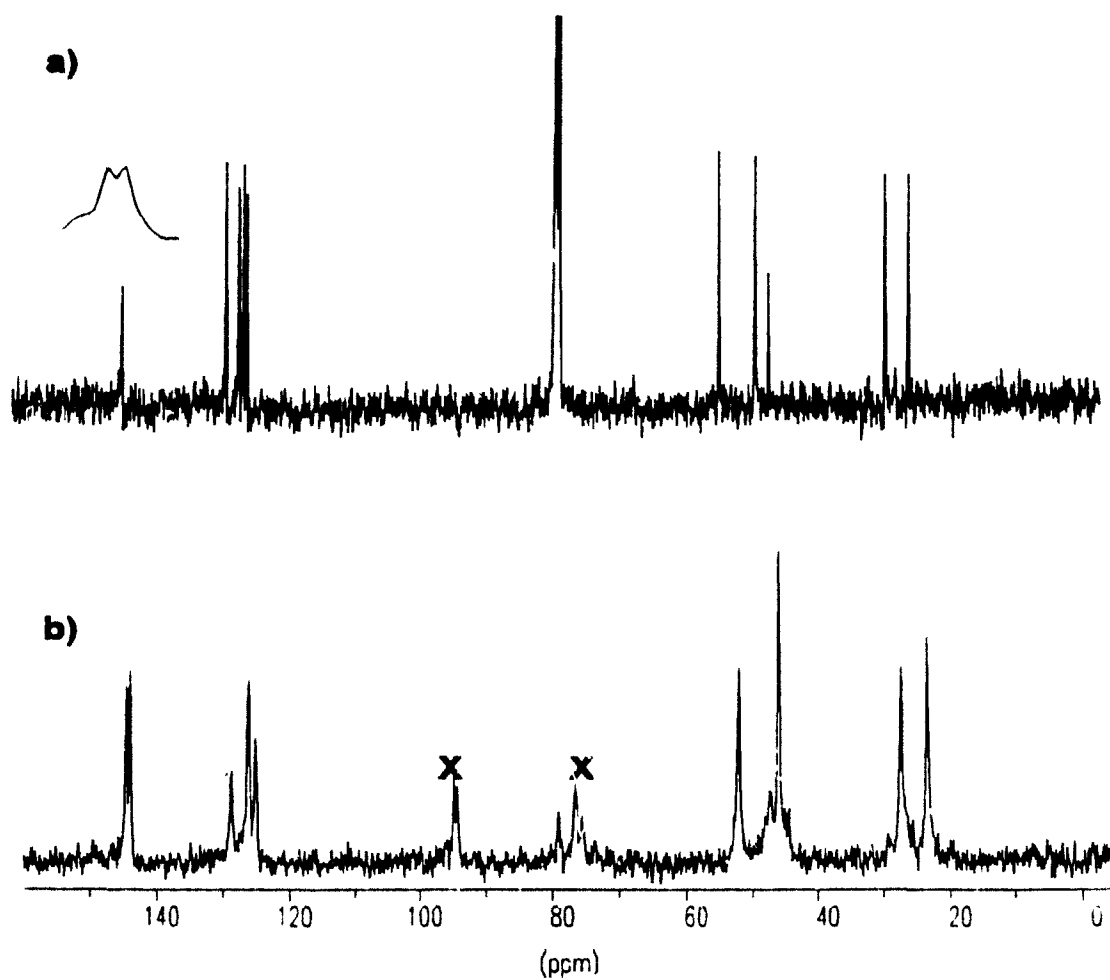


signals. Recording the spectra at both 250 and 400 MHz established that this small peak, having approximately 0.5% of the intensity of the main peak, was indeed a ^{13}C satellite. This signal was not split, indicating that the H(1)-H(1)' vicinal coupling constant was < 1 Hz. The aromatic region consists of two doublets and two triplets as expected for a first-order pattern of a 1,2-disubstituted aromatic ring. The signal of one *ortho* hydrogen is considerably shielded, appearing as a doublet at 6.52 ppm.

The ^{13}C NMR solution spectrum shown in Figure 8a contains 11 signals consistent with C_2 molecular symmetry. Signals of two quaternary carbon atoms (143.3 ppm, 143.2 ppm) and four tertiary carbon atoms (127.5 ppm, 125.6 ppm, 124.9 ppm, 124.4 ppm) are present in the aromatic region and the remaining signals occur at 52.8 (CH), 47.4 (CH), 45.4 (C), 27.5 (CH_3) and 24.0 (CH_3) ppm. A CP/MAS ^{13}C NMR spectrum of this dimer in the solid state is shown in Figure 8b. The MAS spectrum is very similar to the solution spectrum, except that spinning side bands, marked with an X, from the aromatic carbons are present. Chemical shift anisotropies of aromatic carbons are much larger than those of the aliphatic carbons,¹¹⁹ making removal of spinning side bands of aromatic carbons by MAS difficult.

Both the ^1H and ^{13}C NMR spectra are consistent with a single conformer or a conformational average that has C_2 symmetry. Examination of models of the racemic compound indicates that all conformations have C_2 symmetry. The observation of a significantly deshielded *ortho* aromatic proton and the similarity of the solid state and solution ^{13}C NMR spectra suggests that, in solution, the compound exists mainly in the

Figure 8. a) A 65 MHz ^{13}C NMR solution spectrum of the racemic dimer, **29a**. b) A MAS ^{13}C NMR spectrum from the solid state for the racemic dimer, **29a**. The signals marked with an X are spinning side bands.



conformer observed for the solid state which has a H-C(1)-C(1)'-H torsional angle close to 100°. Further support for this assertion comes from the ^{13}C satellite data; $^3J_{\text{H(1)-H(1)'}}$ was < 1 Hz. A value of 0.6 Hz is calculated for an H-C(1)'-C(1)-H angle of 100° using Altona's version of the Karplus equation.¹¹⁷

3.2.5 Calculations for the Racemic Dimer

The coordinates for the racemic dimer were again generated using PCMODEL and minima were calculated using MM3 (94). Seven minima were found, VI-XII, all of which have both of the five-membered rings in an envelope conformation, with C(2) and C(2)' being significantly out of the plane. Minima were calculated that had the C(1)-C(2)-C(3)-C(4) and C(1)'-C(2)'-C(3)''-C(4)'' torsional angles both positive, both negative and of opposite sign. The energies of the seven minima relative to the global minimum and select geometrical data are given in Table 16.

The MM3 global minimum, VII, has a C(2)'-C(1)'-C(1)-C(2) torsional angle of 170.5°. The structure of this conformer is not consistent with the experimental data. The ^1H NMR spectrum shows a shielded *ortho* aromatic proton at 6.5 ppm which is the result of an *ortho* aromatic proton on one aromatic ring in the shielding cone of the other aromatic ring. The calculated C(2)'-C(1)'-C(1)-C(2) torsional angle of 170.5° positions the two aromatic rings *anti* and no unusual shielding effects would be expected. As well, the experimental evidence strongly suggests that the conformation that is populated in solution is very similar to that of the crystalline material. The C(2)'-C(1)'-C(1)-C(2) torsional angle in the crystal structure is 131.0°. Conformer XI

Table 16. Select Geometrical Data for Conformers of the Racemic Dimer.

Feature	VI		VII		
	MM3	AM1	MM3	AM1	
Relative energy (kJ/mol)	1.1 ^a	5.2 ^b	0.0 ^a	0.3 ^b	
C(2)'-C(1)'-C(1)-C(2)	101.4	97.6	170.5	142.7	
H-C(1)'-C(1)-H	-153.9	-145.1	-72.5	-95.1	
C(1)-C(2)-C(3)-C(4)	36.0	16.1	34.2	10.1	
C(1)'-C(2)'-C(3)'-C(4)'	36.0	16.1	34.2	10.1	
C(1) - C(1)'	1.583	1.529	1.581	1.527	
C(1) - C(2)	1.578	1.571	1.574	1.571	

Feature	VIII		IX	X	
	MM3	AM1	MM3	MM3	AM1
Relative energy (kJ/mol)	17.2 ^a	12.0 ^b	22.6 ^a	28.1 ^a	7.7 ^b
C(2)'-C(1)'-C(1)-C(2)	294.9	286.6	136.0	295.8	-71.3
H-C(1)'-C(1)-H	46.1	48.8	-102.7	51.9	48.8
C(1)-C(2)-C(3)-C(4)	33.1	9.8	-36.4	-37.4	9.8
C(1)'-C(2)'-C(3)'-C(4)'	33.1	33.1	34.6	28.8	3.6
C(1) - C(1)'	1.571	1.527	1.575	1.560	1.527
C(1) - C(2)	1.574	1.563	1.572	1.571	1.563

continued...

Table 16. continued

Feature	XI			XII	
	MM3	AM1	STO-3G	crystal ^c structure	MM3
Relative energy (kJ/mol)	15.6 ^a	0.0 ^b			58.1 ^a
C(2)'-C(1)'-C(1)-C(2)	139.6	129.7	132.6	131.0(4)	302.1
H-C(1)'-C(1)-H	-95.0	-104.5	-98.7	-100	61.3
C(1)-C(2)-C(3)-C(4)	-35.9	-12.6	-30.8	-31.9(3)	-39.5
C(1)'-C(2)'-C(3)'-C(4)'	-35.9	-12.6	-30.8	-31.9	-39.5
C(1) - C(1)'	1.555	1.520	1.565	1.554(5)	1.554
C(1) - C(2)	1.571	1.570	1.579	1.563(4)	1.575

^aWith respect to the global MM3 minimum.

^bWith respect to the global AM1 minimum.

^cThe crystal structure data is given for the *S,S* enantiomer because the calculations were done for the *S,S* enantiomer. The ORTEP representation shown in Figure 5 is for the *R,R* enantiomer.

that has a C(2)'-C(1)'-C(1)-C(2) torsional angle of 139.6° is consistent with the experimental data, however, it is calculated to be 15.6 kJ/mol (3.7 kcal/mol) higher in energy than the global minimum.

AM1 calculations were done on the MM3 minima. Only five minima were found. The global minimum, XI, has a C(2)'-C(1)'-C(1)-C(2) torsional angle of 129.7° and is consistent with the experimental data. However, conformer VII with a C(2)'-C(1)'-C(1)-C(2) torsional angle of 142.7° is only 0.3 kJ/mol (0.07 kcal/mol) higher in energy. Both of these torsional angles would have the two aromatic rings offset face-to-face stacked and would be consistent with the NMR data. The decision as to which one of these calculated structures is consistent with the experimental evidence can be made by comparing the calculated torsional angles in the five-membered rings to the corresponding torsional angles in the crystal structure. The C(1)-C(2)-C(3)-C(4) and C(1)'-C(2)'-C(3)'-C(4)' torsional angles in the crystal structure are both negative. This corresponds to a structure which has each five-membered ring puckered away from the adjacent half of the molecule. This can easily be seen in the ORTEP representation (Figure 5). The MM3 conformer, XI, with a C(2)'-C(1)'-C(1)-C(2) torsional angle of 129.7° has both the five-membered ring torsional angles negative.

The calculated AM1 global minimum is the structure that most closely fits all of the experimental data. However, AM1 gives two conformers of nearly equal energy. No temperature effects were observed in the NMR spectra. This means that either the AM1 global minimum should be lower in energy than calculated or the

barrier to interconversion between XI and VII is very small. Again, the AM1 calculations have considerably flattened out the five-membered rings. The C(1)-C(2)-C(3)-C(4) torsional angle in the AM1 global minimum is -12.6° whereas it is -31.9° in the crystal structure.

Single-point STO-3G calculations were done on the two lowest energy AM1 minima and the order of stability was reversed, XI was now calculated to be 8.0 kJ/mol higher in energy than VII.

STO-3G optimizations are being done on the MM3 minimized geometries. The STO-3G optimized geometry of conformer XI had a C(2)'-C(1)'-C(1)-C(2) torsional angle of 132.6° and both of the five-membered rings had negative torsional angles. As can be seen from Table 16 agreement between the STO-3G optimized geometry of this conformer and the crystal structure data is excellent. STO-3G calculations are being done on the other conformers. The relative STO-3G energies of the conformers XI and VII may help to decide if conformer XI is highly populated or if both XI and VII are populated and are rapidly interconverting.

3.2.6 Conclusions

Surprisingly, many of the results of the MM3 calculations were not consistent with the experimental evidence. For the *meso* dimer, the structure of the MM3 global minimum was consistent with the experimental evidence, however, this was not so for the racemic dimer. For the racemic dimer the structure that was consistent with the experimental data was calculated to be 15.6 kJ/mol (3.7 kcal/mol) higher in energy

than the global minimum. NMR evidence suggests that this conformer is highly populated in solution, therefore, it should be significantly lower in energy. For the *meso* dimer the smallest calculated barrier on the energy surface was 17.9 kJ/mol (4.3 kcal/mol) while the experimental barrier was 61.7 kJ/mol (14.7 kcal/mol). One possible explanation for the failure of MM3 is pi stacking. The conformers that have the two aromatic rings offset face-to-face stacked could be much lower in energy than calculated. This would lower the energy of the global minima for the *meso* dimer resulting in a larger barrier. It would also lower the energy of conformer XI of the racemic dimer which has the two aromatic rings stacked. If pi stacking is the explanation the magnitude of the stacking interaction would have to be ~40 kJ/mol (9.6 kcal/mol). There is no literature precedence for pi stacking interactions of this magnitude, pi stacking interactions are on the order of 2 kJ/mol (0.5 kcal/mol).^{110,111} Dimers **29a** and **30a** have interesting conformational properties that cannot be successfully modeled at the level of theory that is practical for molecules of this size.

3.4 Experimental

3.4.1 General experimental

The ^{13}C NMR spectrum of the solid sample was measured on a Bruker AMX 400 NMR spectrometer with magic angle spinning at 5 kHz. For more general experimental details see experimental section 1.5.1.

3.4.2 Characterization of the Dimers

Racemic Bis 1,1'-(2,2,2',2'-Tetramethylindan) (29a): recrystallized from hexanes: mp 187-188 °C; ^1H NMR δ 7.23 (d, 1H, $J = 7.5$ Hz), 7.10 (t, 1H, $J = 7.5$ Hz), 6.91 (t, 1H, $J = 7.5$ Hz), 6.52 (d, 1H, $J = 7.5$ Hz), 3.07 (s, 1H), 2.84 (d, 1H, $J = -15.0$ Hz), 2.77 (d, 1H, $J = 15.0$ Hz), 1.30 (s, 3H), 1.00 (s, 3H); ^{13}C NMR δ 143.3 (C), 143.2 (C), 127.5 (CH), 125.6 (CH), 124.9 (CH), 124.4 (CH), 52.8 (CH), 47.4 (CH₂), 45.4 (C), 27.5 (CH₃), 24.0 (CH₃); GC/MS m/z 290 (M⁺, 0.2), 146 (18), 145 (100), 130 (11), 129 (14), 128 (12), 117 (20), 115 (18), 91 (18).

Meso Bis 1,1'-(2,2,2',2'-Tetramethylindan) (30a): ^1H NMR (233 K) δ 7.40 (d, 1H, $J = 7.30$ Hz), 7.32-7.24 (m, 2H), 7.19 (d, 1H, $J = 7.0$ Hz), 7.13-7.11 (m, 2H), 6.87 (td, 1H, $J_1 = 6.65$ Hz, $J_2 = 2.1$ Hz), 6.07 (d, 1H, $J = 7.56$ Hz), 3.18 (s, 1H), 3.07 (d, 1H, $J = -16.05$ Hz), 2.65 (d, 1H, 16.05 Hz), 2.32 (s, 2H), 1.35 (s, 3H), 1.09 (s, 3H), 1.00 (s, 3H), 0.82 (s, 3H). ^{13}C NMR (233 K) δ 149.5, 144.9, 143.5, 143.1, 128.6, 126.5, 125.9, 125.4, 125.3, 124.6, 62.3 (CH), 56.5 (CH), 48.4 (CH₂), 47.4 (CH₂), 41.2 (C), 41.0 (C), 34.2 (CH₃), 33.0 (CH₃), 25.8 (CH₃), 23.9 (CH₃):

GC/MS m/z 290 (M^+ , 0.1), 146 (20), 145 (100), 130 (14), 129 (21), 128 (19), 117 (23), 115 (24), 91 (21).

Racemic Bis 1,1'-(6,6'-Dimethoxy-2,2,2',2'-tetramethylindan) (29b):

recrystallized from ethanol: mp 139-142 °C; ^1H NMR δ 7.08 (d, 1H, $J = 8.2$ Hz), 6.63 (dd, 1H, $J_1 = 8.1$ Hz, $J_2 = 2.3$ Hz), 6.12 (brs, 1H), 3.49 (s, 3H), 3.00 (s, 1H), 2.72 (d, 1H, $J = -14.7$ Hz), 2.65 (d, 1H, $J = -14.7$ Hz), 1.24 (s, 3H), 0.98 (s, 3H); ^{13}C NMR δ 158.4 (C), 145.0 (C), 135.3 (C), 124.6 (CH), 113.8 (CH), 111.4 (CH), 55.3 ($\text{CH}_3\text{-O}$), 52.9 (CH), 46.5 (CH_2), 45.7 (C), 27.6 (CH_3), 24.1 (CH_3); GC/MS m/z 350 (M^+ , 6), 176 (15), 175 (100).

Meso Bis 1,1'-(6,6'-Dimethoxy-2,2,2',2'-tetramethylindan) (30b): This compound was isolated as a mixture and was not separated.

Racemic Bis 1,1'-(5,5'-Dimethoxy-2,2,2',2'-tetramethylindan) (29c):

recrystallized from hexanes: mp 187-188 °C; ^1H NMR δ 6.78 (s, 1H), 6.49-6.39 (m, 2H), 3.75 (s, 3H), 2.95 (s, 1H), 2.78 (d, 1H, $J = 15.2$ Hz), 2.69 (d, 1H, $J = -15.2$ Hz), 1.26 (s, 3H), 0.97 (s, 3H); ^{13}C NMR δ 158.1 (C), 144.9 (C), 135.3 (C), 128.0 (CH), 110.3 (CH), 110.2 (CH), 55.3 ($\text{CH}_3\text{-O}$), 52.1 (CH), 47.6 (CH_2), 45.6 (C), 27.4 (CH_3), 24.0 (CH_3); GC/MS m/z 350 (M^+ , 0.4), 176 (14), 175 (100).

Meso Bis 1,1'-(5,5'-Dimethoxy-2,2,2',2'-tetramethylindan) (30c): ^1H NMR (250

MHz, 233K) δ 7.28 (d, 1H, $J = 7.9$ Hz), 6.85 (d, 1H, $J = 7.9$ Hz), 6.74 (s, 1H), 6.67 (s, 1H), 6.44 (d, 1H, $J = 8.6$ Hz), 6.00 (d, 1H, $J = 8.0$ Hz), 3.92 (s, 3H), 3.77 (s, 3H), 3.08-3.00 (m, 3H), ~2.60 (d, 1H, $J = -15.8$ Hz, the other half of the AB quartet is obscured under the multiplet at 3.08-3.00 ppm), 2.62 (s, 2H), 1.33 (s, 3H), 1.09 (s, 3H), 0.99 (s, 3H), 0.82 (s, 3H); ^{13}C NMR δ 158.3 (C), 158.2 (C), 144.9, 144.5, 141.4, 125.8, 112.1, 111.6, 109.3, 109.2, 125.88, 125.85, 61.8 ($\text{CH}_2\text{-O}$), 55.5 (CH), 55.3 (CH), 48.5 (C), 47.5 (C), 41.5 (CH_2), 41.3 (CH_2), 34.3 (CH_3), 33.0 (CH_3), 25.8 (CH_3), 24.0 (CH_3); GC/MS m/z 350 (M^+ , 0.3), 176 (13), 175 (100).

References

1. F.A. Carey and R.J. Sundberg. *Advanced Organic Chemistry*. 3rd ed. Plenum Press, New York. 1990. p. 198.
2. E.R. Thornton. *Solvolysis Mechanisms*. The Ronald Press Company, New York. 1964.
3. A. Streitwieser Jr. *Solvolytic Displacement Reactions*. McGraw-Hill, New York. 1962.
4. E. Havinga, R.O. de Jongh, and W. Dorst. *Rec. Trav. Chim.* **75**, 378 (1956).
5. H.E. Zimmerman and V.R. Sandel. *J. Am. Chem. Soc.* **85**, 915 (1963).
6. The yields given are based on isolated product yields. Where two numbers are given two separate determinations were made.
7. H.E. Zimmerman and S. Somasekhara. *J. Am. Chem. Soc.* **85**, 922 (1963).
8. P. Wan, B. Chak, and E. Krough. *J. Photochem. Photobiol. A.* **46**, 49 (1989) and references therein.
9. J. McEwen and K. Yates. *J. Phys. Org. Chem.* **193**, 4 (1991) and references therein.
10. B. Matuszewski, R.S. Givens, and C.V. Neywick. *J. Am. Chem. Soc.* **95**, 595 (1973).
11. D.C. Appleton, D.C. Bull, R.S. Givens, V. Lillis, J. McKenna, J.M. McKenna, S. Thackery, and A.R. Walley. *J. Chem. Soc. Perkin Trans. 2.* **77** (1980).
12. D.P. DeCosta and J.A. Pincock. *J. Am. Chem. Soc.* **115**, 2180 (1993).
13. Data taken from ref 12.
14. R.A. Marcus. *Annu. Rev. Phys. Chem.* **155**, 15 (1964).
15. D.F. McMillen and D.M. Golden. *Annu. Rev. Phys. Chem.* **33**, 493 (1982).
16. Preliminary work on this project was done by James Hilborn and some results were presented in his thesis, ref 17. Some of the results will be presented here again for clarity and continuity. Where possible the work done by Jim Hilborn will be indicated.

17. Jim Hilborn. Ph.D. Thesis, Dalhousie University (1990).
18. J.W. Hilborn and J.A. Pincock. *Can. J. Chem.* **70**, 992 (1992).
19. W.C. Gardiner. *Rates and Mechanisms of Chemical Reactions*. Benjamin, New York. 1969. p. 168.
20. J. Chateaufneuf, J. Luszyk, and K.U. Ingold. *J. Am. Chem. Soc.* **110**, 2877, 2886 (1988).
21. R.F. Langler, Z. Marini, and J.A. Pincock. *Can. J. Chem.* **56**, 903 (1978).
22. S.J. Cristol and T.H. Bindel. *Organic Photochemistry*. Marcel Dekker, New York. vol. 6 1983.
23. S.J. Cristol and T.H. Bindel. *J. Org. Chem.* **45**, 951 (1980).
24. S.J. Cristol and T.H. Bindel. *J. Am. Chem. Soc.* **103**, 7287 (1981).
25. G.H. Slocum and G. B Schuster. *J. Org. Chem.* **49**, 2177 (1984).
26. For esters **1a-d,f** and **2a-d,f** these values were determined by Jim Hilborn, ref 17.
27. S.L. Murov, I. Carmichael and G.L. Hug. *Handbook of Photochemistry*. Marcel Dekker, New York. 1993. p. 50.
28. B. Foster, B. Gaillard, N. Mathur, A.L. Pincock, J.A. Pincock and C. Sehmby. *Can. J. Chem.* **65**, 1599 (1987).
29. D.A. LaBianca, D. Huppert, D.F. Kelley and G.S. Hammond. *J. Am. Chem. Soc.* **94**, 3679 (1972).
30. S.L. Murov. *Handbook of Photochemistry*. Marcel Dekker, New York. 1973. p. 55.
31. Dr. L.J. Johnston, Steacie Institute for Molecular Sciences, National Research Council, Ottawa. unpublished results.
32. H.E. Zimmerman. *Angew. Chem. Int. Ed. Engl.* **8**, 1 (1969).
33. J.M. Kim and J.A. Pincock. *Can. J. Chem.* in press.
34. D. Griller, K.U. Ingold. *Acc. Chem. Res.* **13**, 317 (1980).
35. B.A. Sim, P.H. Milne, D. Griller and D.D.M. Wayner. *J. Am. Chem. Soc.* **112**, 6635 (1990).

36. (a) R.P. Van Duyne and S.F. Fischer. *Chem Phys.* **5**, 183 (1974). (b) J. Ulstrup and J. Jortner. *J. Chem. Phys.* **63**, 4358 (1975). (c) P. Siders and R.A. Marcus. *J. Am. Chem. Soc.* **103**, 741, 748 (1981). (d) B.S. Brunschweig, J. Logan, M.D. Newton and N.J. Sutin. *J. Am. Chem. Soc.* **102**, 5798 (1980).
37. Fitting software provided by Dr. Samir Farid, Eastman Kodak Co., CRL, Rochester, NY, 14640-2109.
38. R.M. Silverstein, G.C. Bassler and T.C. Morrill. *Spectrometric Identification of Organic Compounds*. 5th ed. J. Wiley and Sons, New York. 1991. p. 93.
39. I.R. Gould, R. Moody and S. Farid. *J. Am. Chem. Soc.* **110**, 7242 (1988) and references therein.
40. G.L. Closs, L.T. Calcaterra, N.J. Green, K.W. Penfield and J.R. Miller. *J. Phys. Chem.* **90**, 3673 (1986).
41. P. Wan, B. Chak and C. Li. *Tetrahedron Lett.* **27**, 2937 (1986).
42. P. Wan and B. Chak. *J. Chem. Soc. Perkin Trans 2* 751 (1986).
43. R. Pollard, S. Wu, G. Zhang, and P. Wan. *J. Org. Chem.* **58**, 2605 (1993).
44. R. Mosi, G. Zhang, and P. Wan. *J. Org. Chem.* **60**, 411 (1995).
45. N. Mathivanan, F. Cozens, R.A. McClelland, and S. Steeken. *J. Am. Chem. Soc.* **114**, 2198 (1992).
46. A.J. Kresge, Y. Chiang, L.E. Hakka. *J. Am. Chem. Soc.* **93**, 6167 (1971).
47. A.J. Kresge, H.J. Chen, L.E. Hakka, J.E. Kouba. *J. Am. Chem. Soc.* **93**, 6174 (1971).
48. A.J. Kresge, S.G. Mylonakis, Y. Sato, V.P. Vitullo. *J. Am. Chem. Soc.* **93**, 6181 (1971).
49. D.P. DeCosta and J.A. Pincock. *Can. J. Chem.* **70**, 1879 (1992).
50. J. Kawakami and M. Iwamura. *J. Phys. Org. Chem.* **7**, 31 (1994).
51. (a) L. Meites and P. Zuman. *CRC Handbook Series in Organic Electrochemistry*. CRC Press Inc., Ohio. 1976. Vol 1. #AT20 p. 472. (b) *Ibid* #AN62 p. 353. (c) *Ibid* #BB60 p. 532. (d) *Ibid* #AP79 p. 389.
52. H. Shizuka and J. Tobita. *J. Am. Chem. Soc.* **104**, 6919 (1972).

53. J.M. Kim and J.A. Pincock. unpublished results.
54. M. Christl. *Angew. Chem. Int. Ed. Engl.* **20**, 529 (1981).
55. K.E. Wilzbach, A.L. Harkness and L. Kaplan. *J. Am. Chem. Soc.* **90**, 1116 (1968).
56. J.I. Seeman. *Chem. Rev.* **83**, 83 (1983).
57. P.J. Wagner. *Acc. Chem. Res.* **16**, 461 (1983).
58. F.D. Lewis, R.W. Johnson and D.E. Johnson. *J. Am. Chem. Soc.* **96**, 6090 (1974).
59. W.J. Parr and T. Schaefer. *Acc. Chem. Res.* **13**, 400 (1980).
60. T. Schaefer, K.J. Cox, C.L. Morier, C. Beaulieu, R. Sebastian and G. Penner. *Can. J. Chem.* **68**, 1553 (1990).
61. N.J. Turro. *Modern Molecular Photochemistry*. University Science Books, California. 1991. p. 170-72.
62. N.J. Bunce. *J. Photochem.* **38**, 99 (1987).
63. R.E. Pearson and J.C. Martin. *J. Am. Chem. Soc.* **85**, 354, 3142 (1963).
64. C. Walling, A.L. Reiger and D.D. Tanner. *J. Am. Chem. Soc.* **85**, 3129 (1963).
65. C. Walling and A.L. Rieger. *J. Am. Chem. Soc.* **85**, 3135 (1963).
66. Ref # 27, p 12.
67. C.J. Pouchert. *Aldrich Library of NMR Spectra*. Aldrich Chemical Co. Inc., U.S.A. 1983. ed. 2, Vol. 1 p. 949-C.
68. Ref 67 p 947-C.
69. Ref 67 p 950-A.
70. H.C. Brown, S. Narasimhan and Y.M. Choi. *J. Org. Chem.* **47**, 4702 (1982).
71. M. Lissel, B. Neumann and S. Schmidt. *Liebigs Ann. Chem.* 263 (1987).
72. A. Orliac-Le Moing, J. Delaunay, A. LeBouc and J. Simonet. *Tetrahedron*, **20**, 4483 (1985).

73. R.L. Metcalf, E.R. Metcalf and W.C. Mitcheli. *Proc. Natl. Acad. Sci. U.S.A.* **83**, 1549 (1986).
74. G.S. Groenewold, M.L. Gross and R. Zey. *Org. Mass. Spect.* **17**, 416 (1982).
75. H.A. Staab and W. Rohr. *Syntheses Using Heterocyclic Amides (Azolides) in Newer Methods of Preparative Organic Chemistry*. Academic Press, Germany, 1968.
76. J.G.D. Carpenter and J.W. Moore. *J. Chem. Soc., C*, 1610 (1969).
77. H. Tomioka, K. Tabayashi, Y. Ozak and Y. Izawa. *Tetrahedron* **41**, 1435 (1985).
78. Huang-Minlon. *J. Am. Chem. Soc.* **68**, 2487 (1946).
79. A. Jaxa-Chamiec, V.P. Shah and L.J. Kruses. *J. Chem. Soc., Perkin Trans. I* 1705 (1989).
80. E.A. Carress and I.E. Rosenberg. *J. Org. Chem.* **37**, 3160 (1972).
81. J.E. Herweh and C.E. Hoyle. *J. Org. Chem.* **45**, 2195 (1980).
82. R. Martin. *Org. Prep. Proced. Int.* **24**, 369 (1992).
83. D. Bellus. *Adv. Photochem.* **8**, 109 (1971).
84. G. Kraupp. *Angew. Chem. Int. Ed. Engl.* **19**, 243 (1980).
85. J.F. Cameron and J.M.J. Fréchet. *J. Org. Chem.* **55**, 5919 (1990).
86. C.K. Saucers, W.P. Jencks, and S. Groh. *J. Am. Chem. Soc.* **97**, 5546 (1975).
87. C. Faurholt. *Z. Phys. Chem.* **126**, 72 (1927).
88. J. Chateaufneuf, J. Lusztyk, B. Maillard, and K.U. Ingold. *J. Am. Chem. Soc.* **110**, 6727 (1988).
89. D.H. Williams and I. Fleming. *Spectroscopic Methods in Organic Chemistry*. 4th ed. McGraw-Hill, London. 1987. p. 139.
90. M. Fujio, M. Goto, T. Susuki, I. Akasaka, M. Mishima, and Y. Tsuno. *Bull. Chem. Soc. Jpn.* **63**, 1146 (1990).
91. D. Kevill and H. Ren. *J. Org. Chem.* **54**, 5654 (1989).

92. Y. Tsuno, M. Sawada, T. Fujii, and Y. Yukawa. *Bull. Chem. Soc. Jpn.* **48**, 3347 (1975).
93. T.J. Stone and W.A. Walters. *J. Chem. Soc.* 213 (1964).
94. D.P. Kelly, J.T. Pinhey, and R.D.G. Rigby. *Aust. J. Chem.* **22**, 977 (1969).
95. S.L. Johnson and D.L. Morrison. *J. Am. Chem. Soc.* **94**, 1323 (1972).
96. M. Caplow. *J. Am. Chem. Soc.* **90**, 6795 (1968).
97. B. Arnold, L. Donald, A. Jurgens, and J.A. Pincock. *Can. J. Chem.*, **63**, 3140 (1985).
98. T. Nakaya, T. Tomomoto, and M. Imoto. *Bull. Chem. Soc. Jpn.* **40**, 691 (1967).
99. N. Chapman and J. James. *J. Chem. Soc.* 1865 (1953).
100. D. Zhang, Y. Xu, L.L. Lam, and H.H. Huang. *Acta Cryst.* **49**, 1002 (1993).
101. M. Oki. *The Chemistry of Rotational Isomers*. Springer-Verlag, Berlin. 1993.
102. M.A. Cremonini, L. Lunazzi, G. Placucci, R. Okazaki, and G. Yamamoto. *J. Am. Chem. Soc.* **112**, 2915 (1990).
103. W.D. Hounshell, D.A. Dougherty, and K. Mislow. *J. Am. Chem. Soc.* **100**, 3149 (1978).
104. L. Lunazzi, D. Macciantelli, F. Bernardi, and K.U. Ingold. *J. Am. Chem. Soc.* **99**, 4573 (1977).
105. H.D. Beckhaus, C. Ruchardt, and J.E. Anderson. *Tetrahedron.* **38**, 2299 (1982).
106. A.J.A. Reuvers, A. Sinnema, F. van Rantwijk, J.D. Remijnse, and H. van Bekkum. *Tetrahedron.* **25**, 4455 (1969).
107. P. Finocchiaro, D. Gust, W.D. Hounshell, J.P. Hummel, P. Maravigna, and K. Mislow. *J. Am. Chem. Soc.* **98**, 4945 (1976); D.A. Dougherty, K. Mislow, J.F. Blount, J.B. Wooten, and J. Jacobus. *ibid* **99**, 6149 (1977).
108. S. Brownstein, J. Dunogues, D. Lindsay, and K.U. Ingold. *J. Am. Chem. Soc.* **99**, 2073 (1977).

109. H.D. Beckhaus, K.J. McCullough, H. Fritz, C. Ruchardt, B. Kitschhke, H.J. Lindner, D.A. Dougherty, and K. Mislow, *Chem. Ber.* **113**, 1867 (1980).
110. L.F. Newcomb and S.H. Gellman. *J. Am. Chem. Soc.* **116**, 4993 (1994).
111. S. Paliwal, S. Geib, and C.S. Wilcox. *J. Am. Chem. Soc.* **116**, 4497 (1994).
112. W.L. Jorgenson and D.L. Severance. *J. Am. Chem. Soc.* **112**, 4768 (1990).
113. C.A. Hunter and J.K.M. Sanders. *J. Am. Chem. Soc.* **112**, 5525 (1990).
114. P.J. MacLeod, T.B. Grindley, J.A. Pincock and T.S. Cameron manuscript in preparation.
115. The structure was solved by T. S. Cameron Department of Chemistry Dalhousie University.
116. Lists of atomic coordinates, bond lengths and angles, torsion angles, and anisotropic thermal parameters may be purchased from: The depository of Unpublished Data Document Delivery, CISTI, National Research Council of Canada, Ottawa, ON, Canada K1A 0S2.
117. C.A.G. Haasnoot, F.A.A M. DeLeeuw, and C. Altona. *Tetrahedron.* **36**, 2783 (1980).
118. Thanks to Dr. J. S. Grossert for a BASIC computer program that calculates 3J values based on Altona's equation, ref 117.
119. W.S. Veeman. *Progress NMR Spectrosc.* **16**, 193 (1984).